NEDC-23856-1
OCTOBER 1978

OXYGEN SUPPRESSION IN BOILING WATER REACTORS

QUARTERLY REPORT 2
JANUARY 1 TO MARCH 31, 1978

E. L. BURLEY

CONTRACT EY-C-02-2985
COMMONWEALTH RESEARCH CORPORATION
U.S. DEPARTMENT OF ENERGY

GENERAL ELECTRIC

DISCLAIMER

NEDC-23856-1
October 1978

OXYGEN SUPPRESSION IN BOILING WATER REACTORS

QUARTERLY REPORT 2

January 1 to March 31, 1978

Contract EY-C-02-2985

Prepared by E. L. Burley
for the Commonwealth Research Corp.
and the U.S. Department of Energy

Reviewed: M. Siegler for
J. H. Holloway, Manager
Water Chemistry

Reviewed: W R DeHollander
W. R. DeHollander, Manager
Chemical Engineering

Approved: R. A. Proebstle
R. A. Proebstle, Manager
Applied Metallurgy & Chemistry

NUCLEAR ENERGY ENGINEERING DIVISION • GENERAL ELECTRIC COMPANY
SAN JOSE, CALIFORNIA 95125

GENERAL ELECTRIC

682

LEGAL NOTICE

This report was prepared by the General Electric Company (GE) as an account of work sponsored by the Department of Energy (DOE). Neither DOE, members of DOE, nor GE, nor any person acting on behalf of either, including Commonwealth Research Corporation:

a. Makes any warranty or representation, express or implied, with respect to the accuracy, completeness, or usefulness of the information contained in this report, or that the use of any information, apparatus, method, or process disclosed in this report may not infringe privately owned rights; or

b. Assumes any liabilities with respect to the use of, or for damages resulting from the use of, any information, apparatus, method, or process disclosed in this report.

TABLE OF CONTENTS

TABLE OF CONTENTS (Continued)

TABLE OF CONTENTS (Continued)

LIST OF ILLUSTRATIONS

LIST OF ILLUSTRATIONS (Continued)

LIST OF TABLES

1. INTRODUCTION

Boiling water reactors (BWR's) generally use high purity, no-additive feedwater. Primary recirculating coolant is neutral pH, and contains 100 to 300 ppb oxygen and stoichiometrically related dissolved hydrogen. However, oxygenated water increases austenitic stainless steel susceptibility to intergranular stress-corrosion cracking (IGSCC) when other requisite factors such as stress and sensitization are present. Thus, reduction or elimination of the oxygen in BWR water may preclude cracking incidents. One approach to reduction of the BWR coolant oxygen concentration is to adopt alternate water chemistry (AWC) conditions using an additive(s) to suppress or reverse radiolytic oxygen formation. Several additives are available to do this but they have seen only limited and specialized application in BWR's. The objective of this program is to perform an in-depth engineering evaluation of the potential suppression additives supported by critical experiments where required to resolve substantive uncertainties. On the basis of the engineering evaluation, the optimum oxygen suppression approach(es) will be selected and a specific BWR plant recommended for an extended (3-year) plant demonstration experiment.

The program is funded by the U.S. Department of Energy and managed by Commonwealth Research Corporation which will also implement any large-scale reactor tests. The preliminary engineering evaluations and related test work are being done by the General Electric Co.

2. SUMMARY

2.1 HYDROGEN FLOW SHEET

Initial flow sheets for the suppression of oxygen in the reactor water indicated that surprisingly small amounts of hydrogen are required. Now, additional experimental data have been accumulated and correlated to make them applicable to any given BWR. The results for a GE-BWR using data from the Boiling Reactor Experiments (BORAX III, BORAX IV), Experimental Boiling Water Reactor (EBWR), Argonne Low Power Reactor (ALPR), and Heavy Boiling Water Reactor (HBWR), are:

O_2 Level Desired in Reactor Water (ppm)	H_2 Concentration (ppm)		H_2 Addition (lb/h)
	Reactor Core Inlet	Feedwater	
0.01	0.23	2.1	21
0.05	0.13	1.1	11

2.2 AMMONIA CONSUMPTION

Additional calculations have also been made on the use of ammonia as an oxygen suppressing additive. Assuming that minimum ammonia concentration to prevent nitrate/nitrite formation is 10 ppb, the ammonia requirement was calculated to be from 700 to 1200 lb/h depending on the treatment of the data. This range is not unreasonable considering the assumptions required and it agrees well with other experimenters' predictions. It is concluded that ammonia consumption would be about 1000 lb/h in a 2500 MWt BWR.

2.3 HYDRAZINE REQUIREMENT

The calculations on the use of hydrazine as an additive have also been extended and revised. When radiolytic and thermal decomposition rates are superimposed, it is barely possible to keep trace amounts of hydrazine in the core exit water. Approximately 200,000 lb/h of N_2H_4 must be added with the feedwater to

give a core effluent concentration of 8 ppb hydrazine. Since the hydrazine is decomposing so rapidly to NH_3 and H_2, a hydrazine flow sheet is, in effect, an ammonia flow sheet. Considering this case, a hydrazine addition rate of 980 lb/hr to a 2500 MWth BWR yields a satisfactory in-core ammonia concentration and gives oxygen suppression to <10 ppb without undue nitrate formation.

2.4 N-16 MEASUREMENT

Studies to characterize N-16 behavior at Dresden were partially completed. Conclusions drawn from the full-power testing thus far are:

a. On the Dresden site, D-1 is the major and determining contributor to site boundary dose rate.

b. Currently, dose rates from the Dresden 2 main steam lines, just outside the outboard isolation valves, are 1 R/h at 15 cm from the pipe and 0.5 R/h at 1 meter from the pipe.

c. In the steam, the ratio of the concentration of N-16 (7.4 sec)/C-15 (2.5 sec)/O-19 (27 sec) was 11:5:1. Previously, the C-15 fraction was thought to be much lower.

d. The concentrations of N-16 and O-19 in the main steam just past the outboard isolation valve are 20 μCi/g and 1.7 μCi/g, respectively.

e. The N-16 in the main steam is 2.6% unionized, 77% cationic, and 21% anionic. The O-19 form is neutral and probably O_2 or H_2O.

2.5 N-16 MODELING

The data on N-16 behavior are for the no-additive, neutral flow sheet and must be related to the additive flow sheets through the use of a transport model.

Such a model considering source terms, system transit times, and the differing volatilities of the various chemical species encountered is being developed.

2.6 OFF-GAS IMPURITIES

Preparations have been made to measure trace impurity levels in reactor offgas. An existing off-gas test facility at Nine Mile Point (NMP) Nuclear Power Station will be used. Components to be investigated are Kr, Xe, CH_4, higher hydrocarbons, CO_2, CO, NO_2, NO and O_3. Such trace impurity data will be especially useful if off-gas hydrogen recycle is to be considered.

2.7 LEAKAGE MONITOR

Devices with which to measure condenser cooling water leakage in high-conductivity ammonia-bearing condensate have been reviewed. An instrument sensitivity of <1 ppb is required. The evaluation of possible instruments is continuing, but currently the Orion sodium-ion monitor is the recommended device.

2.8 CONSTANT EXTENSION RATE TESTS

Preliminary tests show that the sensitivity of the constant extension rate test (CERT) for detecting stress-corrosion susceptibility of 304 stainless steel in aerated water at 288°C is improved by having circumferential notches with a 0.013 to 0.026-in.-depth in the 1/4-in.-diam tensile bar. Stress-corrosion indices based on ductility criteria [e.g., elongation, % RA (reduction in area)] obtained from the stress/strain curve mirror the microstructurally observed damage as a function of notch depth.

Future work will concentrate on determining the specimen geometry for maximum sensitivity of detection of stress-corrosion cracking in low oxygen water, before continuing on the effect of alternate water chemistry on cracking susceptibility in deoxygenated solutions.

2.9 GENERAL CORROSION TESTING

Constant load, general corrosion and crevice corrosion tests in the hydrogen additive environment are being prepared. Samples of 304, 316L, Alloy 600 and carbon steel will be included.

2.10 STRAINING ELECTRODE STUDIES

Straining electrode studies on sensitized 304 stainless steel will be run at various hydrogen potentials. The data will help relate to other electrode potential studies already done.

2.11 DEMINERALIZER PERFORMANCE

The use of the hydrogen additive flow sheet is not expected to affect the performance of the existing ion-exchange operations. If an ammonia flow sheet is used, however, a deep bed mixed-resin condensate treatment system will exhaust 150 ft^3 of cation resin per hour. For normal sized beds, as found in a BWR, one regeneration each 45 minutes is required; an impossible situation. Use of an ammonia-based cation resin solves the problem in part, but at pH > 10 and about 20 ppm ammonia, significant reductions in sodium removal efficiency and capacity are encountered.

2.12 ADDITIVE ADDITION

Hydrogen or ammonia, if chosen as the additives, would be added to the feedwater between the condensate booster pumps and the feedwater pumps. Hydrazine would be added to the final feedwater to minimize exposure and thermal decomposition at the elevated feedwater temperatures. Hydrogen and hydrazine would be metered into the stream. Ammonia addition rate would be controlled by final feedwater conductivity. Hydrogen addition equipment will merit special attention because of adverse dissolution kinetics, which may hinder complete dissolution.

2.13 HYDROGEN CONSUMPTION

Use of hydrogen additive in a 2500 MWt BWR without recycle will cost about $700/day plus a $100,000 storage facility. Hydrogen purification and recycle is possible and may be economically feasible depending on the details of four purification techniques which are being investigated. Recycle without purification (only oxygen removal in a recombiner) is also possible, if the diluent nitrogen can be tolerated. Such a recycle scheme would reduce hydrogen consumption by two-thirds with minimum capital outlay.

3. DISCUSSION

3.1 TASK A. O_2 CONTROL — ADDITIVE CONCENTRATION REQUIREMENTS (T.L. Wong, D.P. Siegwarth)

Objective This task will establish the basic primary system flow sheets for the additives being considered. Optimum additive levels must be selected to allow a reasonable operating control range, prevent excessive and wasteful use of the chemical, and yet assure that minimum concentration requirements are always met.

Literature information on the addition of hydrogen, ammonia and hydrazine to suppress oxygen formation has been used to predict mass balances for the GE BWR. In general, the results reported in the literature were not applied directly because the test equipment and conditions were significantly different from those for the BWR. The results from several different tests were used, whenever possible, to develop methods of extrapolating the test data to the BWR conditions.

3.1.1 Basis

The calculations for the BWR were based on the design parameters for the Dresden 2 Nuclear Generating Station shown in Table 3-1. The operating parameters given in this Table are based on operating data obtained at Dresden and other BWR's. The tabulated radiolytic gas production rate is an average of data obtained at many of the presently operating BWR's.[1] Experimental measurements of steam and reactor-water gas concentrations (H_2 and O_2) indicate a partition of 100 to 1. The assumption of equilibrium between the two phases (Henry's Law) would yield a higher partition coefficient. The observed lower values are probably a result of steam carry-under (CU) in the steam separators and/or non-equilibrium conditions.

The observed partition coefficient (100/1) was employed to obtain the "Core Exit Water" (water separated from the steam by the separators) concentrations reported in Table A-1 and for all the mass balance calculations in this report.

Table 3-1

CHARACTERISTICS OF DRESDEN 2 BWR

Design Parameters	
Power, MWt	2527
Steam Flow, lb/h	9.765×10^6
Feedwater Flow, lb/h	9.765×10^6
Core Exit Water Flow, lb/h	88.235×10^6
Total Core Flow, lb/h	98.0×10^6
Saturated Water in Vessel, lb	159,440
Subcooled Water in Vessel, lb	374,920
Recirculation Water, lb	41,120
Saturated Steam in Vessel, lb	18,080
Operating Parameters	
Radiolytic Gas Production, scfm*/MWt	0.041
Radiolytic Gas Flow, scfm*	104
Oxygen in Steam, lb/h	185
Hydrogen in Steam, lb/h	23
Concentrations, ppm (weight basis)	
$[O_2]$ Steam	18.9
$[H_2]$ Steam	2.4
$[O_2]$ Feedwater	0.030
$[H_2]$ Feedwater	0.003
$[O_2]$ Core Entrance	0.173
$[H_2]$ Core Entrance	0.021
$[O_2]$ Core Exit Water	0.189
$[H_2]$ Core Exit Water	0.023

*At 32°F and 14.7 psia

3.1.2 Hydrogen Addition

Ionizing radiation splits the water molecule into free radicals.

$$H_2O \xrightarrow{rad} [H]^+ + [OH]^-$$

The quantity of radicals formed depends on the amount of radiation absorbed by the water. The phenomena which have been observed in radiolytic decomposition studies are believed to result from the chemical reactions of the free radicals with themselves and other radicals, ions or molecules in solution. The recombination of the free radicals through a chain of reactions to produce the molecular products H_2 and O_2 is referred to as the "forward" reaction. When the radicals react to reform water it is called the "back" reaction. The amount or degree of water decomposition actually observed depends on the equilibrium between the forward and back reactions. This equilibrium is a function of the type of radiation, solution impurities and characteristics of the system containing the water (such as, flow, geometry, temperature, pressure, removal of gases from solution, etc.).

The G-value, i.e., the number of molecules or radicals produced per 100 eV of ionizing energy absorbed, is conventionally used in radiation chemistry literature to denote the yield of products. The experimentally observed yield of product "X," which may be the outcome of a chain of secondary reactions involving the independently produced species, will be assigned the symbol G(X) for this discussion.

The upper limit of the $G(H_2)$ for a BWR has been predicted to be approximately unity.[2,3] If the characteristics of the reactor are such that the molecular products remain in solution sufficiently long to react with the free radicals, the actual $G(H_2)$ may be less than one because of the back reaction.

Assuming that 4% of the thermal energy is deposited in the water as a fast neutron-gamma contribution, the radiolytic gas ($H_2 + O_2$) production rate for a reactor with pure water as the moderator and coolant is given by:

$$ft^3/day = 430\ G(H_2)\ \dot{Q} \qquad (3\text{-}1)$$

where $\dot{Q}$ = thermal power in megawatts (MWt). This equation was used to calculate $G(H_2)$ for the Borax III and Borax IV, EBWR, ALPR, HBWR, and the BWR. The values for the radiolytic gas production rate were determined from experimental data reported in the literature.[1-5] The results of these calculations are given in Table 3-2.

The variations in the calculated $G(H_2)$ observed for the different reactors are a manifestation of the differences in the reactor design and operating conditions. The decrease in $G(H_2)$ with increasing pressure exhibited by the EBWR and HBWR could result from a combination of several factors, such as, the change in Henry's Law constant with temperature, the decrease in void volume with pressure at a given power, and the increase in the rate of the back reaction with increasing temperature. Since all these factors are interrelated, it was not possible to develop a mechanistic prediction of the pressure effect.

Variations in $G(H_2)$ between reactors operating at the same pressure are shown in Table 3-2 also. These variations must result from differences in design and/or operating characteristics. The rated thermal power, design operating pressures, flow rates and core power densities for these reactors were obtained from the literature and are given in Table 3-3.[6-9] A comparison of $G(H_2)$ with the core coolant power density (i.e., dose rate to the water contained within the core volume) indicates that $G(H_2)$ values increase with power density.

The steady-state concentration of hydrogen in the reactor water has been observed to vary as the square root of the power density.[10] Therefore, the power density and pressure dependency of $G(H_2)$ was assumed to be of the form:

$$G(H_2) = A(Pd)^{1/2}(p)^n \qquad (3\text{-}2)$$

Table 3-2

RADIOLYSIS OF REACTOR WATER

Reactor	$G(H_2)$* Molecules/100 eV	Operating Pressure (psia)	Rated Power (MWt)
Borax III	0.2	315	15
Borax IV	0.21 to 0.25	315	20
EBWR	0.21 to 0.24	315	20
	0.20 to 0.21	415	
	0.16 to 0.18	515	
	0.15 to 0.17	615	
ALPR	0.13	315	3
HBWR	0.092	160	20
	0.079	300	
	0.072	435	
Dresden 2	0.087 - 0.188**	1015	2527

*Ranges calculated from range of data reported in literature.

**Range of experimental measurements at most of the presently operating BWR's.

Table 3-3

CHARACTERISTICS OF BOILING WATER REACTORS

Reactor	Power (MWt)	Operating Pressure (psig)	Flow Rates (lb/h)			Ratio H_2O/Fuel In-Core	Power Density	
			Steam	Core	Feed H_2O		kW/L (core)	kW/L (core coolant)
ALPR	3	300	9.02×10^3	1.173×10^6	9.02×10^3	2	-	17.5
BORAX III	15	300	3×10^4	2.51×10^5	3×10^4	2.8	27	38
BORAX IV	20*	300	7.5×10^4	4.0×10^6	7.5×10^4	1.9	36	56.5
EBWR	20	300-600	6×10^4	3.86×10^6	6×10^4	1.8*	12.6*	21
HBWR	20	150-400	9.48×10^4	1.79×10^6	9.48×10^4	26	5.1	5.4
D-2 and D-3	2527	1000	9.77×10^6	9.8×10^7	9.77×10^6	2.4	36.7	71*
Typical BWR/4	2500	1000	9.7×10^6	7.1×10^7	9.7×10^6	2.4	51	87*

*Estimated Value

where

Pd = core coolant power density, kW/l
p = absolute pressure, psia
n = exponent, non-dimensional
A = constant, consistent units

Because of the previously mentioned difficulty in predicting the operating pressure dependency and a lack of guidance in the literature, the value of n was determined empirically from the data. As shown in Figure 3-1, n = -1/2 provided a reasonable correlation.

Maintaining dissolved hydrogen in water will reduce the radiolytic decomposition of the water because the excess hydrogen enhances the back reaction. The addition of hydrogen to the cooling water of a BWR has been studied in the ALPR, Borax III, Borax IV, EBWR and HBWR. However, because of the differences between these test reactors and the BWR (as presented in Tables 3-2 and 3-3) the results may not be directly applicable to the BWR.

Hammar, et. al.,[5] have reported in detail the results of the deuterium addition studies at the HBWR. Breden[2] reports the feedwater hydrogen concentrations and the resulting oxygen concentrations in the steam for the ALPR, Borax III, Borax IV and EBWR. However, the data are insufficient to determine the actual concentrations in the reactor vessel. Therefore, the reactor flow rates reported in Table 3-3 were used in conjunction with the hydrogen addition data reported by Breden[2] and Hammer[5] to calculate the reactor water hydrogen concentration required for each reactor to maintain the oxygen concentration in the core exit water at a preselected value. Calculations were performed for oxygen concentrations of 10 and 50 ppb, since these are the concentrations of interest for the BWR. The computer program used for these computations and the details of the calculations are given in Appendix A.

The core inlet hydrogen concentration (U_{H_2}) required to maintain a fixed oxygen concentration exhibited a variation between reactors similar to that previously

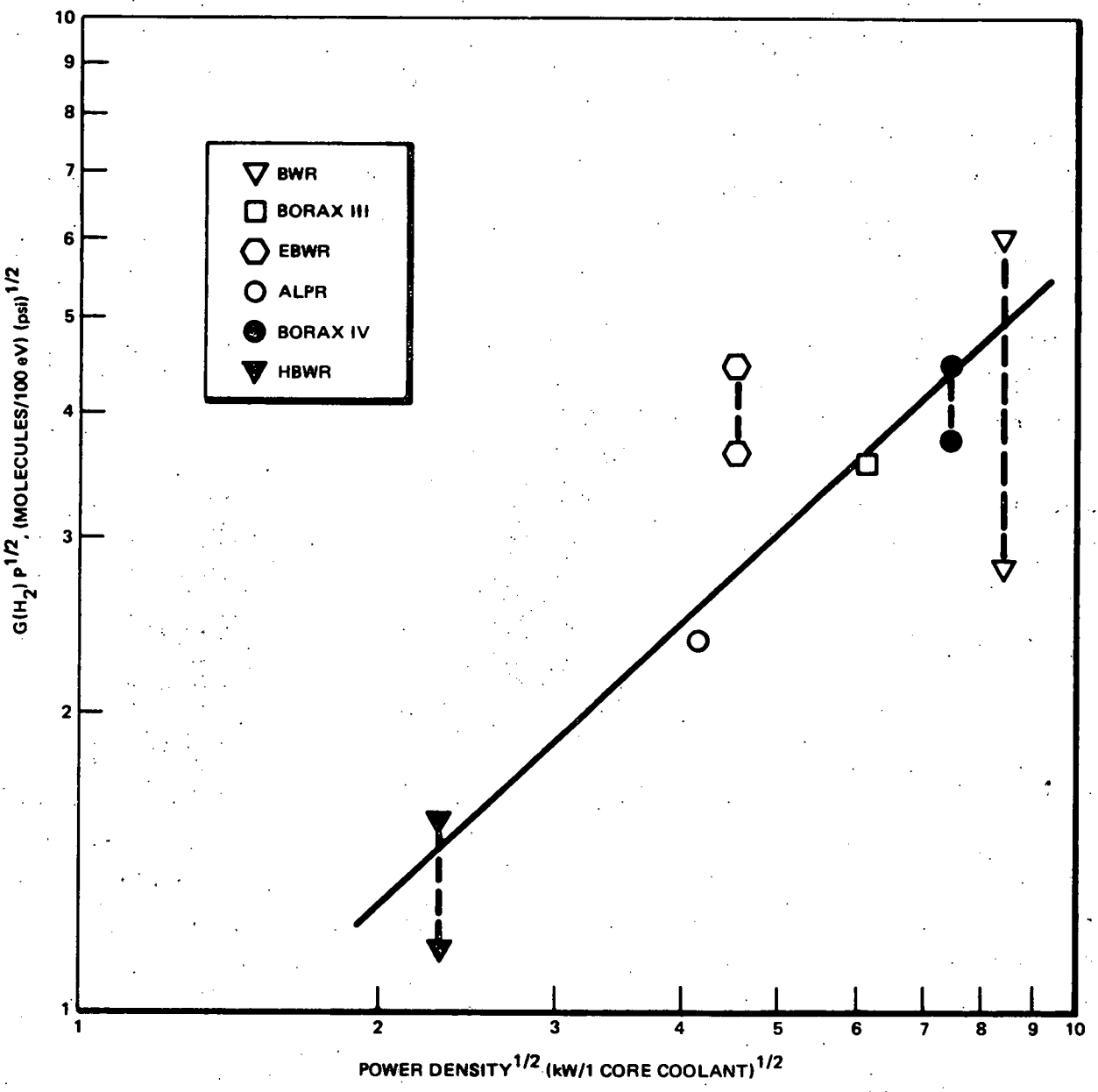

Figure 3-1. Plot of $G(H_2)p^{1/2}$ versus Power Density$^{1/2}$

discussed for $G(H_2)$ in the no-additive case. Therefore, it was assumed that the pressure and power density dependence of U_{H_2} is of the same form:

$$U_{H_2} = A' (Pd/p)^{1/2} \qquad (3\text{-}3)$$

where the symbols have the same significance as in Equation (3-2). As shown in Figure 3-2, Equation (3-3) provides a reasonable correlation of the calculated core inlet hydrogen concentrations.

A means of extrapolating the available test reactor data to the BWR is provided in Figure 3-2. For example, the square root of the power density given in Table 3-3 for Dresden is 8.43. From Figure 3-2, $U_{H_2}\sqrt{p}$ required to maintain 10 ppb oxygen in the core exit water is 7400. Therefore, the core inlet hydrogen concentration is:

$$U_{H_2} = 7400/\sqrt{1015} \approx 230 \text{ ppb.}$$

For 50 ppb oxygen Figure 3-2 gives a hydrogen concentration of 125 ppb.

The results of the mass balance calculations for Dresden using these concentrations are shown in Figures 3-3 and 3-4. The details of the calculations are given in Appendix A. The predicted hydrogen addition requirements for 10 and 50 ppb oxygen in the core exit water are 20.6 and 10.7 lb/h, respectively.

3.1.3 Ammonia Addition

Experiments in operating reactors and reactor test loops have shown that the addition of ammonia to the cooling water of a reactor will reduce the water oxygen concentration.[5,11] The possible sequence of reactions suggested by Anderson in the Appendix of Reference 5 includes the following:

$$NH_3 + OH \rightarrow NH_2 + H_2O$$

$$NH_2 + NH_2 \rightarrow NH_3 + NH$$

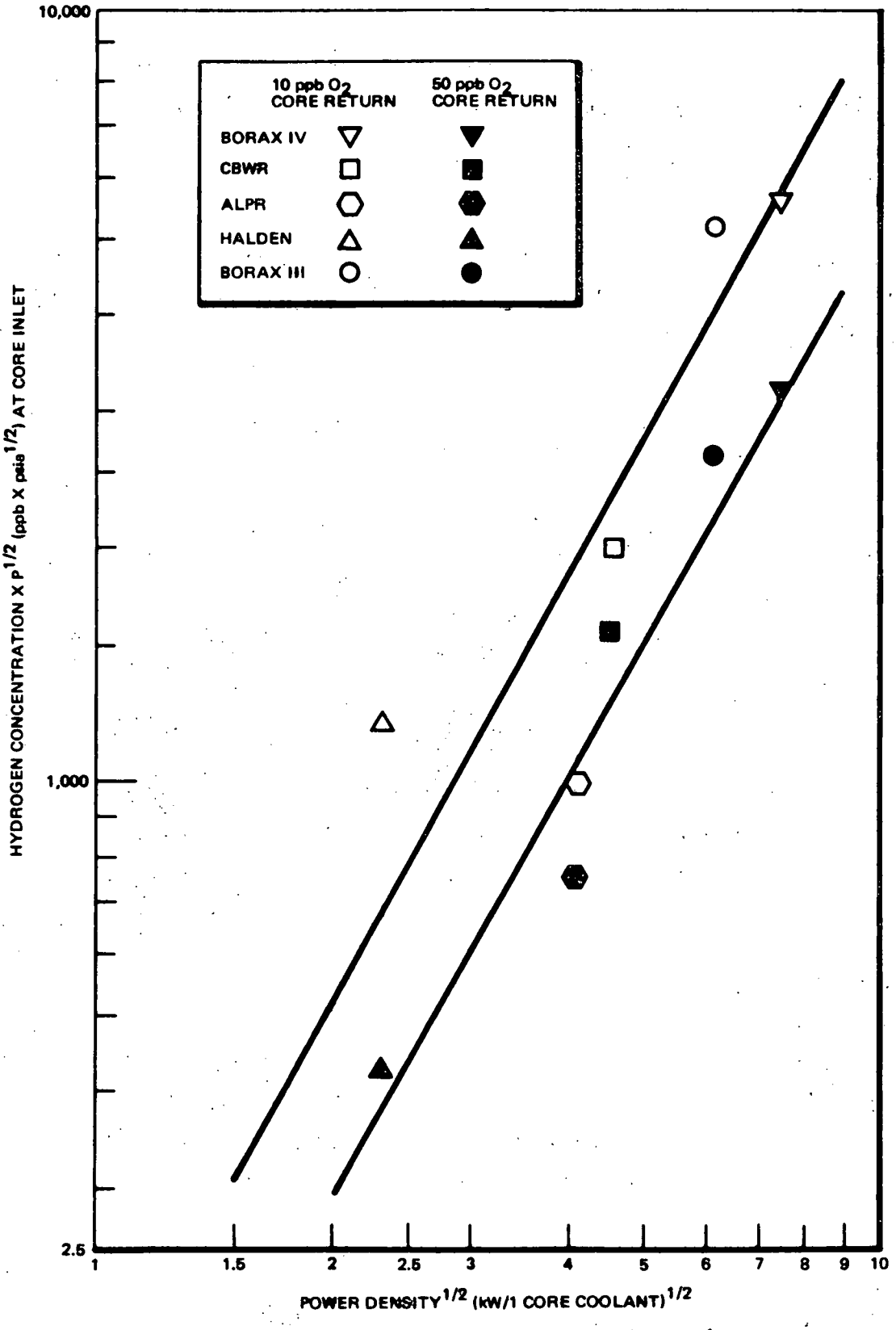

Figure 3-2. Plot of $[H_2]P^{1/2}$ versus $[\text{Power Density}]^{1/2}$

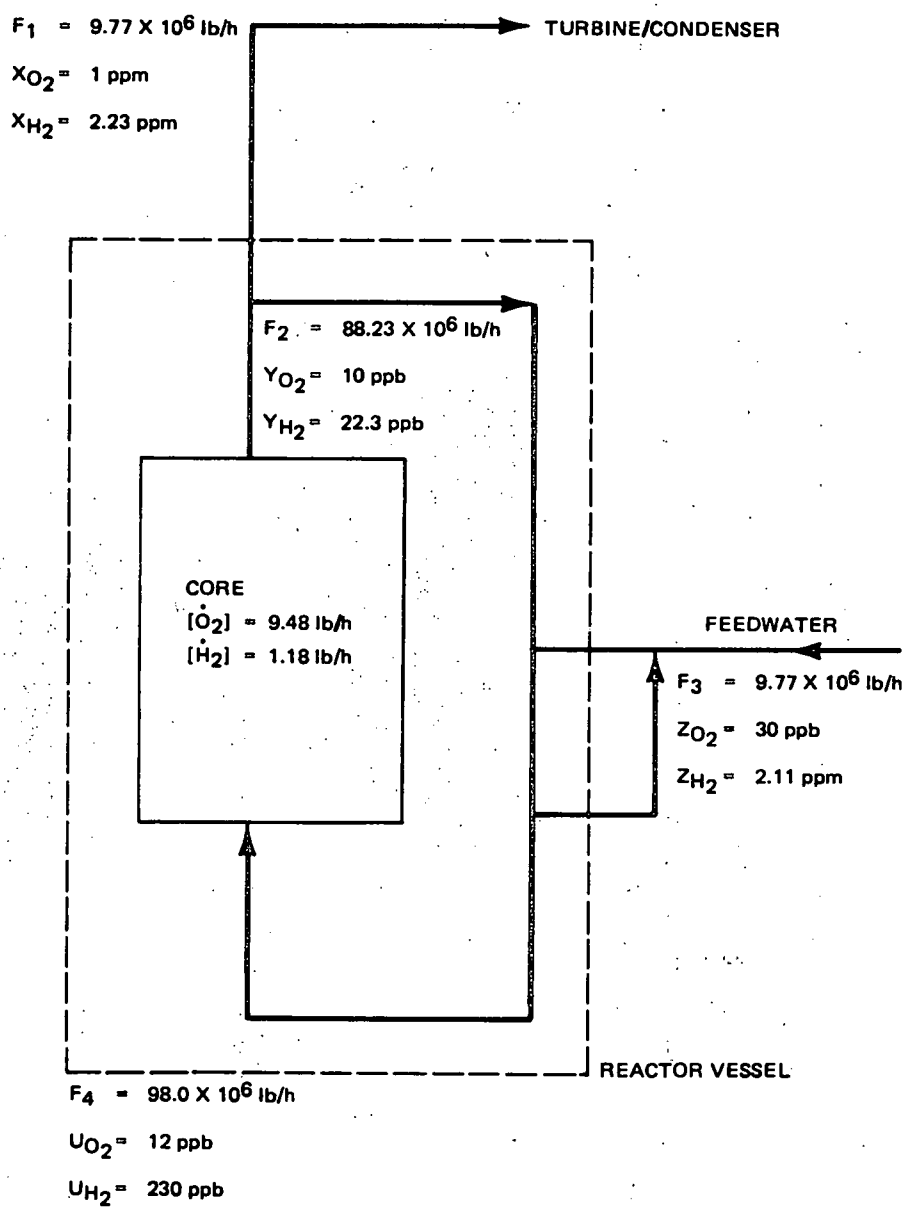

Figure 3-3. Hydrogen Addition for 10 ppb Oxygen in Core Exit Water

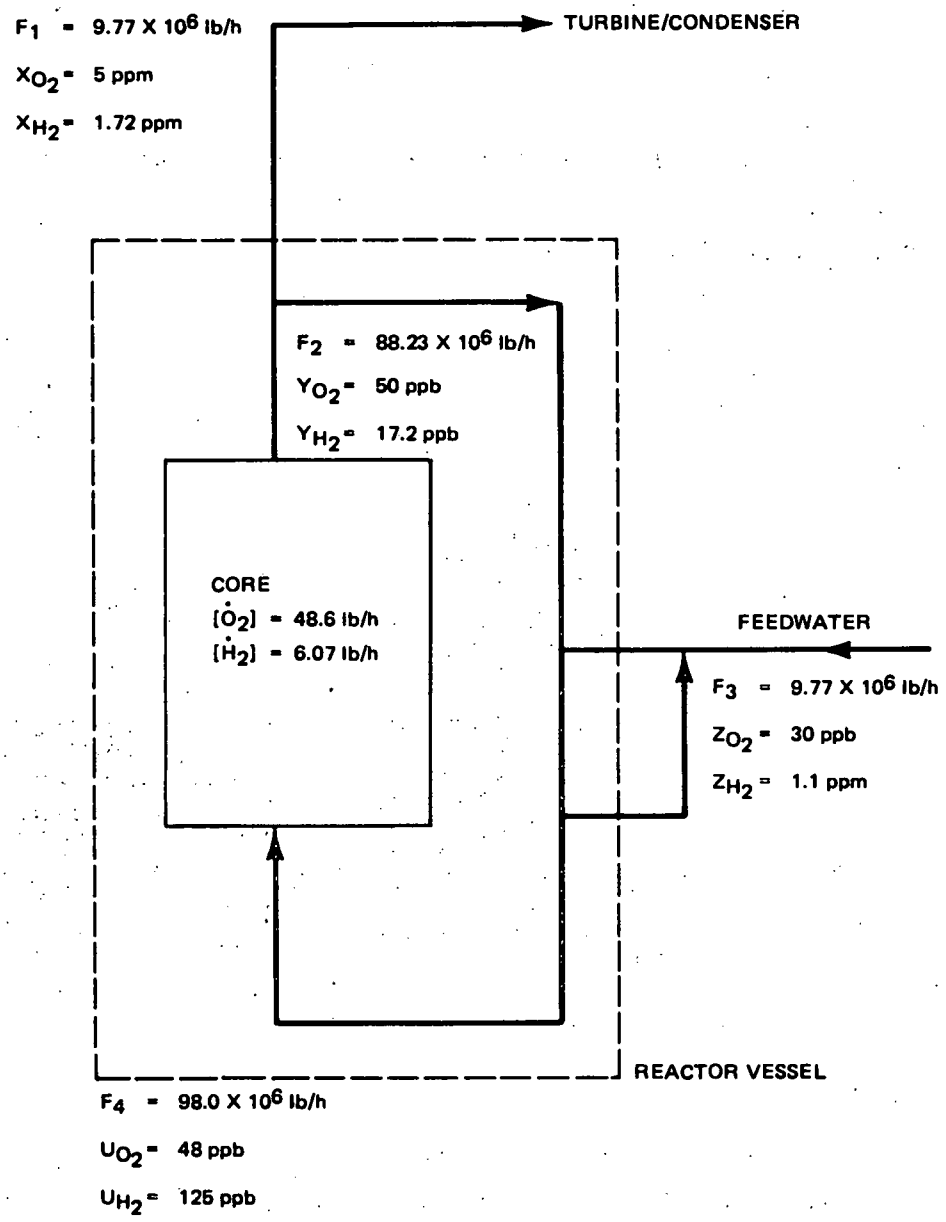

Figure 3-4. Hydrogen Addition For 50 ppb Oxygen in Core Exit Water

$$NH + NH \rightarrow N_2 + H_2$$

Since the OH radical is an intermediate in the formation of molecular oxygen, the oxygen concentration in solution is reduced.

Under conditions where some oxygen remains in solution, the decomposition of ammonia can produce nitrite and nitrate ions by the following reactions:[5]

$$NH_2 + O_2 \rightarrow NH_2O_2$$

$$NH_2O_2 + HO_2 \rightarrow HNO_2 + H_2O_2$$

$$HNO_2 + OH \rightarrow NO_2 + H_2O$$

$$2NO_2 + H_2O \rightarrow HNO_3 + HNO_2$$

The literature data indicate that conditions can be maintained in a BWR to prevent the production of these undesirable by-products. Hammar, et. al.,[5] found that a deuterium concentration in the moderator of >50 ppb was sufficient to prevent nitrate formation.[12] LeSurf and Allison recommend an ammonia concentration in the core exit water of >5 ppm to prevent nitrate formation.[11]

Laboratory tests at Halden indicated that the ammonia radiolytic decomposition rate was proportional to the ammonia concentration and reactor power, and inversely proportional to the deuterium concentration in the moderator.[5] As a result, the HBWR experimental data were correlated with the equation:

$$D = k \dot{Q} [ND_3]_{mod}/[D_2]_{mod} \qquad (3\text{-}4)$$

where

k = Proportionality constant

D = Total decomposition rate, gm/h

$\dot{Q}$ = Reactor Power, MWt

$[ND_3]_{mod}$ = Concentration of ND_3 in the moderator, mg/kg

$[D_2]_{mod}$ = Concentration of deuterium in the moderator [ml (STP/kg].

The proportionality constant (k) calculated from the HBWR September 1964 data (Anderson indicates in Appendix C of Reference 5 that the September data were best) is 8.2.

This equation was used to calculate the rate of ammonia addition required for Dresden 2 to maintain the ammonia concentration in the core exit water at 10 ppm. The nominal value of 10 ppm was chosen to allow operational variations about the nominal value without going below the recommended minimum value of 5 ppm. The results of the calculation are summarized in Figure 3-5. The computer program and calculational details are given in Appendix A. The calculation is based on the assumption that the loss of ammonia from the system is due only to radiolytic decomposition. That is, the ammonia volatilized and leaving the vessel with the steam is recovered in the turbine condenser and steam jet air ejector (SJAE) condensers and thus is recycled back to the reactor.

The calculation predicts that 706 lb/h of ammonia would be required to compensate for the radiolytic decomposition. However, it is not completely obvious that this relation derived from the HBWR experimental data can be directly used to predict ammonia decomposition in the BWR because of the previously discussed differences between the HBWR and BWR's. Therefore, some additional method of predicting the BWR requirements would be invaluable.

The reactor loop test data reported by LeSurf and Allison[11] were used to successfully predict the ammonia radiolytic decomposition rate for the Gentilly reactor (difference between predicted and experimental value approximately 20%). The reactor loop test data for subcooled water and fog (steam-water mixture) coolants reported in Figures 2 and 4 of Reference 11 also predicted the results for boiling tests in the NRX loops within ±15%. Using the core inlet ammonia and hydrogen concentrations given in Figure 3-5 the decomposition rate of ammonia in the subcooled water obtained from Reference 11 is 3.1 mg/wh (watt-hour) and ∿9.5 mg/wh for the fog coolant. The energy absorbed by the steam-water mixture in the channels of the BWR is approximately 2.3% of the thermal power, and the energy absorbed by water outside the channels is approximately 1.7% of the thermal power.[13]

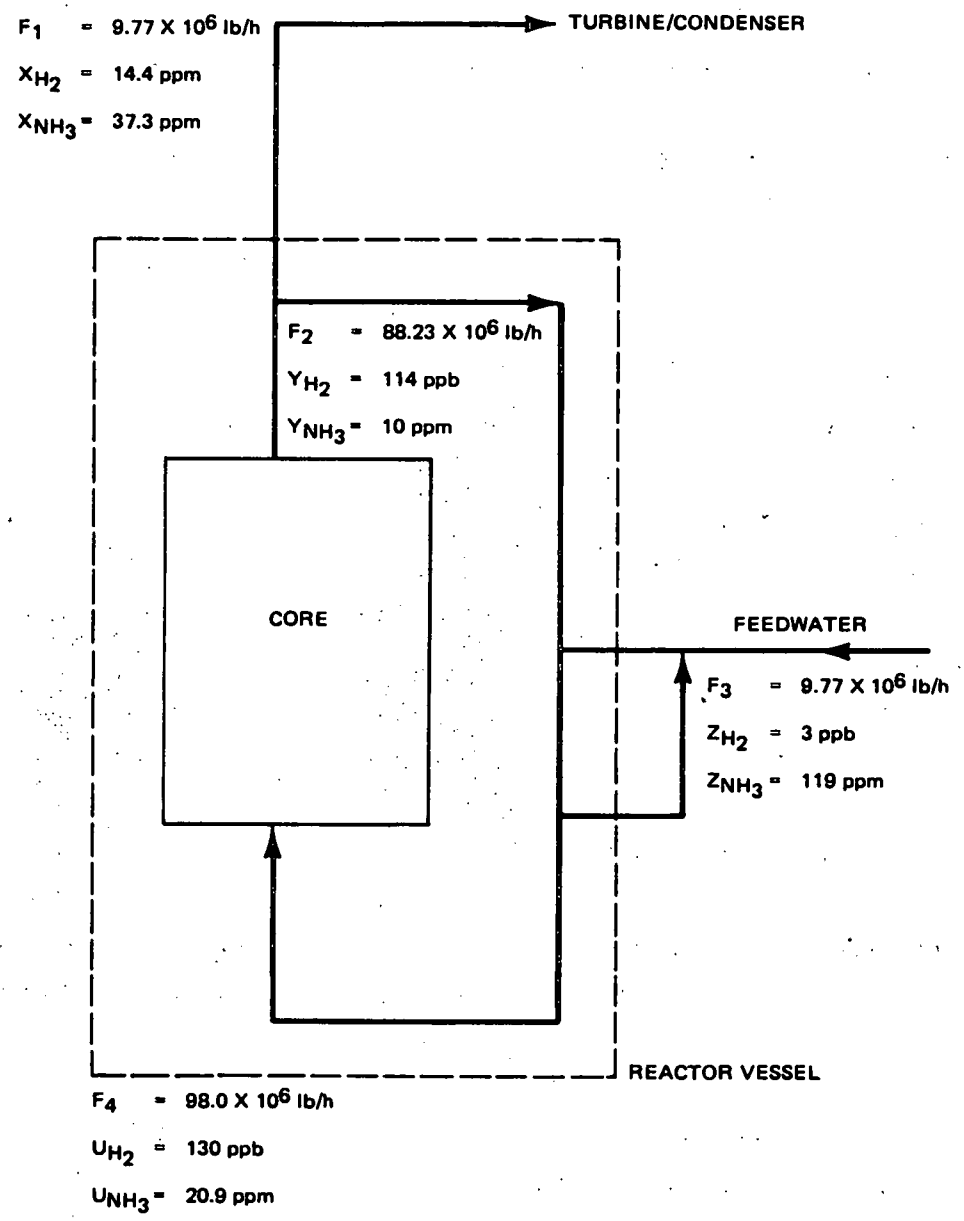

Figure 3-5. Ammonia Addition for 10 ppm Ammonia in Core Exit Water

The assumption that boiling starts, on the average, about one-third the distance from the bottom of the channels leads to:

Energy absorbed in fog region = (0.67) (0.023) MWt.

Energy absorbed in water = [(0.33) (0.023) + 0.017] MWt.

The ammonia radiolytic decomposition rate for Dresden 2 is then:

$$D = \frac{[(0.0154)\ (9.5) + (0.0246)\ (3.1)]\ 2527 \times 10^6}{454000} = 1237 \text{ lb/hr}$$

Although there is a considerable difference between the two estimated ammonia decomposition rates (706 and 1237 lb/h), the values are in reasonable agreement considering the assumptions made in applying the reported data to the BWR. Some additional information on ammonia has been received recently and, when analyzed, may shed more light on the problem. Based on the present calculations it is concluded that the ammonia make-up requirement for a 2500 MWt BWR is on the order of 1000 lb/h.

3.1.4 Hydrazine Addition

Hydrazine has the potential of providing oxygen control in the reactor water by the following two mechanisms: (1) hydrogen produced by hydrazine decomposition suppresses the radiolytic decomposition of water; and (2) hydrazine acts as an oxygen scavenger by chemically reacting with oxygen to form nitrogen and water.

The major consideration for determining the quantity of hydrazine required to maintain a low oxygen concentration in the reactor water is the amount of hydrazine decomposed in the reactor environment. Hydrazine decomposition in the reactor occurs radiolytically and thermally. The radiolytic decomposition of hydrazine is governed by the following reaction

$$\alpha N_2H_4 \xrightarrow{\text{radiation}} \alpha NH_3 + \frac{\alpha}{2} H_2 + \frac{\alpha}{2} N_2$$

The reported experimental data show that the G value (hydrazine molecules decomposed per 100 eV of energy absorbed) increases with increasing hydrazine concentrations.[14,15]

An evaluation of the reported results shows that a correlation of the data on a log-log plot of the G-values versus hydrazine concentration is a straight line (as shown in Figure 3-6). Therefore, the relationship between G value and concentration can be expressed as:

$$G(N_2H_4) = C^{m}_{N_2H_4} \tag{3-5}$$

where

$C_{N_2H_4}$ = concentration of hydrazine (ppm)

m = 0.26 (from slope in Figure 3-6)

In addition to radiolytic decomposition, hydrazine also decomposes thermally. The thermal decomposition of hydrazine is a first-order reaction expressed by the following equation:

$$\frac{dC_{N_2H_4}}{dt} = -kC_{N_2H_4} \tag{3-6}$$

where

k = reaction rate constant ($second^{-1}$)

t = reaction time (second)

Literature values for the reaction rate constant are shown in Figure 3-7.[16] This figure shows that the correlation between the reaction rate constant and temperature is given by the Arrhenius equation:

$$k = k_o e^{-E/RT} \tag{3-7}$$

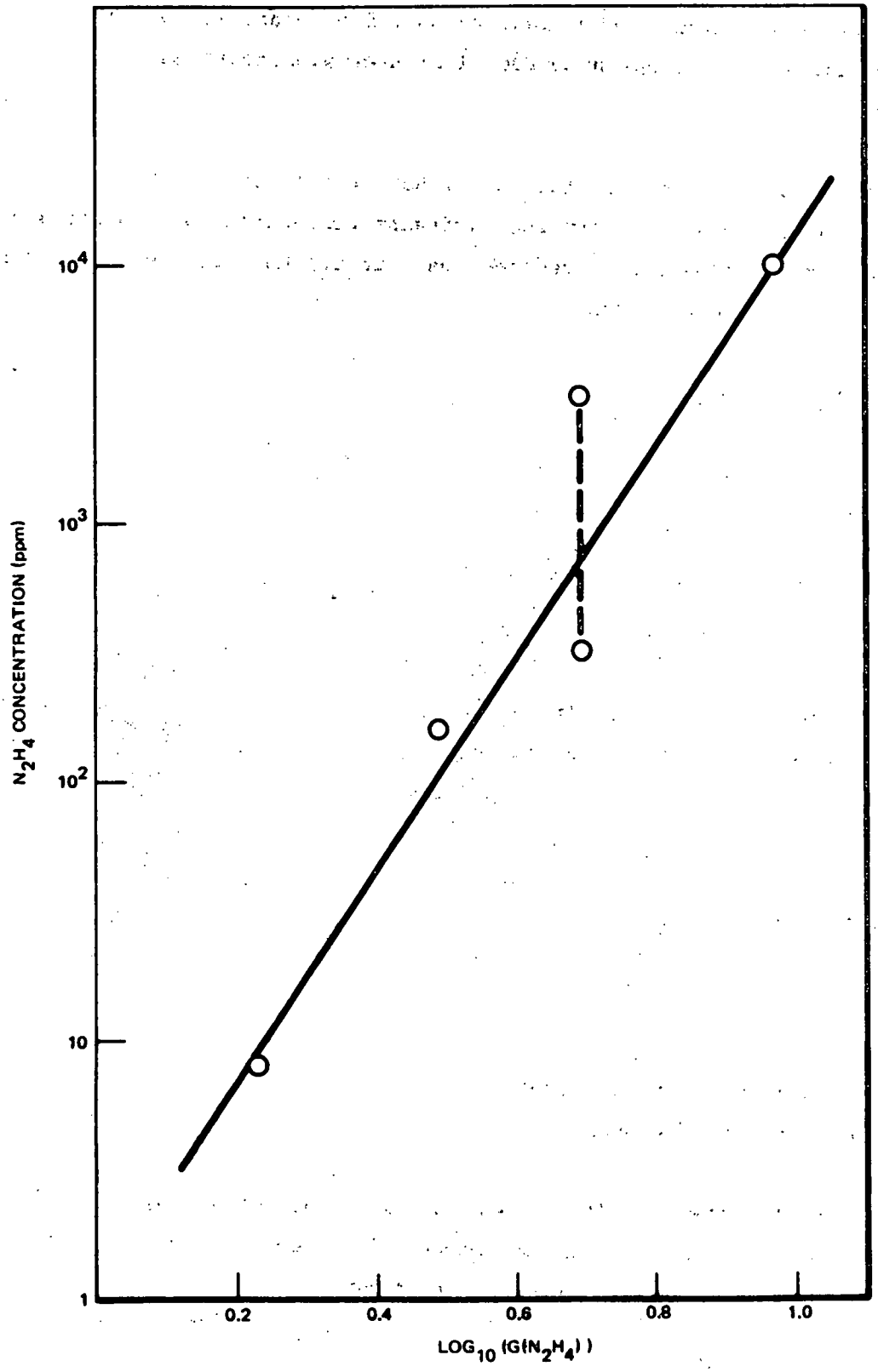

Figure 3-6. Plot of (Log_{10}) G-Values versus Hydrazine Concentration

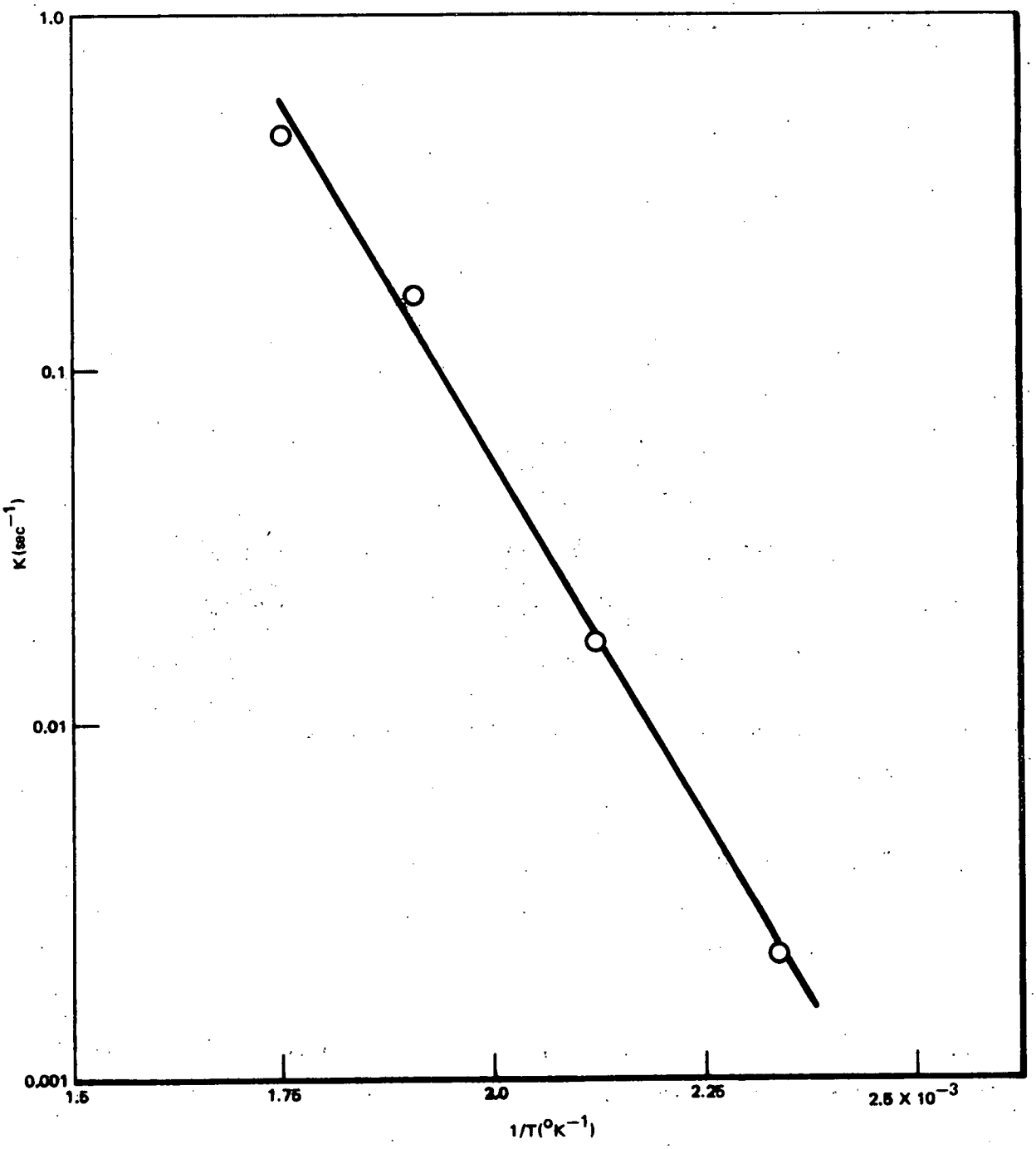

Figure 3-7. Reaction Rate Constant as a Function of Temperatures For Hydrazine Decomposition

In calculating the hydrazine addition requirements, the following decomposition model was used. The mass balance for a differential element of reactor water is

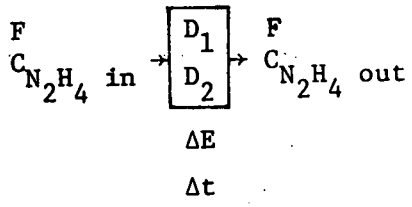

$$FC_{N_2H_4\ in} - FC_{N_2H_4\ out} = D_1\ \Delta E + D_2\ \Delta t$$

where

F = flow rate (lb/h)

$C_{N_2H_4}$ = concentration of hydrazine (ppm)

D_1 = radiolytic decomposition rate ($lb_{N_2H_4}$)/h, MWt

D_2 = thermal decomposition rate $lb_{N_2H_4}/h^2$

ΔE = incremental energy absorbed by the water molecules (MWt)

Δt = incremental residence time for thermal decomposition (sec)

The radiolytic and thermal decomposition rates based on the previously discussed experimental data are:

$$D_1 = A_1\ G\ (N_2H_4) \equiv A_1 C^m_{N_2H_4}$$

$$D_2 = FkC_{N_2H_4}$$

where the terms are those defined previously and A_1 is a constant for obtaining the correct units for D_1. Therefore, the hydrazine mass balance can be expressed as

$$FC_{N_2H_4\ in} - FC_{N_2H_4\ out} = A_1 C^m_{N_2H_4}\ \Delta E + FkC_{N_2H_4}\ \Delta t$$

If ΔE and Δt are assumed to be independent of direction, these terms can be expressed by a common space unit ($\Delta \ell$) with the following relationships

$$B_1 \Delta \ell = \Delta E$$

$$B_2 \Delta \ell = \Delta t$$

The mass balance for hydrazine can be shown in a differential form as:

$$\frac{-dC_{N_2H_4}}{d\ell} = \frac{A_1 B_1 C^m_{N_2H_4} + kB_2 C_{N_2H_4}}{F} \qquad (3\text{-}8)$$

Since a closed form solution does not exist for all values of m, an approximate solution for the above differential equation was obtained by numerical integration.

Two cases were considered in determining the quantity of hydrazine required for oxygen control in the reactor water. In the first case, calculations were made to determine the amount of hydrazine required to maintain a few ppb hydrazine in the core exit water. In this calculation, the suppression of the radiolysis of water by the hydrazine decomposition products (ammonia and hydrogen) was not considered. The calculated results are summarized in Figure 3-8 for the assumptions that radiolytic decomposition results from 100 MW (4% of 2500 MWt) absorbed by the water and the total residence time is 20 seconds for thermal decomposition.[3,17] The other parameters and the computer program used for the calculation are presented in Appendix A. The calculated results show that a hydrazine addition rate of ∿200,000 lb/h is required to obtain 8 ppb hydrazine in the core exit flow. The extremely high addition rate is attributed to the high thermal and radiolytic decomposition rates for hydrazine in the BWR environment.

The calculations for the second case take into consideration the fact that the hydrazine decomposition products (ammonia and hydrogen) suppress the oxygen concentration by the mechanism discussed in Section 3.1.3. The calculated results as shown in Figure 3-9 are based on the following assumptions: (1) hydrazine

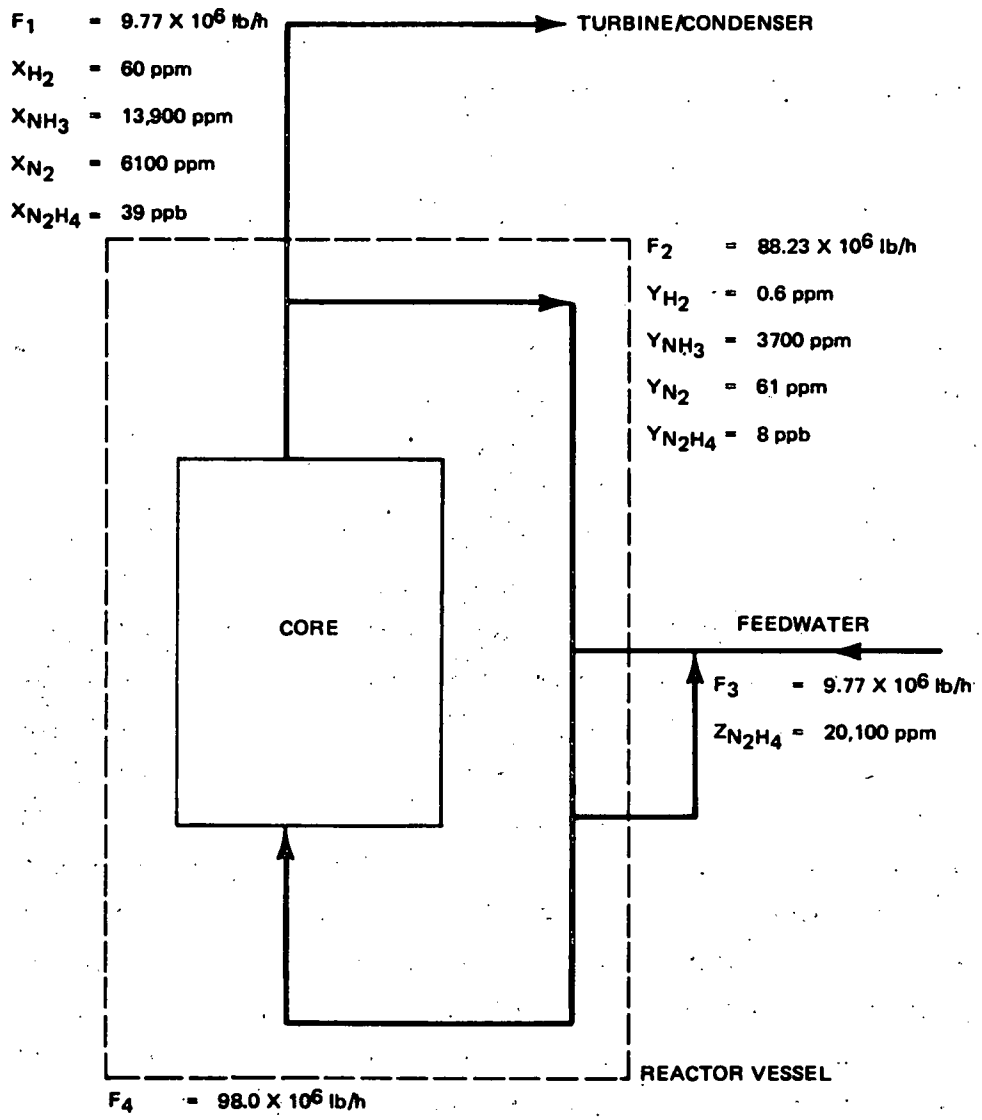

Figure 3-8. Hydrazine Addition - Hydrazine Controlling

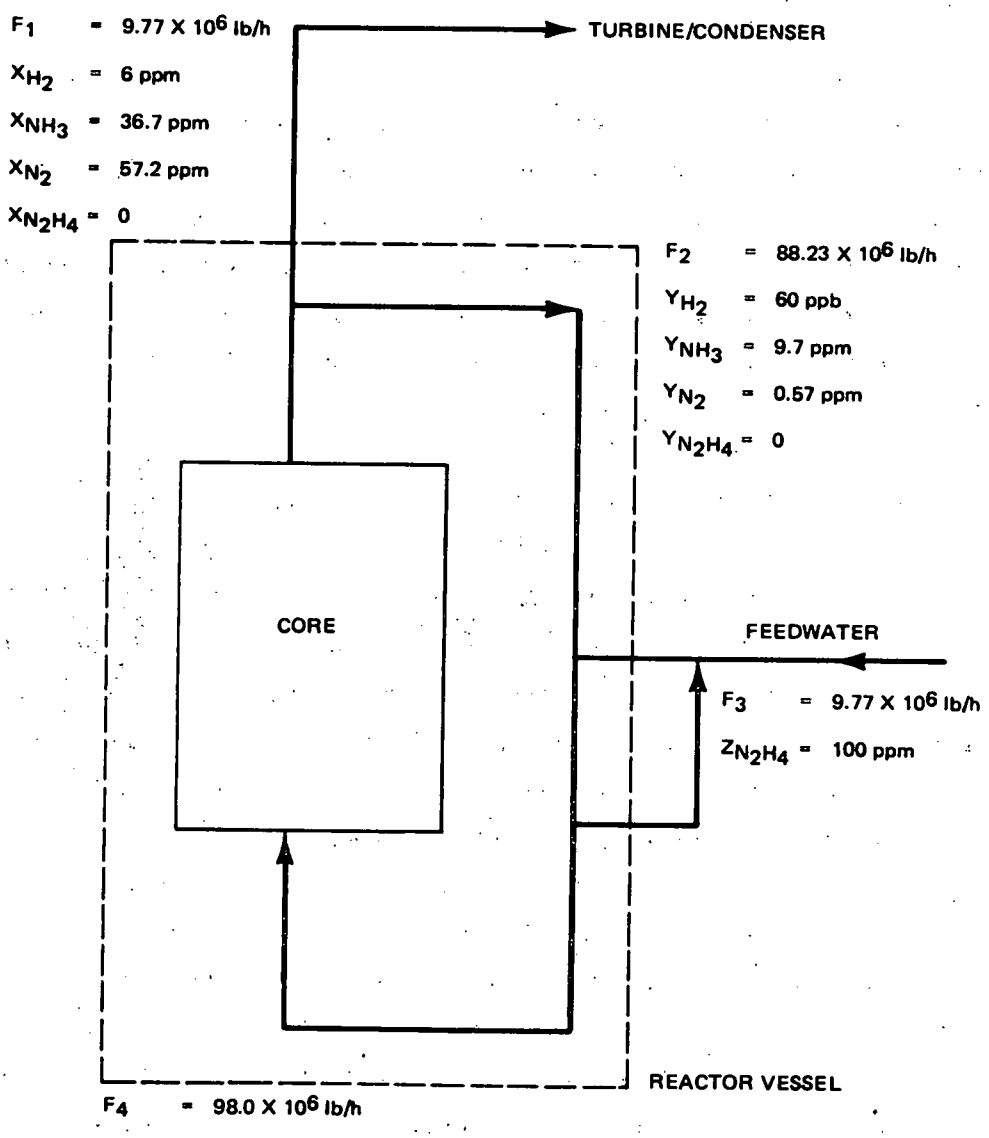

Figure 3-9. Hydrazine Addition - Ammonia Controlling

decomposes thermally and radiolytically by the reactions previously discussed; (2) the ammonia formed by the decomposition of hydrazine decomposes radiolytically and the rate of decomposition is governed by

$$\frac{-dC_{NH_3}}{dt} = \frac{k\dot{Q}C_{NH_3}}{C_{H_2}}$$

and (3) sufficient hydrazine is added to the feedwater to maintain 10 ppm ammonia in the core exit flow (the 10-ppm ammonia concentration is sufficient to suppress the radiolysis of water and prevent the formation of nitrate). The calculated results based on these assumptions show that a hydrazine addition rate of 977 lb/h would be required to maintain 10 ppm ammonia in the core exit water based on a total energy absorbed of 100 MWt and a total residence time of 20 seconds.

3.2 TASK B-1. N-16 DOSE RATE (G.F. Palino, H.R. Helmholz)

Objective. The primary source of radioactivity in the steam from a BWR is N-16 from the O-16 (n,p) reaction. The N-16 is formed in the water phase within the reactor core and then partitioned between the reactor water and steam during the phase separation. With standard BWR water chemistry, the bulk of the N-16 formed is quickly converted to relatively non-volatile anionic species, primarily NO_2^- or NO_3^-. Only a small amount of the N-16 formed in the core goes into the steam phase. As the oxidizing potential of the coolant is reduced by oxygen suppression additives, the proportion of the N-16 converted to relatively volatile, cationic (NH_4^+) species markedly increases and the fraction released to the steam rises commensurately. Measurements at EBWR[18] showed a factor of 10 increase in steam radiation level. All three potential additives, i.e., H_2, NH_3, and N_2H_4, appear to act similarly in increasing the N-16 activity in the steam, but the exact relationships need to be verified quantitatively so that the impact on turbine building shielding and/or operator-environment dose rates can be evaluated.

3.2.1 Measurement Program

The assessment of the impact of addition of chemical additives to suppress oxygen production in the BWR primary system demands reasonable estimates of the current non-additive BWR N-16/C-15 production rates and steam carryover, and of the primary system radiation levels. Consequently, base line studies were performed in January and February 1978 at Dresden 2 to obtain much of this required base line data.

Specifications for the proposed site measurement program were prepared in December 1977.[18] In response to these specifications, a detailed test procedure was prepared.[19] It underwent internal design review and with only minor modifications to the procedure, testing was initiated at Dresden 2. The reduction of the data taken during this study is near completion and some of these data have been summarized in internal General Electric documents, ATRs (Apparent Test Results).[20] The current status of the measurement program is presented in Table 3-4.

Present plans are to return to the Dresden site to install radiation monitors in Dresden 3 and to perform follow-up chemical measurements on both Dresden 2 and Dresden 3. Procedures for the installation of the recording radiation instrumentation have been written[21] and installation work arrangements have been made.

Excerpts from the preliminary test reports and other data packages are presented below. These results appear in a somewhat fragmented form since data reduction is not complete.

3.2.2 Dose Rate Measurements

3.2.2.1 Environmental Radiation Levels

The HPIC (high pressure ion chamber) was set up in a trailer south of the site administration building within the line of sight of both the Dresden 2 and

Table 3-4

STATUS OF D-2/D-3 N-16/N-13 MEASUREMENT PROGRAM

	Completed	Partial Completion	Necessary to Perform	Not Possible	Comments
A. REACTOR WATER					
N-16 Total				X	Sampling system delays were too long
Species (Charge)				X	
N-13 Total	X				
Species (Charge)		X			
Species (Chemical)		X			
Sample Line Delays					
(Recirc.)	X				
(CU Inlet)	X				
B. STEAM					
N-16 Total	X				
Species (Charge)	X				
N-13 Total	X				
Species (Charge)		X			
Species (Chemical)			X		
C-15 Total	X				
Sample Line Delays	X				
C. OFFGAS					
N-16 Total	X				
N-13 Total	X				
Species (Chemical)		X			
C-15 Total	X				Not observed at recombiner outlet.
F-18 Total	X				
Iodine Chemical Species			X		Considerable moisture in the sample line prevented this measurement.
Sample Line Delays	X				Not for recombiner sample line.
Air In-Leakage	X				
D. CONDENSATE					
N-13 Total	X				
Species (Charge)	X				
Species (Chemical)				X	Concentration below the detection limit of system.
Sample Line Delays				X	Concentration of short-lived nuclides below detection limit of system.
System Delays	X				
E. MOISTURE SEPARATOR DRAIN					
N-16 Total				X	Sampling system delays were too long.
N-13 Total	X				
Species (Charge)	X				
Species (Chemical)				X	Too low concentration.
Sample Line Delays	X				
System Delays		X			
F. GAMMA SCANS					
SJAE		X			
Steam Line	X				
CU Inlet			X		
Moisture Separator Drain					
G. DOSIMETRY					
Steam Lines	X				
Turbine Components			X		Will be performed on Dresden 3.
Environmental		X			Dresden 1 dominates the environmental dose rate.
H. PLANT OPERATION DATA	X				All units.

Dresden 1 turbine buildings. The intent of the measurement was to assess the relative contributions of Dresden 2 to the observed total environmental radiation fields (Task G.3 in Table 3-4). The HPIC data, along with the power history data for all three units, are presented in Figure 3-10.

The measurement was initiated in February when Dresden 1 was down for maintenance. Throughout the measurement period, Dresden 3 operated in a coastdown mode over the power range of 475 to 470 MWe and Dresden 2 operated near 800 MWe with the exception of an early morning surveillance power dip on February 5 and a scram on February 8. Dresden 1 returned to power on February 5 and operated in a nearly steady manner (135-145 MWe) from February 6 to the end of the measurement effort on February 9.

The data in Figure 3-10 demonstrate that Dresden 1 is the major contributor to the Dresden site environ radiation level. In general, the observed dose rate, above the level on February 4, mirrored the power history of Dresden 1. The fluctuations in dose rate between February 5 and February 9 were considerably more intense than shown in the figure and are believed to be a result of the Dresden 1 off-gas plenum changing directions with changes in wind direction.

The power dip of Dresden 2 from 810 to 705 MWe that occurred on February 5 was not seen by the HPIC. The scram of Dresden 2 that occurred on February 9 yielded a maximum Dresden 2 contribution to the environmental dose rate of 30 μR/h. The true value may be considerably less based upon a detailed analysis of the timing of the scram relative to the observed change in the HPIC response.

Since the Dresden 3 turbine building was shielded from the HPIC by the Dresden 2 and 3 reactor buildings, its contribution to the dose rate is expected to be considerably less than that of Dresden 2. Therefore, the environmental dose rate measured on February 4 must be from other local sources, and not from the Dresden 2/3 turbine building. A possible source of this radiation field is the condensate storage tanks (CST). This general background is ∿115 μR/h at the trailer (natural background is ∿10 μR/h). At 145 MWe for Dresden 1, the

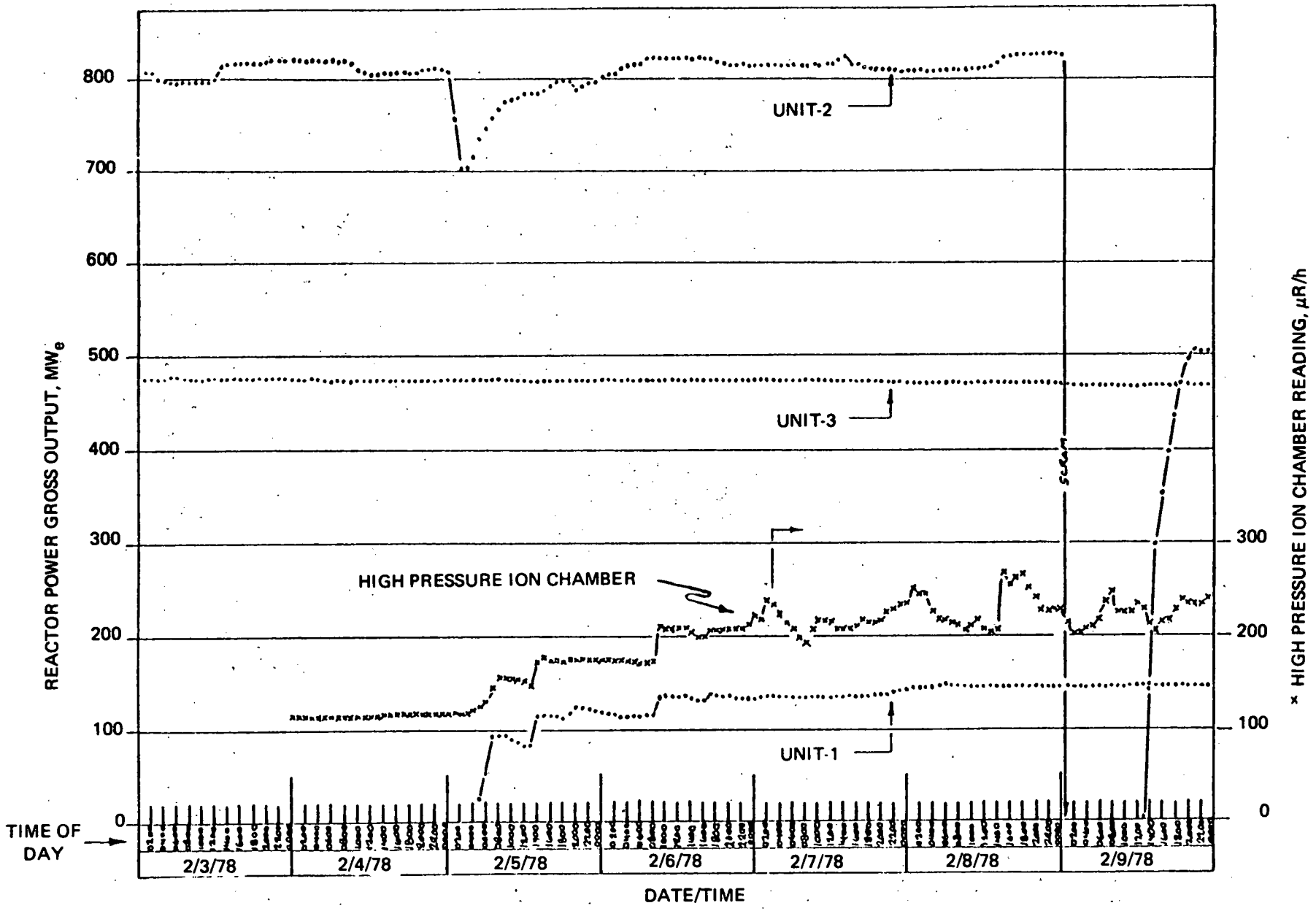

Figure 3-10. Environmental Radiation Levels - Dresden Site

radiation level has increased to ∿210 μR/h with severe fluctuations above this level due to off-gas releases. The present contributions of Dresden 2/3 to the environmental dose rates are quite low and are difficult to estimate with the presence of the other site sources (e.g., CST's Dresden 1 turbine building, and Dresden 1 off-gas releases).

3.2.2.2 Steam Line Radiation Levels

A summary of the dose rate measurements made on the "C" steam line at Dresden 2 is presented in Figure 3-11 and in Table 3-5. The LiF Thermal Luminescense Dosimeters (TLD's) were exposed in sets of two and the reported results are the average net exposure rates. The dose rate measurements were made on 8 February 1978. The TLD measurements were made between the hours of 1100 to 1200 when the reactor power was at 2459 MWt and the total steam flow was 9.52×10^6 lb/h. The survey measurements were made at ∿1630 when the reactor was at 2498 MWt and the total steam flow was 9.69×10^6 lb/h.

The calibration of the Victoreen 470A Panoramic Survey Meter (s/n 1094) was verified upon return from the Dresden site.

The LiF TLDs exposed at the site were read by the Radiation Detection Company, Sunnyvale, California. A calibration set of TLD's were exposed at the VNC Co-60 Instrument Calibration Facility to serve as calibration data for the interpretation of the field exposed TLD's.

The Co-60 source at the Vallecitos Nuclear Center (VNC) Instrument Calibration Facility was calibrated according to standard procedure NSP 5130, Rev. 0. The calibration of this source was necessary to the verification of the survey meter calibration, to the remote area monitor calibration, and to the interpretation of the TLD data.

The separation between the steam lines, outer insulation to outer insulation, is 1.02 meters. The insulation thickness is 9 cm., and the steam lines are 24-in., Schedule 80, carbon steel pipes.

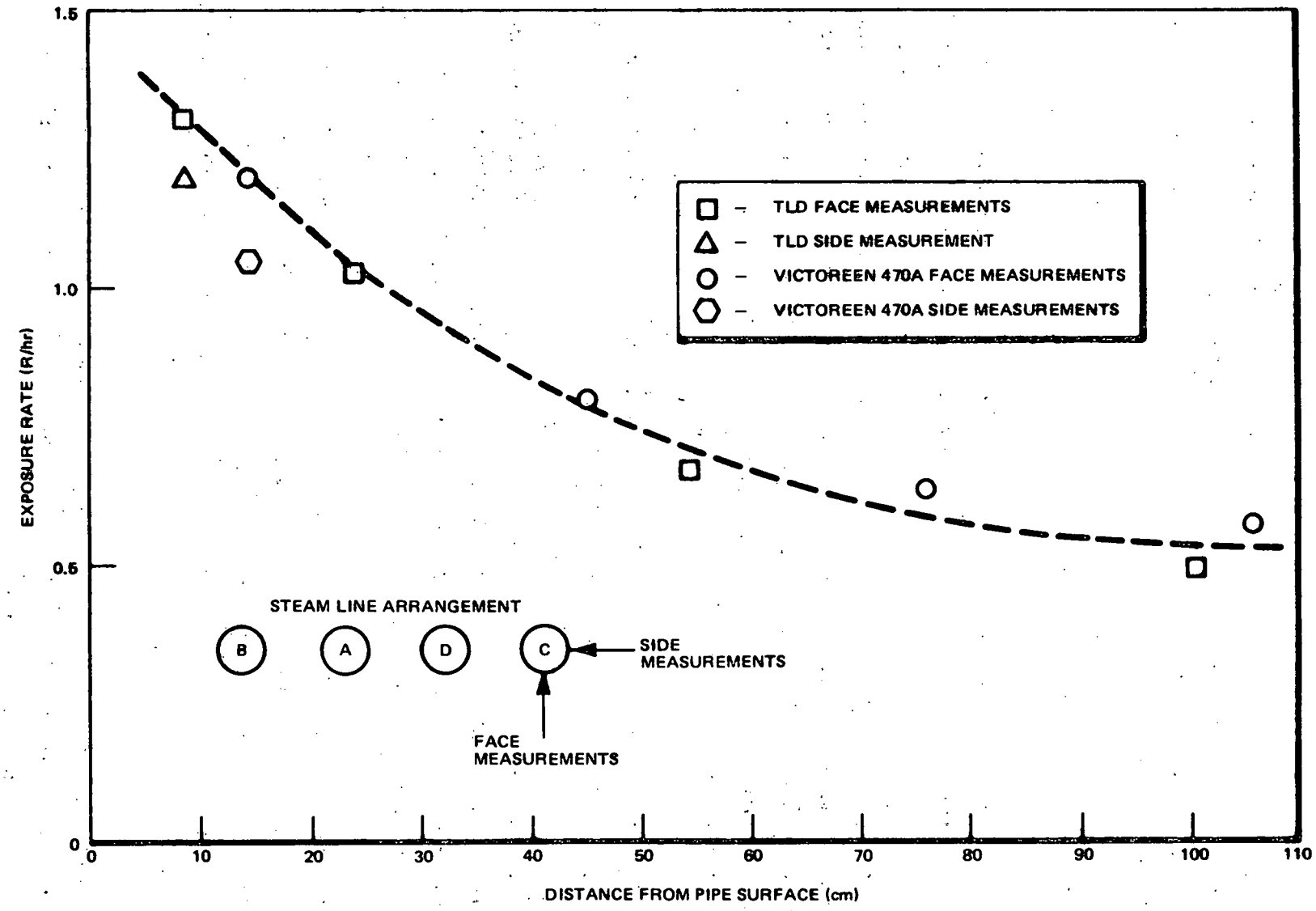

Figure 3-11. Exposure Rate versus Distance From Dresden 2 Steam Line DATE: 8 February 1978

Table 3-5

"C" STEAM LINE DOSE RATE MEASUREMENTS

Victoreen 470A Panoramic Survey Meter Measurements

Distance* (cm)	Exposure Rate (R/h)	Comments**
14.7	1.05	Side Measurement
14.7	1.20	Face Measurement
45.2	0.80	Face Measurement
75.7	0.64	Face Measurement
106.2	0.57	Face Measurement
	LiF TLD Measurements	
9.0	1.10	Side Measurement
9.0	1.31	Face Measurement
24.2	1.03	Face Measurement
54.7	0.67	Face Measurement
100.4	0.49	Face Measurement

*Distance is from outer metal surface of the "C" steam line to the effective center of the detector system.

**See Figure 3-11 for representation of comments.

3.2.3 Ge(Li) Gamma Scan of the "C" Steam Line

Gamma scans, using the General Electric Ge(Li) Pipe Gamma Scanning System, were made of the "C" steam line at the Dresden 2 reactor on February 8, 1978. The reactor power was at 2498 MWt and the total steam flow was 9.69×10^6 lb/h. The radionuclides N-16 (7.35s), C-15 (2.45s), and O-19 (26.9s) were identified in the spectra. The ratio of concentration ($\mu Ci/cm^3$) in the steam line was estimated to be 10.6:5.2:1, respectively. There is considerable uncertainty in these numbers since the spectrometer system is not calibrated for this scan geometry or gamma energy range.[22]

The significance of this observation is that C-15 is a major contributor to the steam line dose rate and that previous interpretations of steam line dose rate in terms of only N-16 contribution are in error.

The steam line dose rate measurements and the gamma scan data were submitted to General Electric Plant Engineering for evaluations in terms of absolute concentration of the dose rate contributing nuclides.

3.2.4 Radionuclide Concentrations in the Dresden 2 "B" Steam Line

3.2.4.1 Absolute Concentration of N-16 and O-19

The absolute concentration of N-16 and O-19 in the "B" steam line was measured to be 17.5 µCi/g and 1.72 µCi/g, respectively. The ratio of nuclide concentration agrees reasonably well with those derived from the gamma scan measurement.

3.2.4.2 N-16 and O-19 Species Analysis

The relative concentrations of N-16 chemical species in the steam sample stream are: 2.6% neutral, 76.7% cationic, and 20.7% anionic. The relative species concentrations were based upon the 5108 keV double escape peak which had the highest signal to background ratio. The uncertainties in the relative species concentrations are considerable as a consequence of a poor photopeak signal to

background ratio. The high background radiation field and flow instabilities of the sampling system resulted in considerable uncertainty in decay corrections.

The chemical form of O-19 is neutral, probably O_2 or H_2O.

3.2.5 Identification of a Previously Unobserved Activation Isotope in the BWR

In the analysis for N-13 and F-18 in the moisture separator drain samples, it was noted that the initial decay of the samples was considerably faster than anticipated. A detailed study of this phenomenon yielded evidence for the short-lived positron emitter O-15 (half-life 2.05 minutes). This activity is associated with a neutral chemical species in water.

This species is probably H_2O-15. The concentration of O-15 in the moisture separator drain was measured at 3.3×10^{-2} μCi/mℓ. This concentration is higher by an order of magnitude than the other positron emitters in the condensate.

3.2.6 Sample Line Delays at Dresden 2

Sample line delays were estimated from the concentration ratio of observable short-lived nuclides at two different sample flow rates. The delay volumes of some of the sampling lines are presented below:

Sample Line	Delay Volume (cm^3)
Steam line	2.75×10^2
Recirculation	1.44×10^4
CU System Inlet	9.85×10^3
Moisture Separator Drain	1.63×10^3

It was not experimentally possible to measure the delay volume of the condensate pump discharge sample line. The delay volume of the SJAE sample line was measured to be 2.36×10^3 cm^3. No estimate was possible for the recombiner outlet sample line.

3.2.7 Condensate and Clean-up System Delays

The liquid delay times in the condensate hotwell of Dresden 2 were measured using the Cs-139/Ba-139 parent-daughter pair. The basic assumption is that the source of liquid phase Cs-139 is the decay of Xe-139 in the steam, and the Ba-139 in the liquid phase results only from the decay of Cs-139. This hotwell delay, which includes sample line delay, was estimated to be 10.8 minutes. The delay volume of the reactor clean-up system from the recirculation line to the root valve of the reactor water clean-up filter inlet sample line was estimated to be $9 \times 10^{2} ft^{3}$. At a flow rate of 4.6×10^{5} lb/h, the flow time from the recirculation line to the sample root valve is about 5.7 minutes. This long delay precludes any measurement of N-16 using the pipe gamma scanning system at the exit of the heat exchangers. To analyze for N-16 on the primary water will require a sample point or gamma scanning location forward of the regenerative heat exchangers.

3.2.8 N-16/N-13/C-15 Transport Model Development

To analyze the data obtained in the radiation study at Dresden and to provide an analytical basis for projections to conditions of additive addition, a transport model of the primary system process streams and partitioning has been formulated. The reactor used in this model development is shown in Figure 3-12. To assist in the presentation of this model, the discussion is segmented into three general subjects: source terms, system delay times, and transport model development.

3.2.8.1 Source Terms

The nuclides of interest are produced in-core by neutron interaction with the coolant flowing through the core. There are two in-core pathways for coolant flow: the in-channel flow, and the leakage flow. To a first approximation, the core average neutron flux is identical in both of these flow paths.

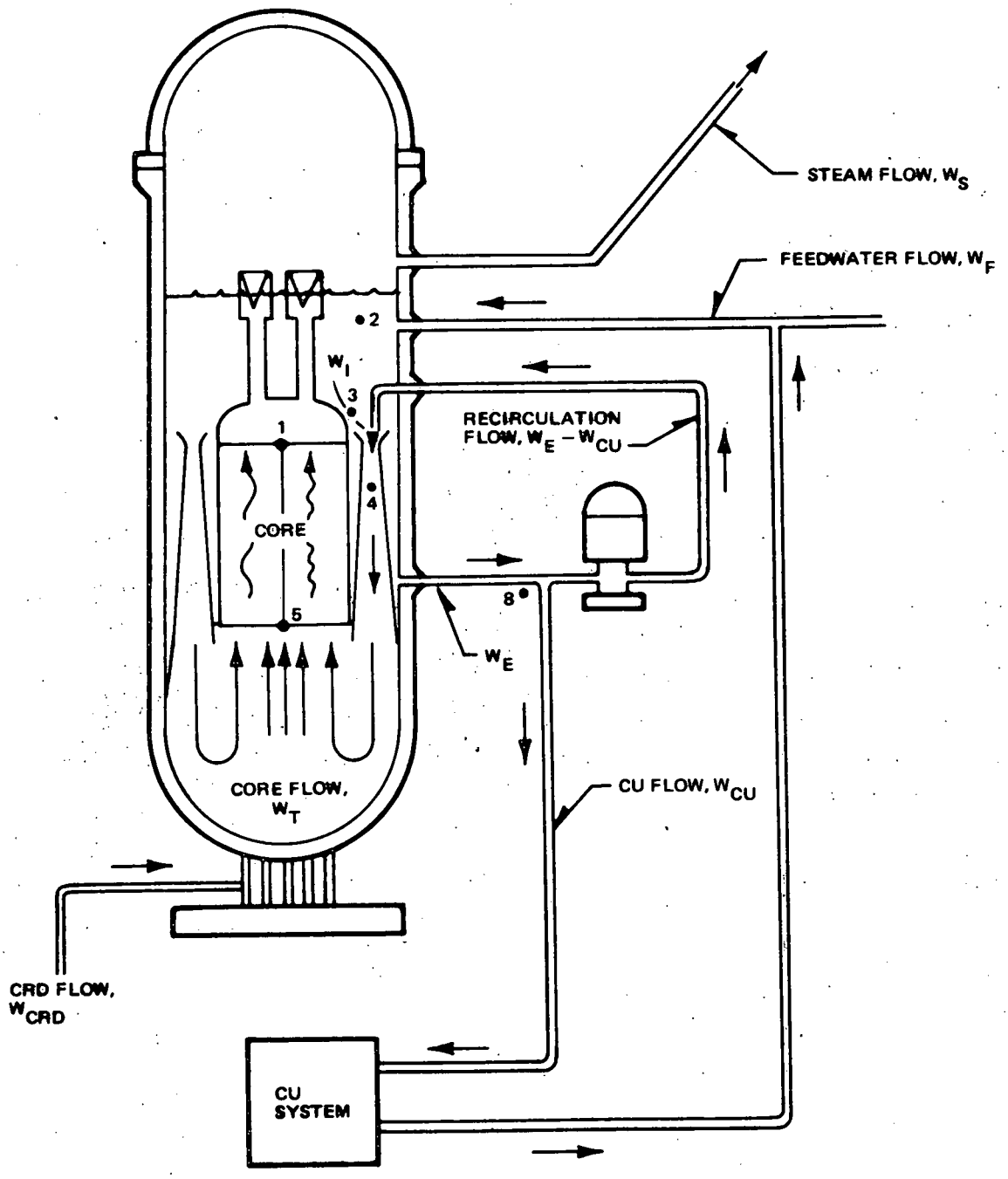

Figure 3-12. Transport Model Development

The number of atoms activated per unit time by in-channel coolant is given by:

$$R_{IC} = N_{IC} V_{IC} \sigma \phi p \frac{(1-e^{-\lambda t_{IC}})}{\lambda t_{IC}} \quad (3\text{-}9)$$

where:

R_{IC} = in-channel coolant activating production rate (atoms/sec),

N_{IC} = concentration of target atoms in the in-channel coolant (atoms/cm^3),

V_{IC} = in-channel volume (cm^3),

σ = cross section of activation (cm^2),

ϕ = neutron flux (n/cm^2-sec),

p = reactor thermal power (watts),

λ = decay constant (sec^{-1}), and

t_{IC} = time for one pass through the core in-channel (sec).

Although the in-channel coolant is made up of subcooled water, saturated water, and saturated steam, for calculational purposes, it can be assumed that the coolant is a homogeneous mixture and t_{IC} is the time for this homogeneous mixture to flow through the core.

The number of atoms activated per unit time by leakage coolant is given by:

$$R_L = N_L V_L \sigma \phi p \frac{(1 - e^{-\lambda t_L})}{\lambda t_L} \quad (3\text{-}10)$$

where

R_L = leakage coolant activity production rate (atoms/sec),

N_L = concentration of target atoms in leakage coolant (atoms/cm^3),

V_L = leakage volume (cm^3), and

t = time for one pass through the core via leakage (sec).

The number of atoms generated in-core and exiting the core per second is given by:

$$R = R_{IC} + R_L \tag{3-11}$$

where:

R = atoms per second exiting the core produced via in-channel and leakage pathways.

The concentration of radioactive atoms in the coolant exiting the core is given by:

$$A_{avg} = \frac{R\lambda}{W_T C} \tag{3-12}$$

where:

A_{avg} = average concentration of exit coolant (μCi/g),

W_T = total core flow (g/sec), and

C = conversion factor between disintegrations per second and microcuries (3.7×10^4 d/s/μCi).

$$A_{avg} = \frac{\sigma \phi P}{W_T C} \left(\frac{N_{IC} V_{IC}}{t_{IC}} (1 - e^{-\lambda t_{IC}}) + \frac{N_L V_L}{t_L} (1 - e^{-\lambda t_L}) \right) \tag{3-13}$$

Another quantity that is useful to define is the generation rate, K(μCi/sec-watt):

$$K = \frac{A_{avg} W_t}{P} = \frac{R\lambda}{PC} \tag{3-14}$$

or

$$K = \frac{\sigma \phi}{C}\left(\frac{N_{IC}V_{IC}}{t_{IC}}(1 - e^{-\lambda t_{IC}}) + \frac{N_L V_L}{t_L}(1 - e^{-\lambda t_L})\right) \quad (3\text{-}15)$$

3.2.8.2 Time Delays in the System

The delay time in any section of the reactor can be calculated using the general expression:

$$t = \frac{V \times \rho}{W} \quad (3\text{-}16)$$

where:

V = volume of the section (cm^3)

ρ = average density of the coolant in the section (g/cm^3), and

W = flow rate through the section (g/sec).

For most calculations where different phases are passing through a section, it is assumed that the mixture is homogeneous. This assumption is not strictly valid for in-channel flow or for flow from the core exit to the separator exit. In these regions, two-phase flow is known to exist.

Another concern is whether flow through a section is slug flow or whether mixing occurs in the section. The decay corrections will be slightly different for each case. For slug flow, the decay correction is $e^{-\lambda t}$; while for flow through a section where perfect mixing occurs, the decay correction is $(1 - e^{-\lambda t})/\lambda t$.

The time delays in the various sections of the reactor primary system are important since the activity that remains with the condensed phase after separation at the steam-water interface is cycled back through again and again until it has decayed to a negligible contributing level.

From inspection of Figure 3-12, it is readily apparent that there are numerous flow paths in the primary system for partitioned activity to return to the core

entrance. The fraction of activity entering the condensed phase at position 1 and surviving the tortuous transit back to that same position is given by:

$$g(t) = \left(\frac{W_I}{W_I + W_E} e^{-\lambda t_{12345}} + \frac{W_E - W_{CU}}{W_I + W_E} e^{-\lambda t_{123845}} \right) x$$

$$\left(\frac{W_L}{W_T} e^{-\lambda t_{561}} + \frac{W_{IC}}{W_T} e^{-\lambda t_{571}} \right) \left(1 - \frac{W_{CU}}{DF(W_I + W_E)} e^{-t_{2382}} \right) \quad (3\text{-}17)$$

where:

$g(t)$ = fraction of activity entering the condensed phase at 1 that survives transit through the primary system in its return to 1.

W_i = flow rates as indicated in Figure 3-10.

DF = decontamination factor for clean-up system, and

T_{ijk} = time for flow along path i, j, k.

The above development considers the alternate flow paths in the core, the clean-up systems flow path, and the clean-up systems removal efficiency. To be strictly correct in this development, one must also consider the activity returning to the vessel with the feedwater. This term is expected to be negligible and has been neglected in this treatment.

3.2.8.3 Model Development to Evaluate Fractionation Coefficient and Distribution Coefficient

The model of activation, transport, partitioning, and decay for the activation products of interest is based upon some fundamental assumptions concerning the partitioning process.

a. Model development (Model A) assuming production of a volatile component that is released to the steam and a nonvolatile component that remains in the water.

$$A_S = \frac{\beta K P}{W_S} \tag{3-18}$$

$$A_L = \frac{(1-\beta) K P}{(W_T - W_S)(1 - g(t))}$$

where:

β = fractionation coefficient (e.g., the fraction of the total activity that is produced in a single pass through the core that enters the steam phase),

A_S = steam phase concentration (μCi/g) at core exit, and

A_L = liquid phase concentration (μCi/g) at core exit.

The distribution coefficient, α, is therefore given by:

$$\alpha = \frac{A_S}{A_L} = \frac{\beta (W_T - W_S)(1 - g(t))}{(1 - \beta) W_S} \tag{3-20}$$

b. Model development (Model B) assuming production of a partially volatile species that partitions itself between the steam and liquid phases.

In this development, it was assumed that the partially volatile material that remains with the liquid can repartition itself in its next return cycle.

$$A_S = \frac{\beta K P}{W_S (1-g(t)) (1-\beta))} \tag{3-21}$$

$$A_L = \frac{(1-\beta)\ K\ P}{(W_T - W_S)\ (1-g(t)\ (1-\beta))} \qquad (3\text{-}22)$$

The distribution coefficient, α, is therefore given by:

$$\alpha = \frac{A_S}{A_L} = \frac{\beta}{(1-\beta)} \frac{W_T - W_S}{W_S} \qquad (3\text{-}23)$$

The differences between these two models are significant in light of the known nitrogen chemical species. The nitrogen species in the reactor system are a mixture of the above model situations. There are volatile species (NO,...), partially volatile species (NH_3, NH_2OH,....), and nonvolatile species (NO_3^-, NO_2^-,....). The volatile and nonvolatile species can be treated using Model A while the partially volatile species must be treated using Model B.

At this time in the development of activation gas release, it is recommended that use be made of Model A.

Application of Model A to the measurements presented in Sections B and C yielded some interesting conclusions concerning the carryover of N-16 and C-15 at Dresden-2. Using the data presented on the control room periodic log for the time period of interest and the General Electric reference drawings 718E901 and 729E493, which detail internal volumes of the reactor primary system, the following estimates of the delay times were calculated.

	Description	Time (sec)
Steam:	Core Exit to Reactor Pressure Vessel (RPV) Exit	6.83
	RPV Exit to Turbine Stop Valves	1.20

	Description		Time (sec)
Liquid:	Core Exit to Core Entrance (direct)	t_{12345}	15.9
	Core Exit to Core Entrance (via Recirc.)	t_{123845}	24.8
	Core Entrance to Core Exit (in-channel)	t_{571}	1.24
	Core Entrance to Core Exit (leakage)	t_{561}	18.9
	Clean-Up System	t_{2382}	∿450 (assumed)

The values of g(t) are calculated to be 0.1471 for N-16 and 4.86×10^{-3} for C-15. The source term, R, for N-16 has been estimated from neutron flux and cross-section data to be 0.63 μCi/sec watt.[6] The production rate for C-15 relative to that of N-16 is estimated to be 0.45 and is based upon relative fission spectra cross-sections and isotopic abundance of target nuclei.

The data from Sections B and C yield concentrations of N-16 and C-15 in the steam at the core exit (A_S) of 35 μCi/g and 70 μCi/g, respectively. Equation (3-18) predicts values for the fractionation coefficient, β, of 0.027 for N-16 and 0.12 for C-15. The liquid phase concentration at the core exit (D_L) is calculated according to Equation (3-19), to be 170 μCi/g for N-16 and 57 μCi/g for C-15. Therefore, the activity in the recirculation lines will be due only to N-16 since the delay times in the system are such to reduce the C-15 to near negligible levels.

An interesting observation that can be made from these data is that additive addition has the potential of increasing the carryover by a factor of 33 for N-16 and a factor of 8 for C-15, although the actual increase may be considerably less. Better definition of this observation awaits the dosimetry measurements on Dresden 3 and additional refined steam line measurements on Dresden 2.

3.3 TASK B-2. ADDITIVE VOLATILITY/DECOMPOSITION — OFF-GAS SYSTEM SIZING (R.J. Law, F. A. Arlt)

Objective. Each of the potential oxygen suppression additives and its volatile decomposition products will be continuously stripped into the steam phase in the reactor vessel. These volatile components are subsequently extracted from the condenser by the SJAE and, with any fission product gases present, constitute the inlet flow of the off-gas treatment system. The exact magnitude of the inlet gas flow to the off-gas for each additive must be determined. It is possible that the gas flow will be several times larger than that in the current, no-additive situation and will dictate an increase in the size of the system components and piping. In addition, the altered composition (including trace impurities) of the off-gas may alter the recombiner performance, affect the hydrogen explosion hazard, and will be of special significance if hydrogen is to be recycled as the feedwater additive.

Off-gas base line impurity studies are to be conducted to evaluate:

a. potential interactions of additives with impurities, and

b. modification requirements to proposed recovery and/or removal methods and equipment.

3.3.1 Test Facility

Impurity measurements will be conducted at the Nine Mile Point 1 (NMP-1) Nuclear Power Station, Lycoming, New York, using the off-gas sampling location presently available for the improved noble gas retention pilot plant. The sample location is downstream of the recombiner at the entrance to the 30-min. hold-up pipe.

3.3.2 Test Instrumentation

The analytical instruments for each impurity to be measured, Kr, Xe, CH_4, higher hydrocarbons, CO_2, CO, NO_2, NO and O_3 are listed in Table 3-6 with the detection limits and expected concentrations. The expected concentrations are the values

Table 3-6

OFF-GAS ANALYSIS EQUIPMENT FOR BASE LINE STUDY

Species	Technique	Equipment	Detection Limit(s) (vol ppm)	Expected Concentration (vol ppm)
Kr	Gas Chromatography[b] Mass Spectroscopy[c]	Tracor, MT150 Gas Chromatograph UTI, Q-30C Mass Spectrometer	1	1
Xe	Gas Chromatography Mass Spectroscophy		0.1	0.1 to 0.2
CH_4	Gas Chromatography		1	4
Higher Organics	Gas Chromatography		1	4
CO_2	Gas Chromatography		10	300
CO	Gas Chromatography		1	0.5
NO_2	Electrochemical Cell	Dynasciences, NX-110 Air Pollution Monitor, NO_2 Cell	0.5	?
NO	Oxidation to NO_2 then measurement with NO_2 Cell		0.5	?
O_3	Ultraviolet Absorption	Dasibi 8000 Ozone Monitor	0.1	0.1 to 0.2

[a] GE study at KRB

[b] Primary measurement

[c] Secondary or backup

previously obtained at KRB.[23] The detection limits listed for each instrument are distinct, measureable quantities. If lower concentrations are detected, they will be reported as estimated values. The primary instrument for measuring the impurities Kr, Xe, hydrocarbons, CO and CO_2, will be a modified Tracor Model MT-150 Gas Chromatograph. A UTI Model Q-30C Mass Spectrometer will be used as a secondary or back-up instrument. Improvements have been made to the chromatograph equipment and procedures for analyses of Kr and CH_4 to increase the sensitivity and ease of operation. A schematic of the modified chromatograph flow system is in Figure 3-13. Typical outputs for CH_4 and Kr are shown in Figures 3-14 and 3-15, respectively. It is anticipated that similar improvements will be accomplished for the other impurity measurements.

Measurements for the oxides of nitrogen will be made with a Dynascience Air Pollution Monitor using only the NO_2 cell. Once the NO_2 concentration has been determined, a chromium trioxide packed oxidizing column will be used to convert the NO to the NO_2. The NO concentration will be determined from the difference in the NO_2 concentrations measured, with and without the chromium trioxide column in place. Ozone concentrations will be measured with a Dasibi Model 8000 dual beam ultraviolet absorption monitor.

3.3.3 Calibration

All concentration calibrations, except for ozone, will be conducted with certified or primary standard gas mixtures shown in Table 3-7. Using these base concentrations, a critical flow orifice blending system will be used to dilute the concentrations to 1/10 or 1/100 of their original levels, as indicated on the right side of Table 3-7. A schematic of the gas blending system is shown in Figure 3-16. Since ozone mixtures cannot be stored, two different O_3 generators will be used to calibrate the O_3 monitor. A standard 1% KI-wet chemistry analysis has been tested and will be used to calibrate the generators.

All nonstandard calibration techniques have been written.

This test work will be conducted in compliance with NEDE-21109, Engineering Operating Procedures. The final impurity determinations at NMP-1 will be conducted only after careful documentation of the plant's performance.

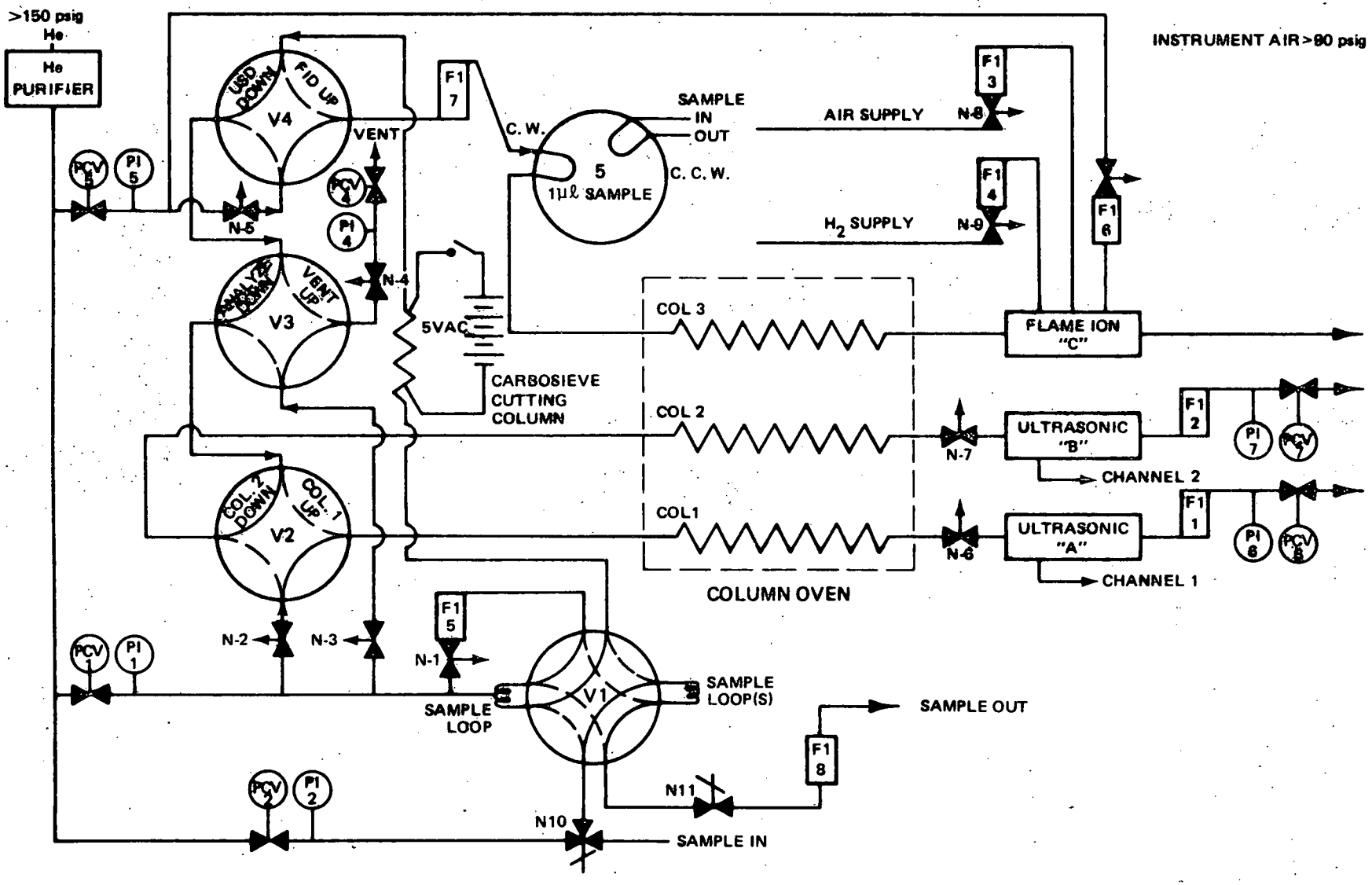

Figure 3-13. Tracor Gas Chromatograph Schematic

COLUMN: SPHEROCARB – 100-120 MESH, 10-ft LONG
1/8-in. o.d. x 0.016-in. WALL AT 100° C

DETECTOR: FLAME IONIZATION DETECTOR AT 180°C BASE TEMPERATURE
FLOWS: HYDROGEN AT 60 sccm = 44 cc/min ON ROTAMETER
AIR AT 0.7 scfh = 0.7 scfh ON ROTAMETER
He PURGE AT 3.5 ON BLACK BALL
TOTAL DISCHARGE TO ATMOSPHERE

RATES AT PRESSURES:

COLUMN = 60 sccm	VENT = 60 sccm
PI-1 = 80 psig	PI-4 = 49 psig
PI-2 = 49 psig	

CUTTING COLUMN:
CARBOSIEVE S – 60/80 MESH, 9-in. LONG
3/16-in. o.d. x 0.010-in. WALL
ADSORB AT ROOM TEMPERATURE,
DESORB AT 200°C. 80% POWER FOR 6 min.
APPROX 2 min CUTTING TIME

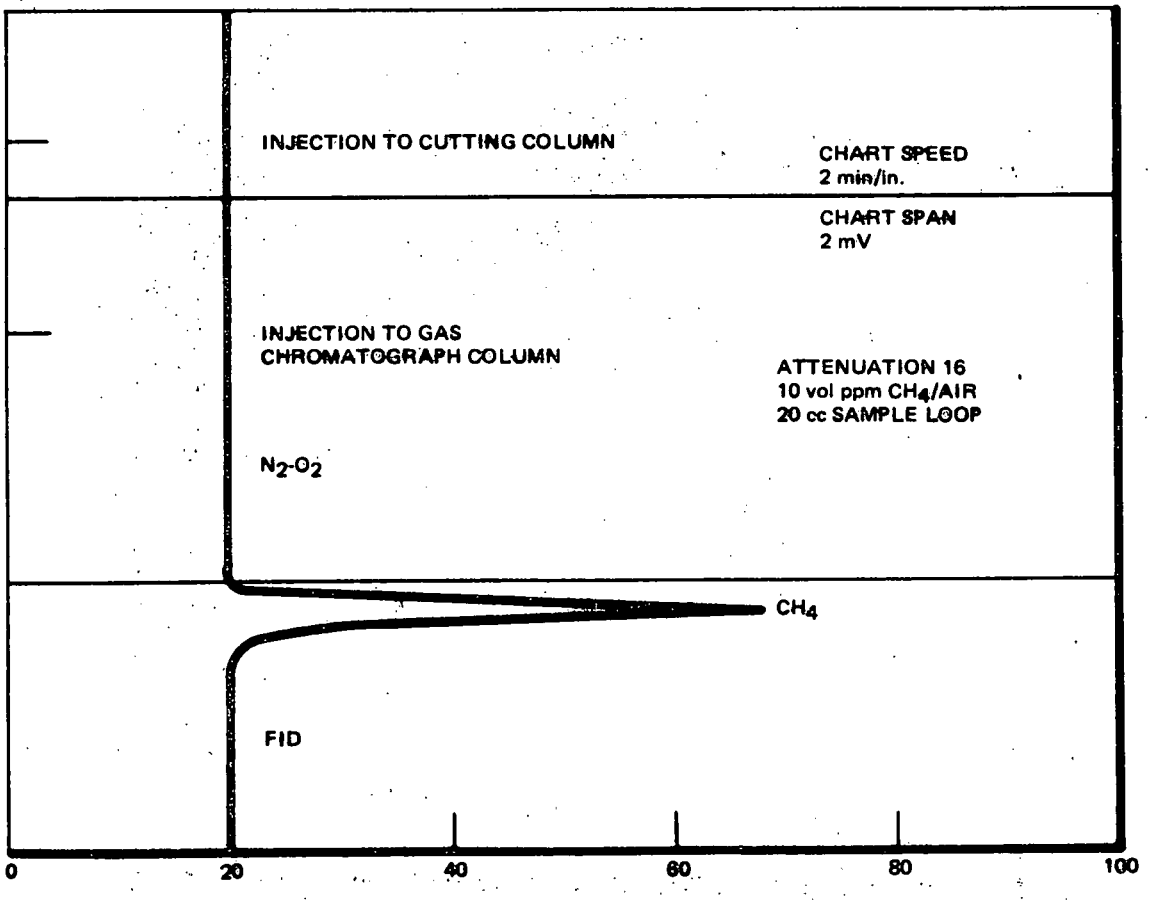

Figure 3-14. Conditions for CH_4 Detection with the Tracor MT-150 with Modified Cutting Column

COLUMN: SPHEROCARB – 100-120 MESH 6-ft LONG
1/8-in. o.d. x 0.016-in. WALL AT 30°C

DETECTOR: ULTRASONIC DETECTOR AT 150°C

RATES AT PRESSURES:
COLUMN = 60 sccm
VENT = 60 sccm
PI 1 = 80 psig
PI 2 = 49 psig
PI 4 = 49 psig

CUTTING COLUMN:
CARBOSIEVE S – 60-80 MESH, 13-1/2-in. LONG
3/16-in. o.d. x 0.010-in. WALL
16 min CUTTING TIME
ROOM TEMPERATURE ADSORB,
200°C DESORB AT 80% POWER

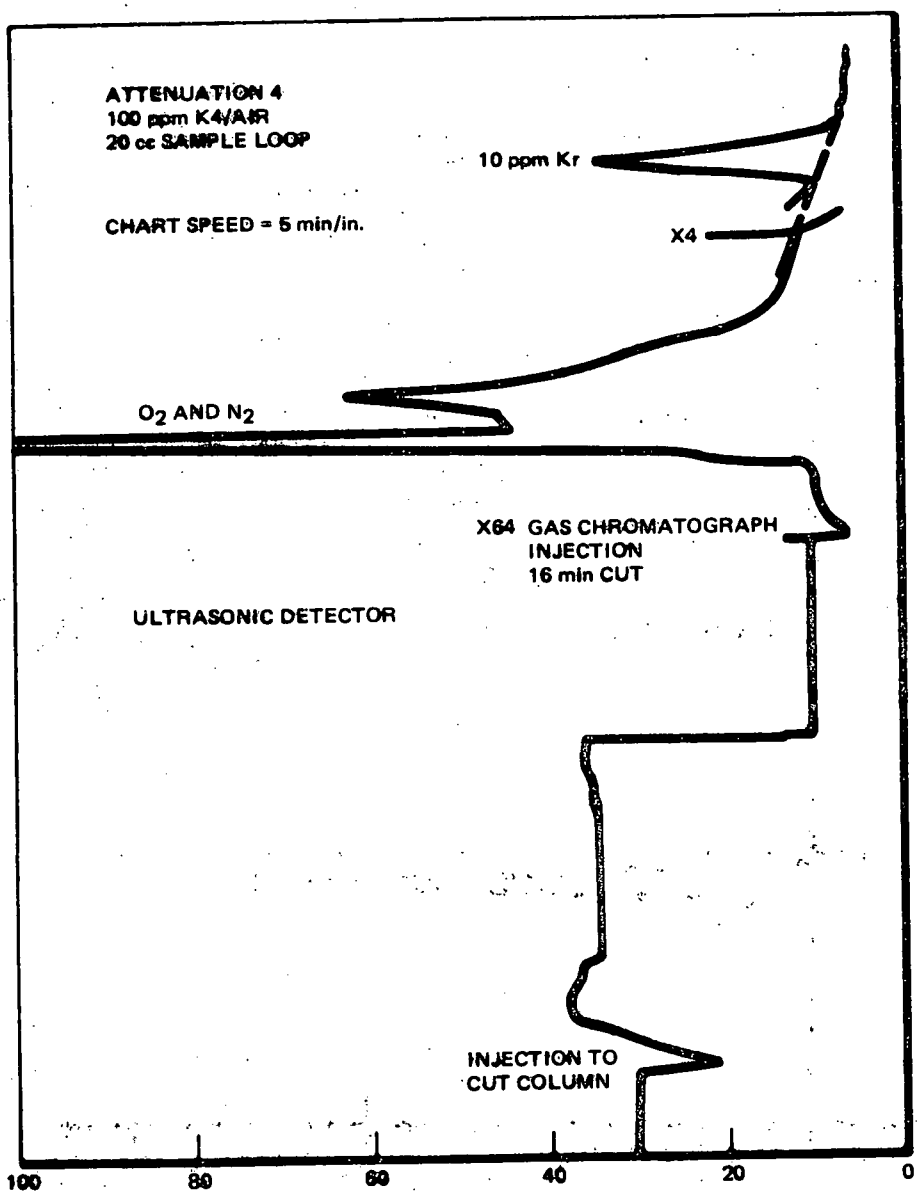

Figure 3-15. Conditions for Krypton Detection with the Tracon MT-150 with Modified Cutting Column

Table 3-7

CALIBRATION GAS SOURCES

			Nominal Concentrations (vol ppm) Using CFO Dilution Panel		
				Critical	Flow Orifice
Kr	D-1 Cylinder	1.0% Kr/N_2	10,000	1,000	100
	B Cylinder	10 vol ppm Kr/N_2	10	1	0.1
Xe	D-1 Cylinder	0.1% Xe/N_2	1,000	100	10
	B Cylinder	10 vol ppm Xe/N_2	10	1	0.1
CH_4	B Cylinder	100 vol ppm CH_4/N_2	100	10	1
CO_2	B Cylinder	1.0% CO_2/N_2	10,000	1,000	100
CO	B Cylinder	10 vol ppm CO/N_2	10	1	0.1
NO_2	B Cylinder	100 vol ppm NO_2/N_2	100	10	1
NO	B Cylinder	100 vol ppm NO/N_2	100	10	1
O_3	Pen Ray Ultraviolet Generator SOG-2 (I_2 standardization)		Self-adjustable range 4 -- 0.4 vol ppm		
O_3	MEC-1000 Ultraviolet Generator		Self-adjustable range 1 -- 0.01 vol ppm		

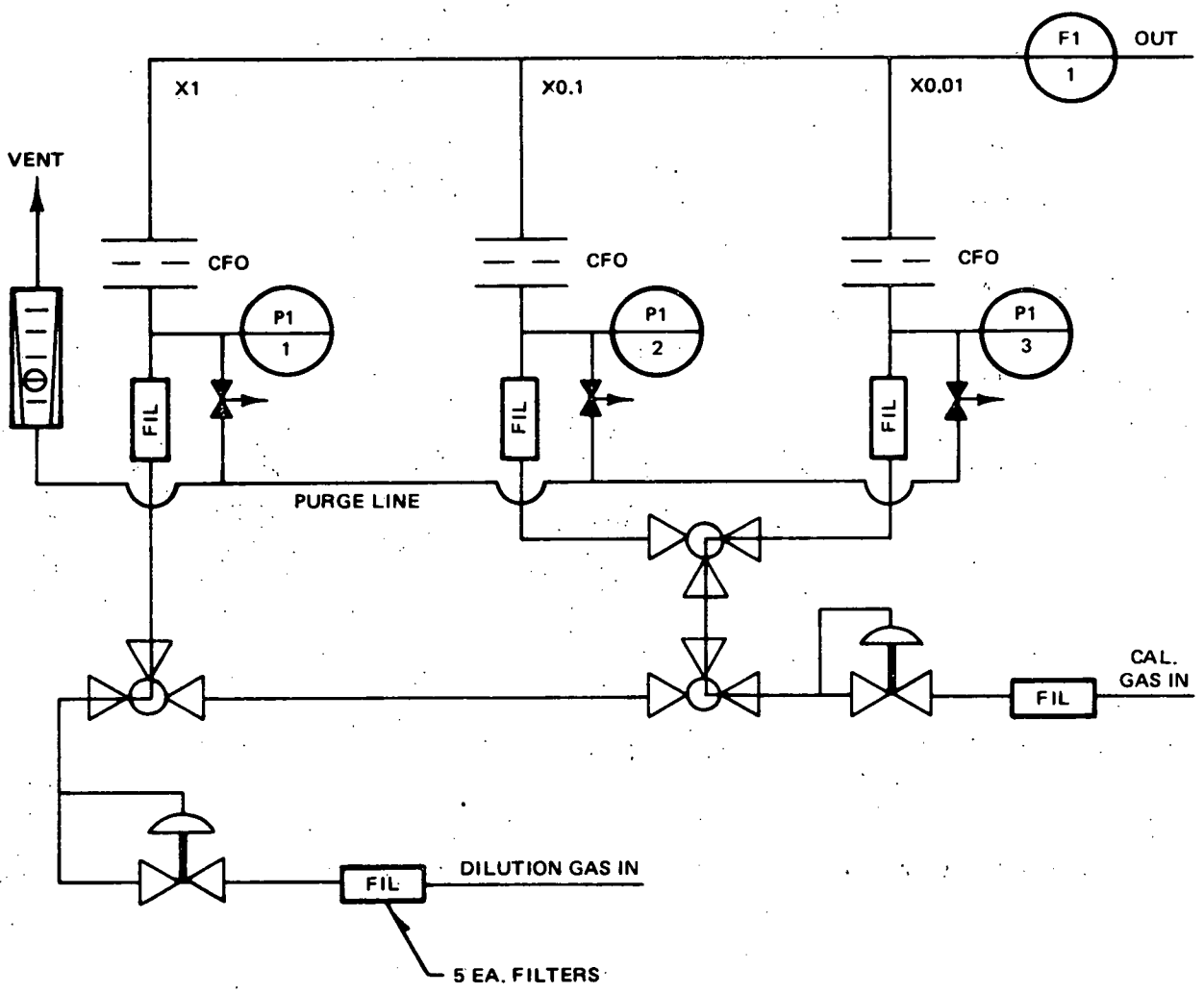

Figure 3-16. Gas Blending System

3.4 TASK B-3. COOLANT LEAKAGE MONITORING (L.L. Sundberg, J.H. Holloway)

Objective. Uncorrected condenser leakage can quickly exhaust the BWR full flow, condensate demineralizers and inject undesirable impurities, including chloride, into the reactor water. With ionic additives such as NH_3 or N_2H_4, the condensate conductivity becomes about 35 μS/cm and simple conductivity is no longer a sensitive leakage monitoring technique. An alternative leakage monitoring technique must be selected and evaluated.

3.4.1 Required Sensitivity

Three parameters must be known to determine the feasibility of measuring trace element intrusions into the condenser: (1) elemental concentration of the cooling water; (2) the rate of cooling water in-leakage; and (3) the condensate flow. Other than the ionization products of water, the most likely candidates (ion) to monitor in the condensate are Na^+ or $C\ell^-$ with lesser amounts of Ca^{+2}, Mg^{+2}, K^+, and $SO_4^=$. Based on the following assumptions, the requisite sensitivity for the monitoring system may be calculated.

Condensate flow:	1×10^7 lb/h ≃ 4.5×10^6 ℓ/h
In-leakage rate:	1 gpm ≃ 240 ℓ/h
Cooling Water Species Concentration:	5 ppm ≡ 5 mg/ℓ ≡ 5000 μg/ℓ

Condensate impurity concentration:

$$\frac{5000\ \mu g/\ \times\ 240\ \ell/h}{4.5 \times 10^6\ \ell/h} = 0.3\ \mu g/\ell \equiv 0.3\ ppb$$

Increased condensate flow, decreased in-leakage rate, or decreased cooling water impurity concentration would require instrumentation with even lower sensitivities.

3.4.2 Instrumentation - Ion-Selective Electrodes

Considering on-line analysis for sodium or chloride, the most suitable method appears to be ion-selective electrodes. The status of "low-level" chloride

monitors is not encouraging, for the manufacturer of the only unit suitable recently recalled all units from the field because of electrode instability. Redevelopment is estimated to take 6 months. If, and when a successful prototype is operating, a sensitivity of <1 ppb is predicted by the vendor.

Three sodium ion monitoring systems were reviewed. These systems were Leeds and Northup, Technicon, and Orion. All systems require the addition of a base to raise the pH of the system to 11-12. This base is needed to reduce the concentration of H^+, to which the electrode will also respond. The Na^+/NH_4^+ selectivity coefficient would have to be assessed. Measurements at low temperature are advisable since the ion product of water decreases with decreasing temperature.

Leeds and Northrup (Model 7070)

Quoted Sensitivity - 0.1 ppb
Additive Base - dimethylamine (g) to pH 11.3
Range - 0.1 to 100 ppb
Sample flow rate - 125 mℓ/min
Cost - $4500
Delivery - 14 weeks
Maximum ambient temperature - 105°F
Additional features (good):

Provides multistream monitoring with sequential stream selection. Preprogrammed solenoid valves select one stream at a time, while others are discharged to drain. Variable programmed sample times for each stream. Possible to monitor cooling water, condensate, feedwater, reactor water semicontinuously.

(NOTE: Two users of this unit were dissatisfied with its performance)

Orion

Quoted Sensitivity - 0.1 ppb
Additive Base - NH_3 (g)
Range - 0.1 to 1000 ppb
Sample flow rate - 200 mℓ/min
Cost - $4000
Delivery - 1 week
Maximum Ambient Temperature - 110°F
Additional Features (good):
Multistream (2) analysis
Built-in particulate filtration system
Additive base consumption should be minimal if the additive is ammonia

Technicon

This unit was examined because of its successful implementation at Gentilly. Surprisingly, Technicon has no sodium monitors on the shelf. The procurement sequence is: A sales representative sends an instrumental specification sheet, which is filled in for sensitivity, flow rate, etc. This sheet is forwarded to development for review, where it may be accepted as a project. Nominal lead time (6 mo) and development charges ($14,000) yield a product, fully warranted, whose acceptance is based on successful implementation under the conditions specified.

3.4.3 Recommendations

At the moment, the Orion sodium monitor appears to be the method recommended. An installed Leeds and Northrup system will be examined. Instrumental specification sheets from Technicon have been promised. Upon receipt, they will be returned for feasibility/cost-lead time evaluation. Monthly progress reports from Orion on their low-level chloride monitor have also been arranged.

3.5 TASK B-4. PLANT MATERIALS COMPATIBILITY (B. M. Gordon, R. L. Cowan)

Objective - A primary concern in the application of an AWC to the BWR is the possibility of materials-coolant incompatibilities which might be introduced. This task, in addition to evaluating the necessary and limiting additive and oxygen concentrations necessary to mitigate stress-corrosion cracking tendencies in the primary coolant loops, will investigate the general corrosion behavior of normally encountered BWR materials in the proposed additive chemistry environment.

The tests in the program are specifically designed to not only demonstrate that the various AWC's do indeed prevent stress-corrosion cracking of typical BWR structural materials, but also do not in themselves produce any detrimental or unacceptable corrosion problems.

3.5.1 Initial Constant Extension Rate Tests (F. Peter Ford, CR&D Schenectady)

3.5.1.1 Test Basis

An initial series of CERT's is being run at GE Corporate Research and Development Center in Schenectady. This series is designed to show that the contemplated oxygen and additive concentrations are indeed beneficial and that plausible excesses of additive are not detrimental. The additive concentrations to be tested are given in Table 3-8.

There are no relevant data in the literature on these alloy/environment stress-corrosion systems at 288°C, and our state of theoretical knowledge is insufficient to definitely state the effect of the chemical additives over the required design life of the reactor. Albeit, the degree of stress-corrosion susceptibility is likely to be small, on the basis of operating experience in all volatile treatment (AVT) dosed boilers. However, the possibility of cracking does need to be defined together with an examination of secondary topics such as the possible effect of by-products, e.g., NO_3^-, on the cracking behavior.

Table 3-8

CONSTANT EXTENSION RATE TEST ENVIRONMENTS

	Range (ppm)	Initial Value to be Investigated (ppm)
Ammonia	12 to 30	20
Hydrazine	0.4	0.4
Hydrazine	0.1 to 0.15	0.1
+		
Morpholine	3 to 8	5
Ammonia	0.3 to 1.5	10
+		
Hydrazine	0.05 to 1.0	0.5
Hydrogen	0.1 to 0.3	0.23

To achieve the stated objective, the following sequential tasks must be accomplished:

a. Task A. Construct and commission experimental loop and test equipment.

b. Task B. Evolve a testing technique capable of resolving low amounts of stress-corrosion susceptibility within the project time period.

c. Task C. Determine the effects of nominal chemical additions to H_2O/0.01 ppm O_2 with respect to stress-corrosion resistance of sensitized 304 stainless steel at 288°C.

d. Task D. Determine how the conclusion in Task C is affected by varying the addition between upper and lower composition limits, and by the presence of breakdown products, e.g., NO_3^-.

e. Task E. Final report.

To achieve the objective within the projected time period (1 year), it is necessary to evolve a rapid stress-corrosion test in which there is some confidence in its applicability to the service behavior of 304 stainless steel. The CERT is rapid, (compared with other test techniques) and there is a growing amount of data for 304 using this method for comparison with service performance; in addition, since it is a dynamic strain test, it simulates the changing load period during operation most likely to be of stress-corrosion cracking danger. However, because of the inherent nature of the test, it is limited to the resolution of cracking in relatively stress-corrosion susceptible alloy/environment systems (i.e., since it is a dynamic tensile test, there is only a finite time the test can run before ductile failure will occur). Thus, in Task B above, the resolution power of the CERT test must be improved if the results are to be conclusive. There are three possible approaches:

a. Lower the strain rate during the test. Because of the time limitation on the project and the number of environmental variables to be investigated, the slowest strain rate that can be practically employed is approximately $10^{-4}min^{-1}$.

b. Use a very susceptible metallurgical condition for the stainless steel. In these tests, the steel will be furnace sensitized and given a further low temperature sensitization. Such a treatment will give a condition extremely susceptible to IGSCC and should increase the sensitivity to changes in the environment, e.g., O_2 content, thereby making it easier to pick up small changes in this failure mode due to amine addition. It should be noted that this microstructural accelerating factor will not help if the failure mode is transgranular, which might be possible in the lower oxygen conditions.

c. Introduce a defected surface condition prior to the test. The CERT testing[24,25] of stainless steel (and carbon steels) has shown that cracking in low oxygen (0.2 ppm O_2) water at 288°C may be detected by CERT when using shot-peened specimens. Presumably, the defects produced by this surface treatment ensure that stress-corrosion cracking is initiated early in the CERT test thereby maximizing the time for crack propagation to have an effect on the tensile properties. Thus, in Task B of this present program, the effect of (reproducible) surface notches on the behavior in the CERT test will be investigated in 288°C water with oxygen contents varying from 8 ppm O_2 to 0.01 ppm O_2.

3.5.1.2 Experimental Procedures

Task A. Construction of Experimental Loop and Test Equipment

The schematic line diagram of the loop (Figure 3-17) indicates the flow pattern of solution to and from the autoclave. Deionized water is delivered from a mixed-resin bed to either the 30-gal make-up tank or 100-gal main reservoir; these tanks are made of linear polyethylene. Aeration, or deaeration is accomplished by saturating with argon, argon/oxygen mixtures or bottled synthetic air (21% O_2, 79% N_2). The solution is pressurized via a Pulsafeeder pump to 1500 psig and delivered at 85 cc/min through a primary header circuit of commercially pure titanium. Outlets to various testing stations, are valved off this circuit. Sampling points are available at the exits to the tanks (SP1 and SP2) and the autoclave (SP3).

The conductivity of the feedwater from the deionizing beds is $\sim$0.4 μmhos/cm. In the initial test, the feedwater to the autoclave was 1.3 μmhos/cm (despite the fact that the main reservoir underwent multiple rinsing during commissioning); however, in subsequent tests, the conductivity dropped to 0.9 μmhos/cm. The rise in conductivity in traversing the autoclave circuit was $\leq$0.05 μmhos/cm.

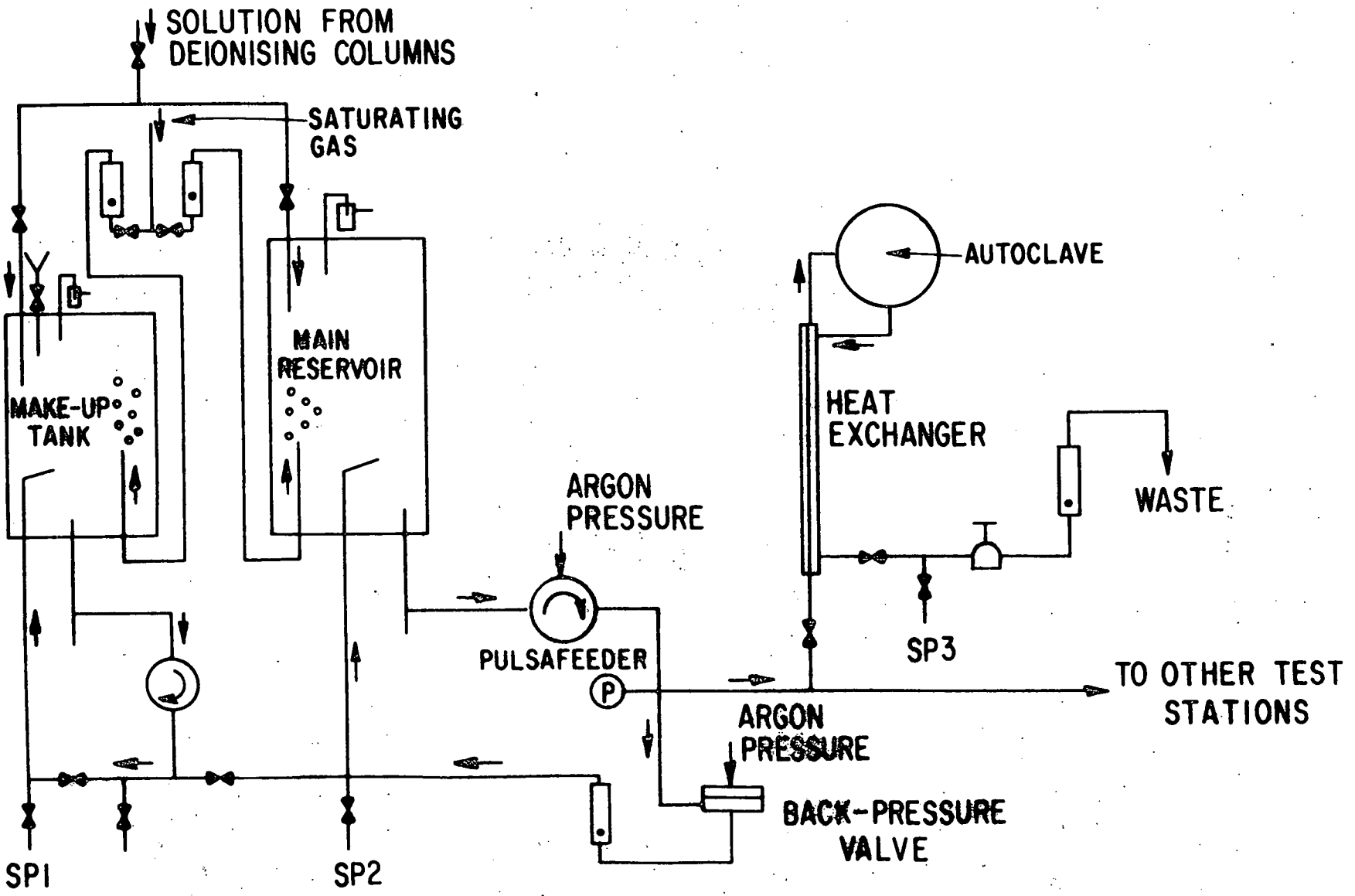

MAIN PIPE MATERIAL:	COMMERCIAL PURITY TITANIUM
TANK MATERIAL:	LINEAR POLYETHYLENE
AUTOCLAVE MATERIAL:	6 A1–4V–TITANIUM

Figure 3-17. Off-Chemistry Loop

Automatic analytical facilities for pH, conductivity and oxygen content (Figure 3-18) are attached to the sampling points to give a continuous data readout for these parameters. (Note that this facility was not commissioned during the preliminary tests in air-saturated water, the analyses being taken on aliquots removed at intervals during these tests. The automatic analytical facility will be used in subsequent experiments.)

The 6AL-4V titanium autoclave of 1-liter capacity (Figure 3-19) containing specimen grips and compression tube, was mounted in an Instron (Model 1131) tensile machine. Solution was delivered to the autoclave at 20 cc/min (residence time ∿50 minutes) via a coaxial titanium heat exchanger and was subsequently dumped to drains.

Task B. Evolution of Test Technique Capable of Resolving Low Amounts of Stress-Corrosion Susceptibility

The 304 stainless steel used in these experiments had the following composition:

Cr	18.4%
Ni	8.45%
Mn	1.65%
Si	0.34%
Cu	0.30%
Mo	0.84%
P	0.038%
S	0.024%
C	0.063%

After rough machining into 1/2-in.-diam x 4-in.-length bars, the material was solution annealed at 1100°C for 1/2 hour and water-quenched. The specimens were then centerless ground to 1/4-in.-diam tensile bars (Figure 3-20) with a 30-deg angle notch (root radius 0.001 in.) of varying depth at the mid-length position. The tensile bars were encapsulated in quartz, evacuated to 10^{-6} torr and furnace sensitized at 650°C for 24 hours, air-cooled to room temperature, low-temperature sensitized at 500°C for 24 hours and air cooled to room temperature.

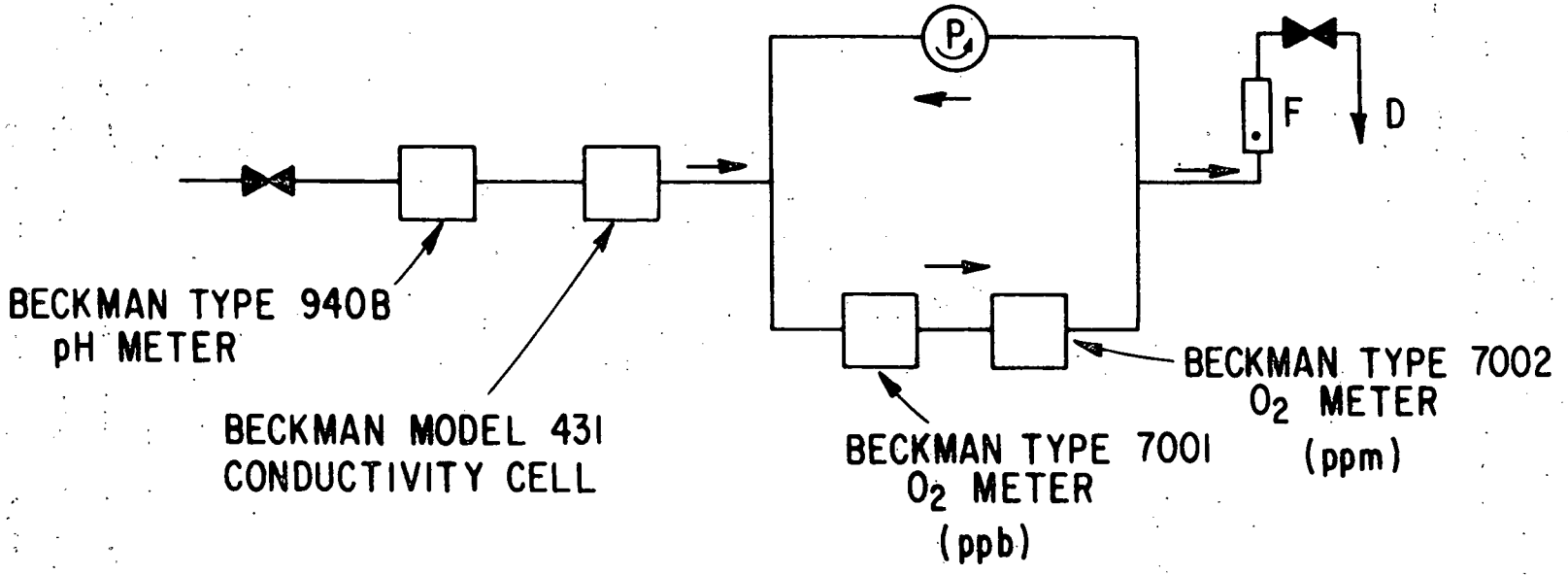

Figure 3-18. Analytical Facility for Oxygen, pH and Conductivity

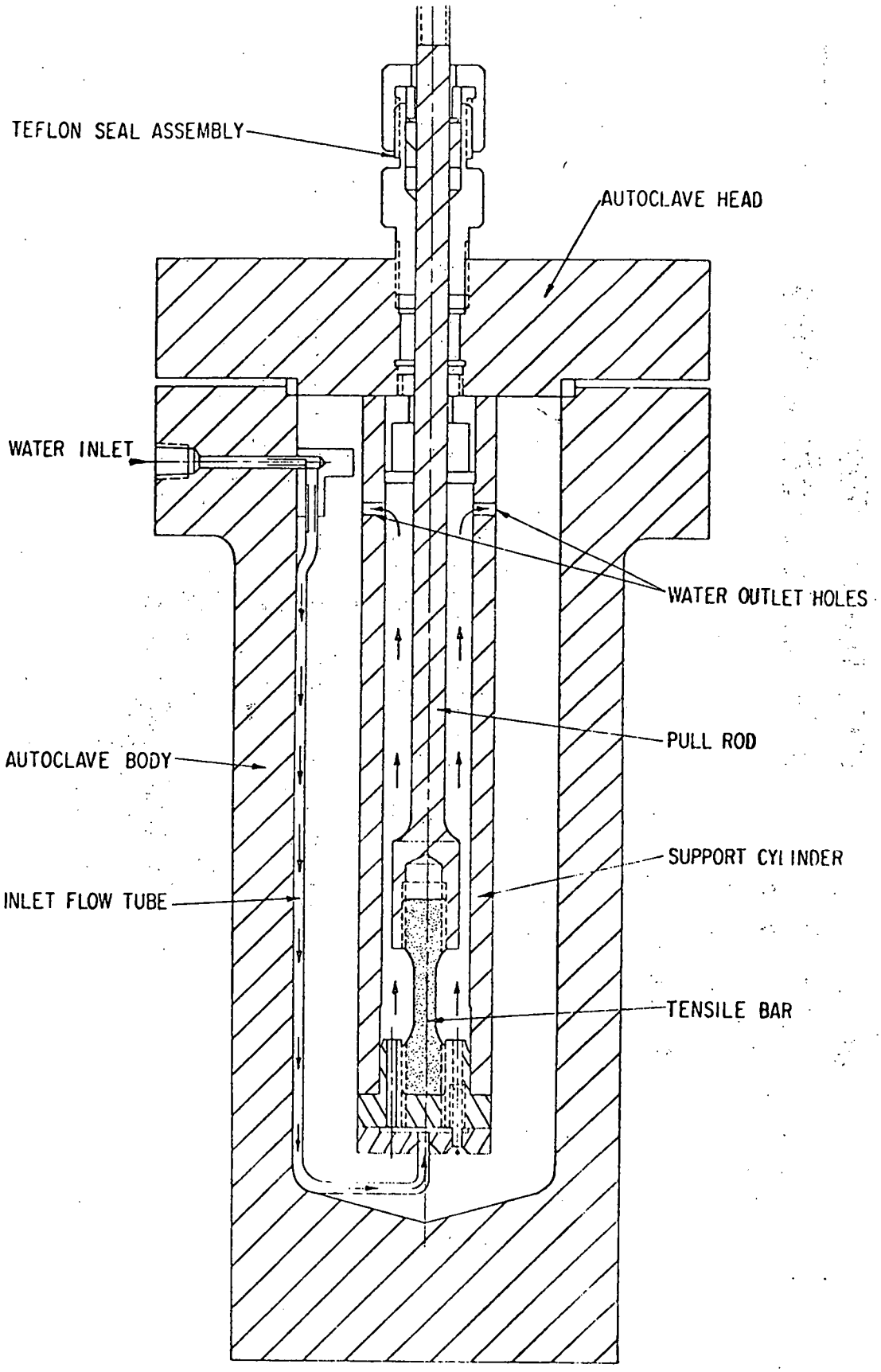

Figure 3-19. Assembly Diagram of Autoclave and Tensile Bar, Grips, etc.

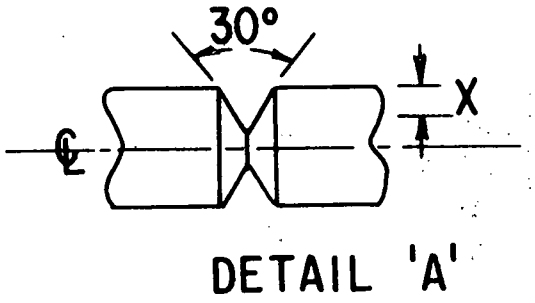

ROOT RADIUS 0.001"
X(ins); 0, 0.013, 0.026, 0.052

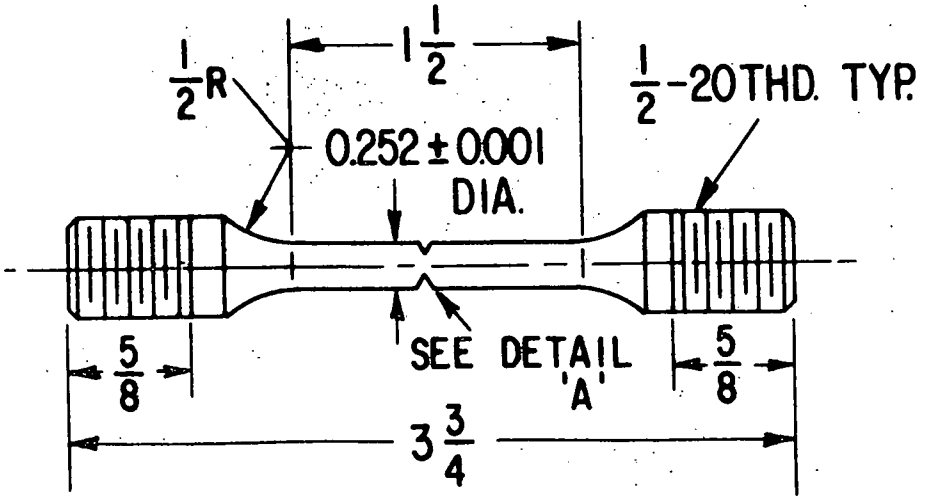

Figure 3-20. Details of Tensile Bar and Notch Geometry

These heat-treated tensile specimens were subjected to constant extension rate testing according to the following environment/notch depth matrix:

Environment	Notch Depth (in.) 0	0.013	0.026	0.052
	Specimen Number			
Argon	1A1	1A5	1A9	1A13
H_2O/8 ppm O_2	1A2	1A6	1A10	1A14
H_2O/0.2 ppm O_2	1A3	1A7	1A11	1A15
H_2O/0.01 ppm O_2	1A4	1A8	1A12	1A16

To date, tests have been completed in argon and H_2O/8 ppm O_2 at 288°C. The testing chronology following alignment of the specimen in the autoclave was as follows: (For aqueous environment)

a. Pressurize autoclave with water to 1500 psig and adjust flow to 20 cc/min

b. Heat autoclave to 288°C

c. Connect tie-rod to Instron cross-head and start extension at 2×10^{-4} in./min. This corresponds to a nominal strain rate of 1.33×10^{-4} min^{-1}.

3.5.1.3 Results

The nominal engineering stress/strain curves for testing in argon and H_2O/8 ppm O_2 are shown in Figures 3-21 for various notch depths. In these curves, the nominal engineering stress is defined as the load/cross-sectional area at notch root and the strain as the instantaneous cross head extension/ initial gage-length. Further data are given in Table 3-9, including the fracture stress (= final load/final area at notch root), and the tensile stress values based on the unnotched specimen cross-sectional area.

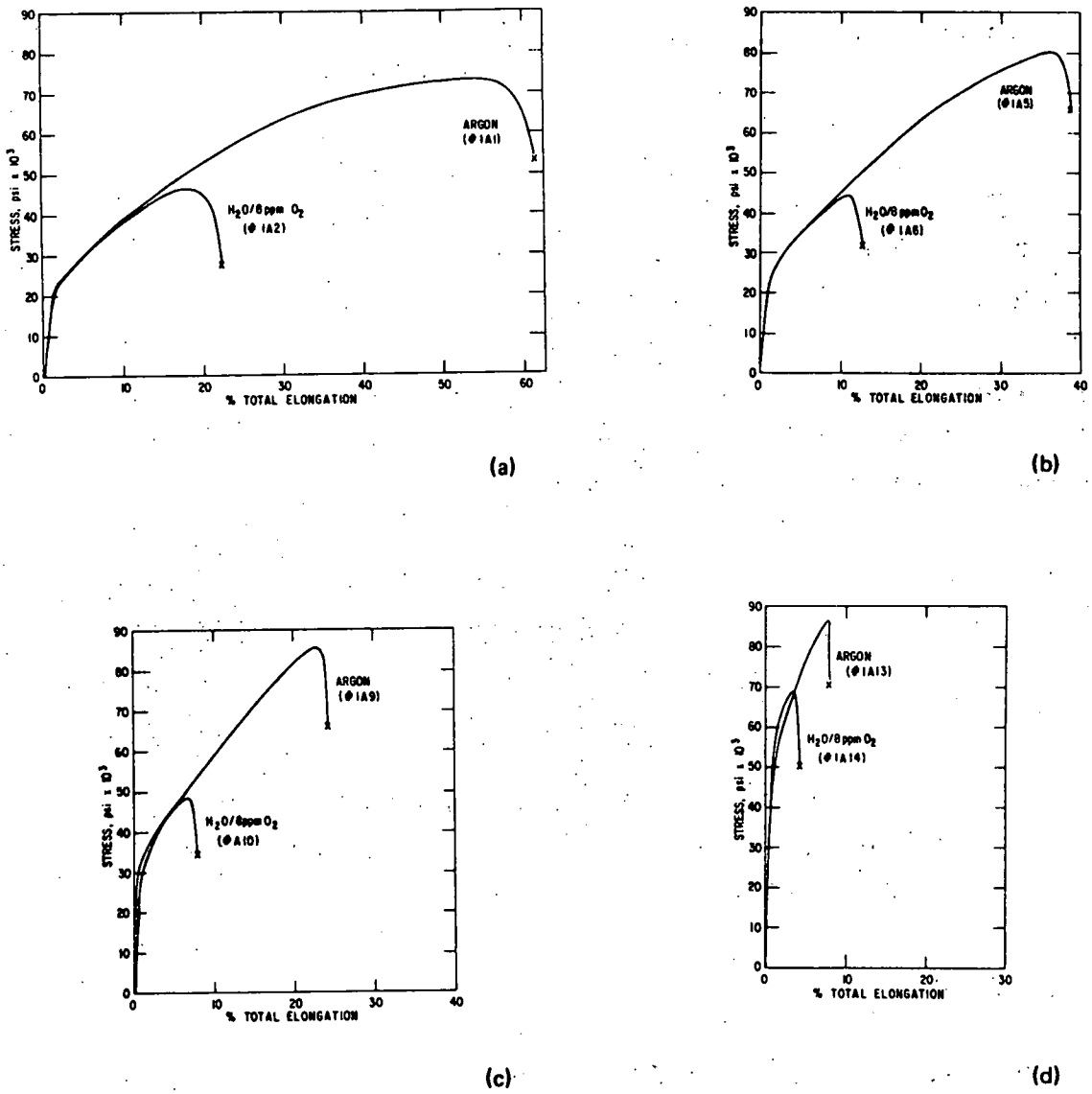

$\dot{\epsilon}$; 1.3×10^{-4} min^{-1}

(a) UNNOTCHED BAR

(b) 0.013-in. DEPTH NOTCH

(c) 0.026-in. DEPTH NOTCH

(d) 0.052-in. DEPTH NOTCH

Figure 3-21. Stress Elongation Curves in Argon and H_2O/8 ppm O_2 at 288°C

Table 3-9

CONSTANT EXTENSION RATE TEST RESULTS

Environment	Specimen Number	Nominal Notch Depth (in.)	Gage Length Diameter (in.)	Notch Root Diameter (in.)	Yield Stress (psi)[a,b]		UTS (psi)[a]		% RA	Total Elongation (in.)	Plastic[c] Strain to Fracture (%)	True[d] Fracture Stress (%)	% IGSCC on Fracture Face	Average Crack Penetration (in.)	Test Time (h)	Average Crack Velocity (mils/day)
					Area 1	Area 2	Area 2	Area 2	Area 2							
	1A1	0	0.2515	-	22,250	22,250	73,000	73,000	67	0.925	59	167,176	-	-	-	-
Argon	1A5	0.013	0.2562	0.2288	18,430	23,105	63,820	80,010	46	0.585	37	122,092	-	-	-	-
288°C	1A9	0.026	0.2532	0.2013	17,875	28,275	54,120	85,611	28	0.365	23	91,654	-	-	-	-
	1A13	0.052	0.2532	0.1525	15,890	43,790	31,780	87,575	12	0.115	7.6	80,604	-	-	-	-
	1A2	0	0.2520	0	17,500	17,500	46,300	46,300	22	0.338	22.4	35,941	65	0.0454	28.16	38.64
H_2O/8 ppm O_2	1A6	0.013	0.2593	0.2318	18,936	23,695	35,506	44,430	15	0.190	12.13	37,709	78	0.1567	15.83	237.36
288°C	1A10	0.026	0.2562	0.2013	16,294	23,390	29,969	48,540	6	0.119	6.2	36,757	78	0.0518	9.98	124.56
	1A14	0.052	0.2562	0.1495	16,100	47,295	23,277	68,375	4	0.0653	4.33	52,871	28	0.009	5.3	40.56

Notes

[a]For Area 1 = Initial cross-sectional area of unnotched gage-length
For Area 2 = Initial cross-sectional area across notch root

[b]Yield stress = limit of proportionality

[c]Based on nominal gage length of 1.50 in.

[d]Defined as load at failure/final cross-sectional area at notch root

All tests conducted in argon exhibited 100% ductile fracture, while intergranular cracking was observed on those specimens strained in H_2O/8 ppm O_2. The % IGSCC on the fracture face on these latter specimens and the average crack velocities (determined from the average crack penetration distance and testing time) are recorded in Table 3-9.

These tests are to determine the specimen geometry giving the greatest sensitivity to stress-corrosion cracking. The data in Table 3-9 and Figure 3-22 indicate that, as expected, there is an increase in test sensitivity to IGSCC (as measured by the average crack velocity and % IGSCC on the fracture surface) at intermediate notch depths. The lower sensitivity on the smooth specimen is probably related to the test time spent in initiating the cracks (i.e., the real crack velocity will be higher than the quoted average velocity, but the propagation period is short). In contrast, the decrease in crack velocity at the deeper notch depths may be related to the elastic constraint effects associated with such a geometry - and the effect that this will have on the fundamental parameters involved in crack propagation, e.g., the oxide rupture rate at the crack-tip.

In Figure 3-23 and Table 3-10, various stress-corrosion indices derived from the stress-strain curves are presented as a function of the notch depth, to determine which index mirrors the observed stress-corrosion behavior most accurately. It is seen that the ratio of fracture stress in solution/fracture stress in argon favored by Battelle[26] does not accurately indicate the increased sensitivity at the intermediate notch depth. By comparison, the other indices based on elongation or % RA parameters and the GE stress-corrosion index,[27] which is related in part to the energy involved in fracture, do predict the observed stress-corrosion behavior.

3.5.1.4 Conclusions

On the basis of these preliminary tests, it has been confirmed that the sensitivity of the CERT test for detecting stress-corrosion susceptibility of 304 stainless steel in aerated water at 288°C is improved by having circumferential notches 0.013 to 0.026 in. in depth in the 1/4-in.-diam tensile bar. Stress-corrosion indices based on ductility criteria (e.g., elongation, % R.A.)

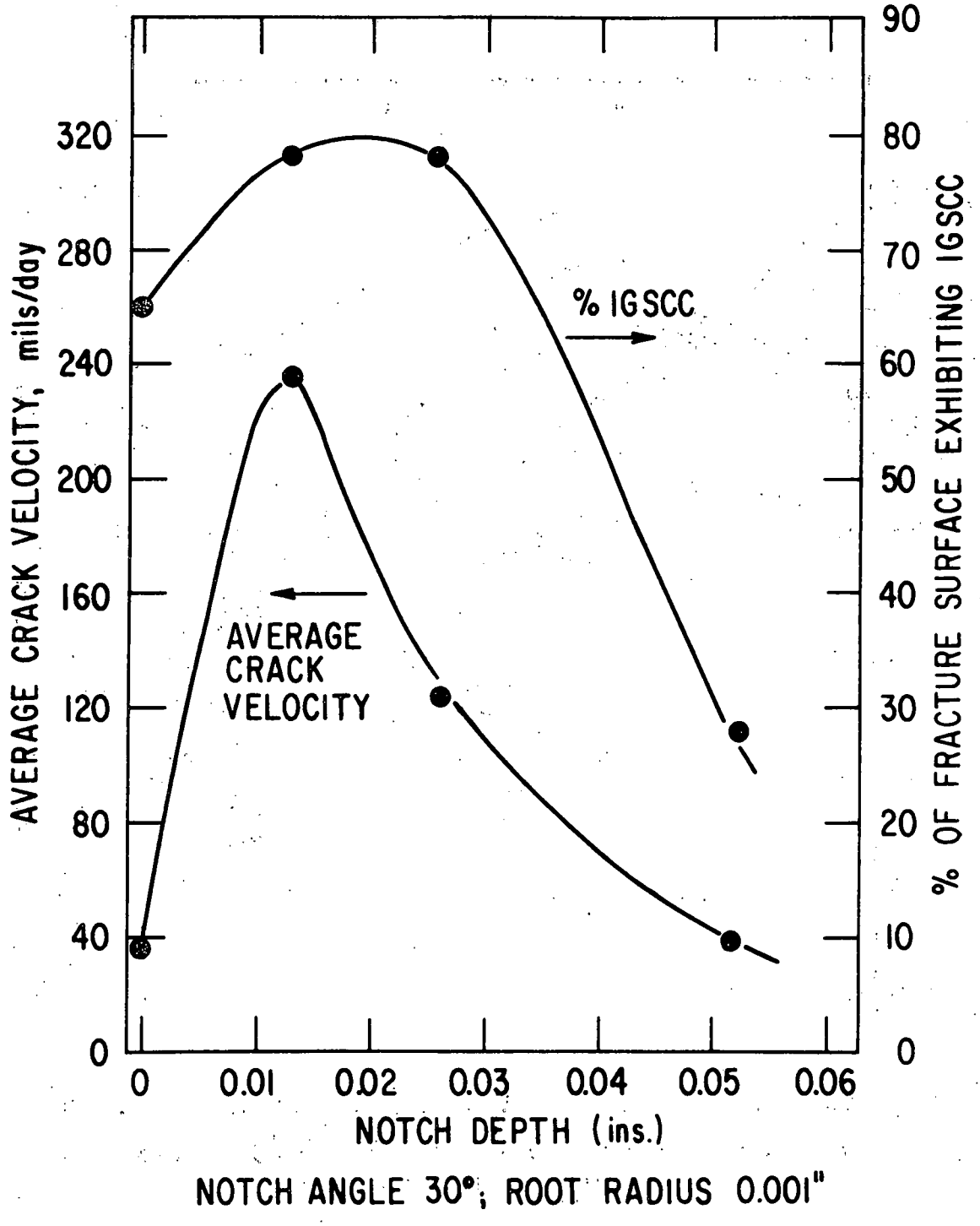

Figure 3-22. Variation of % IGSCC on Fracture Surface and Average Crack Velocity in H_2O/8 ppm O_2 at 288°C, as Function of Initial Notch Depth

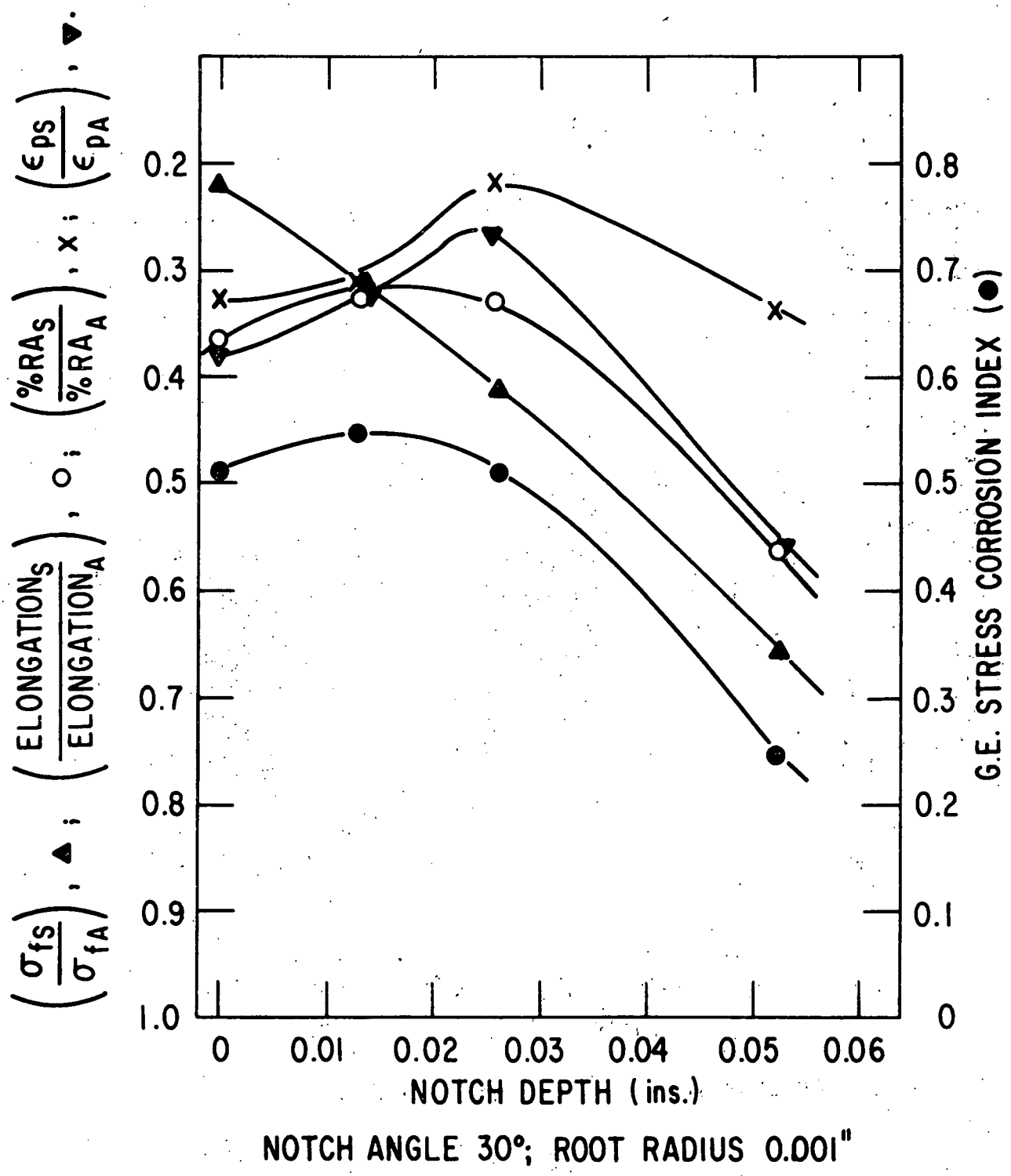

Figure 3-23. Variation of Stress-Corrosion Indices from Stress-Elongation Curve, as a Function of Notch Depth, for H_2O/8 ppm O_2 at 288°C

Table 3-10

COMPARISON BETWEEN OBSERVED STRESS-CORROSION BEHAVIOR AND INDICES DERIVED FROM STRESS/STRAIN CURVE DURING CERT

Notch Depth (in.)	Observed SCC Behavior: % IGSCC on Fracture Face	Observed SCC Behavior: Average Crack Velocity (mils/day)	Stress-Corrosion Indices from Stress/Strain Curve: $\frac{\text{Elongation}_S}{\text{Elongation}_A}$	$\frac{\%RA_S}{\%RA_A}$	$\frac{\text{Plastic Strains to Fracture}_S^*}{\text{Plastic Strains to Fracture}_A^*}$	GE Stress-Corrosion** Index
0	65	38.64	0.365	0.328	0.379	0.5117
0.013	78	237.36	0.324	0.326	0.327	0.545
0.026	78	124.56	0.326	0.214	0.269	0.510
0.052	28	40.56	0.565	0.333	0.569	0.243

Notes:

*Subscript "S" = test in H_2O/8 ppm O_2; subscript "A" = test in argon.

**GE stress-corrosion index $= 1 - \frac{\sigma_W(1 + E_S)}{\sigma_A(1 + E_A)}$ (6)

Where σ = maximum breaking stress (in this case, based on area at notch root)

E = maximum strain (in this case, based on gage length of 1.500 in.)

obtained from the stress/strain curve mirror the microstructurally observed damage as a function of notch depth.

Future work will concentrate on determining the specimen geometry for maximum sensitivity of detection of stress-corrosion cracking in low oxygen water, before continuing on the effect of additive additions on the cracking susceptibility in deoxygenated solutions.

3.5.2 Constant Load, General Corrosion, Crevice Corrosion Tests (B. Gordon, W. Walker)

Tests at San Jose using "Keno", constant-load autoclave (32 station) have been designed. A detail of the tensile loading device is presented in Figure 3-24. The specimen is loaded by a 1000-psi pressure differential between the autoclave operating pressure acting on the load piston and the manifold side of the piston which is vented to the atmosphere through the bottom of the autoclave. The loading device in the autoclave is shown in Figure 3-25. If a specimen fails, a numbered stainless steel ball related to that specimen is forced out of its seal, drops down the manifold and out of the autoclave into a ball-processing device, detailed in Figure 3-26. The failure time and identity of the failed specimens are thus uniquely recorded. The ball-processing device assures that in the case of multiple failures over a brief time, separate strip chart indications are obtained for each failure.

Specimens will be made of two heats of Type 304, one heat of Type 316L and one heat of Alloy 600 fabricated from 6-in.-diam Schedule 80 pipe. All specimens will be in the furnace-sensitized-and-welded plus low-temperature-sensitized (LTS) condition so that performance under identical conditions can be measured and compared. The stress level will be 136% of the materials 550°F 0.2% offset yield strength. The stress level will be set on this fixed load (785 lb) device by controlling the cross-sectional area of each specimen. Quadruplicate specimens will be used. To increase the severity of the test, and to prevent any of the pistons from becoming "stuck," the specimens will be cycled at least once per week from zero to full load.

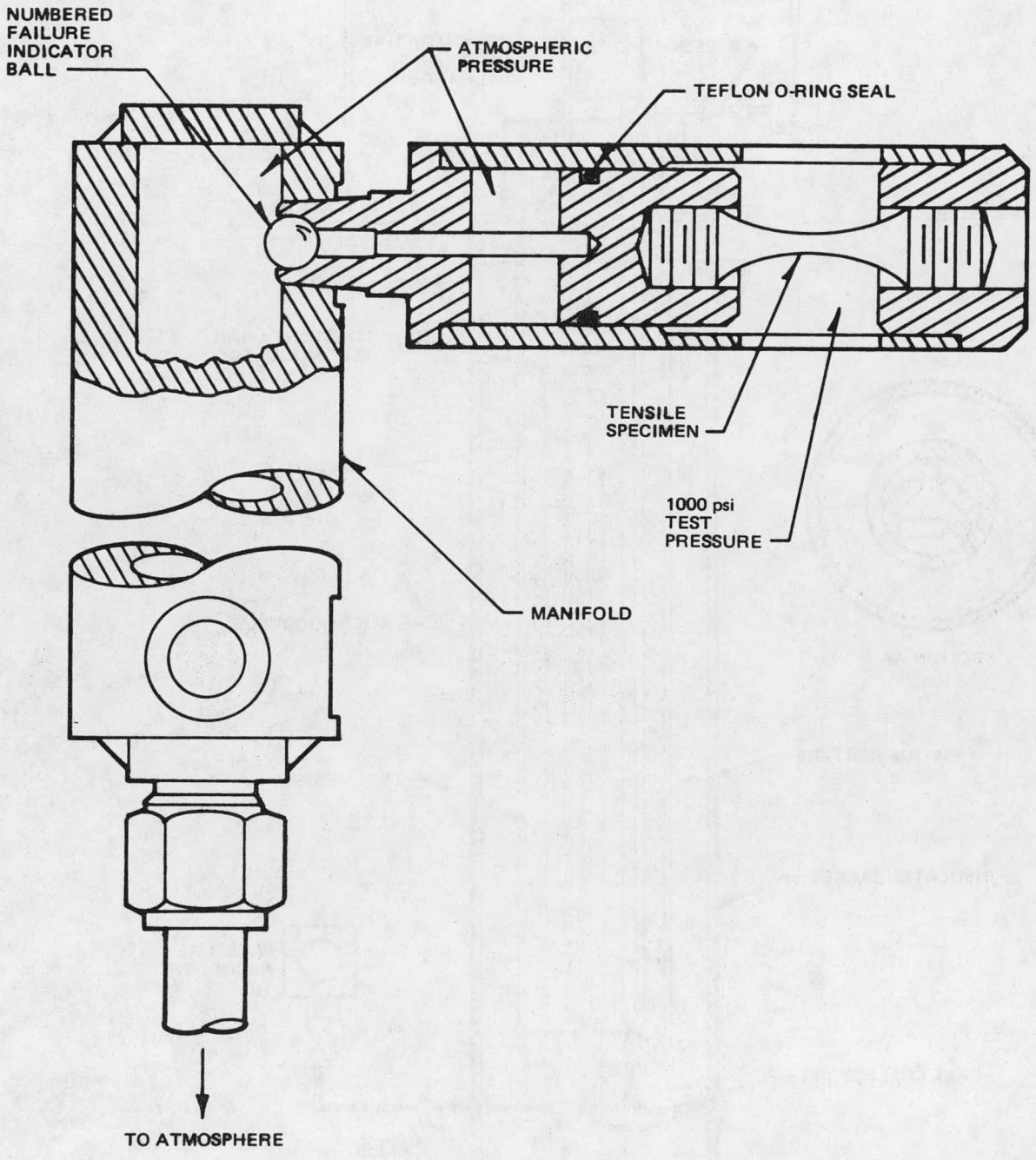

Figure 3-24. Detail of Constant Load Uniaxial Tensile Stress Corrosion Specimen Loading Device

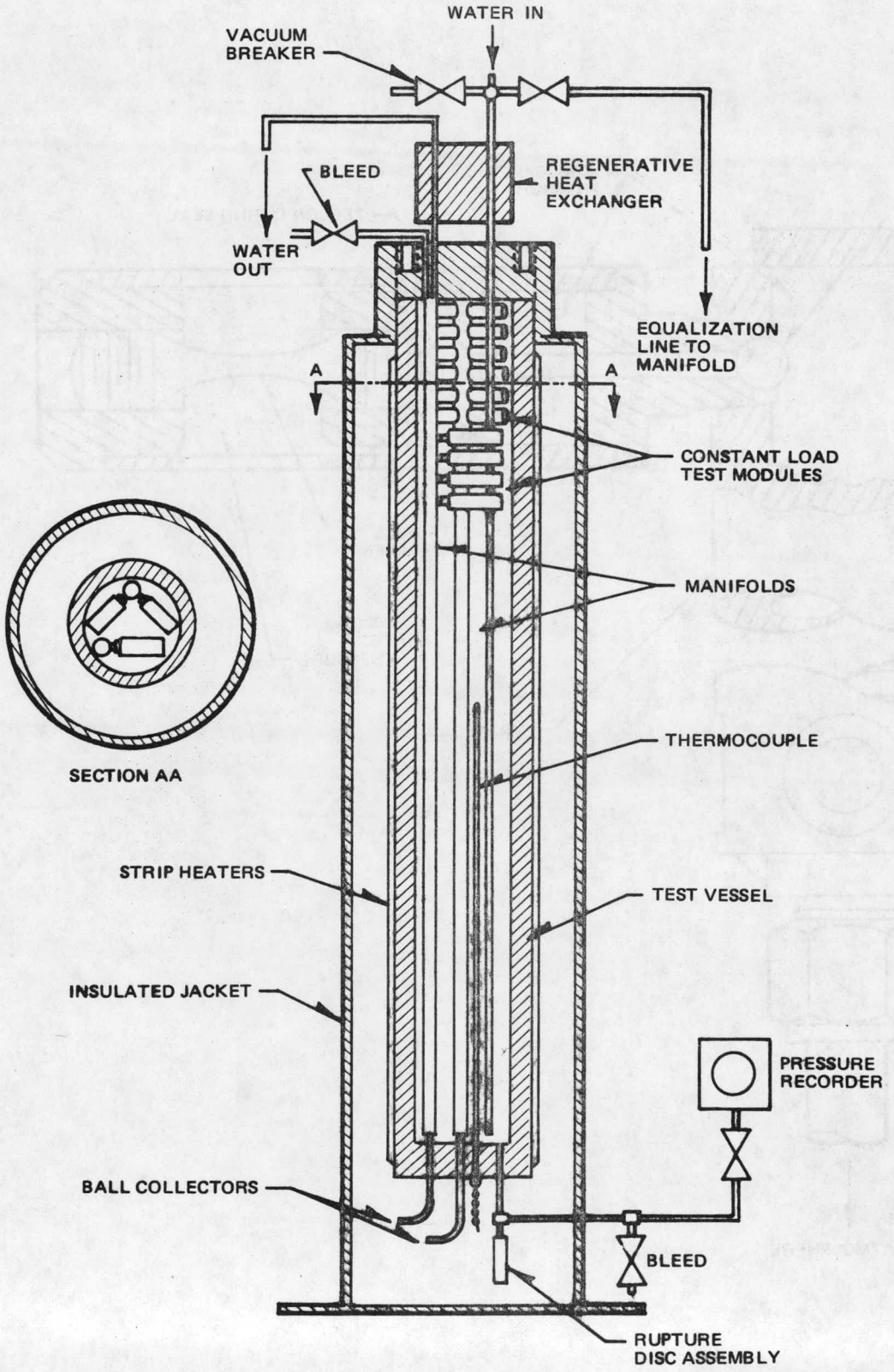

Figure 3-25. Assembly of Constant Load Tensile Test Vessel

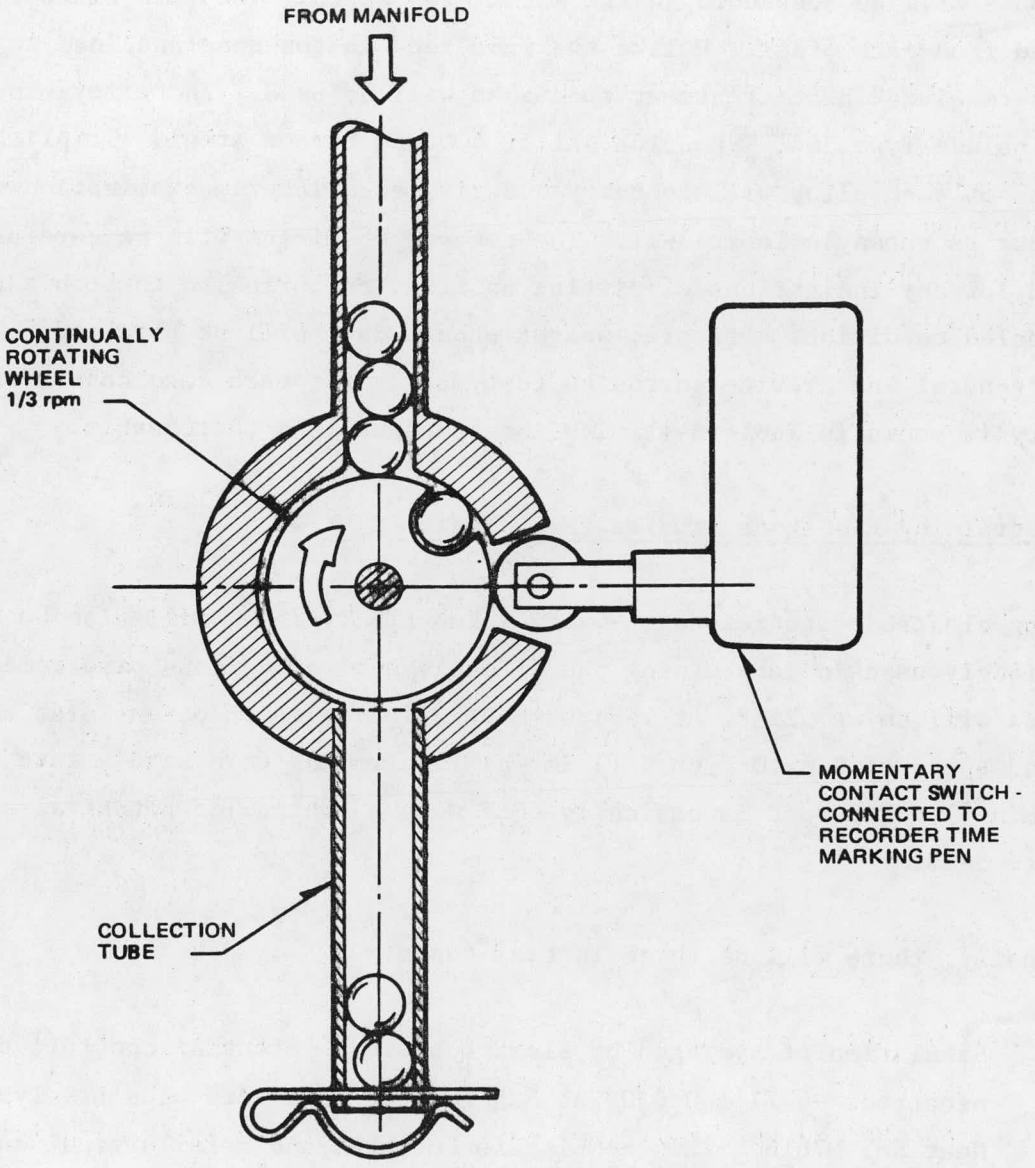

Figure 3-26. Ball Processing Device—Constant Load Test

General and crevice corrosion tests will be performed with the constant load tests on a space available basis or in a separate autoclave. Standard type corrosion weight-change coupons will be used. Crevice corrosion coupons will consist of two general corrosion coupons bolted together with a shim between. The coupons will be suspended in the autoclaves so that they are electrically insulated from each other. Unlike the specimens in the constant load tests, only "as-received" heat treatment specimens will be used. The alloys to be tested include Type 304, Type 316L, Alloy 600 and carbon steel. Triplicate specimens of each alloy will be removed during each interim examination which will occur as shown in Table 3-11. The removed specimens will be carefully examined for any indications of pitting and crevice corrosion in both the scaled and descaled condition. Descaled weight change data will be obtained. The overall general and crevice corrosion test matrix for each candidate additive chemistry is shown in Table 3-11 with the constant load test matrix.

3.5.3 Straining Electrode Studies (M.E. Indig)

Straining electrode studies on as-welded plus LTS Type 304 will also be conducted. As previously used in determining the effectiveness of various pipe remedies, the tests will be at 525°F, at various controlled hydrogen potentials, and at a crosshead speed of 2.5×10^{-3} cm/h (1 in./h) (equivalent to a strain rate of 2×10^{-5} min^{-1}). The test is basically CERT with a controlled potential as shown in Figure 3-27.

Specifically, there will be three initial tests:

a. Simulation of hydrogen by electrochemical potential control, straining electrode -0.77 ± 0.050V at 525°F using as-welded plus LTS Type 304 Heat No. M7616. This combination of heat and metallurgical condition is known to produce a specimen severely susceptible to IGSCC at very low dissolved oxygen concentrations (<50 ppb).

b. Same conditions as Test 1, but in the presence of hydrogen.

c. Pure water CERT at 525°F using pure H_2 addition. Chemical control will be used and electrochemical potentials of the strained and unstrained specimen will be measured.

Table 3-11

TEST MATRICES FOR CONSTANT LOAD AND GENERAL/CREVICE CORROSION TESTS

A. Constant Load

Alloy	Number of Specimens: Furnace Sensitized	Number of Specimens: Welded + LTS	
Type 304-1	4	4	
Type 304-2	4	4	32 total specimens
Type 316L	4	4	
Alloy 600	4	4	

B. General/Crevice Corrosion

	Number of Specimens						
Alloy	1 week	2 weeks	1 month	2 months	4 months	8 months	16 months or Termination
304	3	3	3	3	3	3	3
316L	3	3	3	3	3	3	3
600	3	3	3	3	3	3	3
Carbon Steel	3	3	3	3	3	3	3
304/304*	1	1	1	1	1	1	1
316L/316L	1	1	1	1	1	1	1
600/600	1	1	1	1	1	1	1
CS/CS	1	1	1	1	1	1	1
304/600	2	2	2	2	2	2	2
316L/600	2	2	2	2	2	2	2
CS/600	2	2	2	2	2	2	2
CS/304	2	2	2	2	2	2	2
CS/316L	2	2	2	2	2	2	2

*Number represents pairs of specimens for crevice tests.

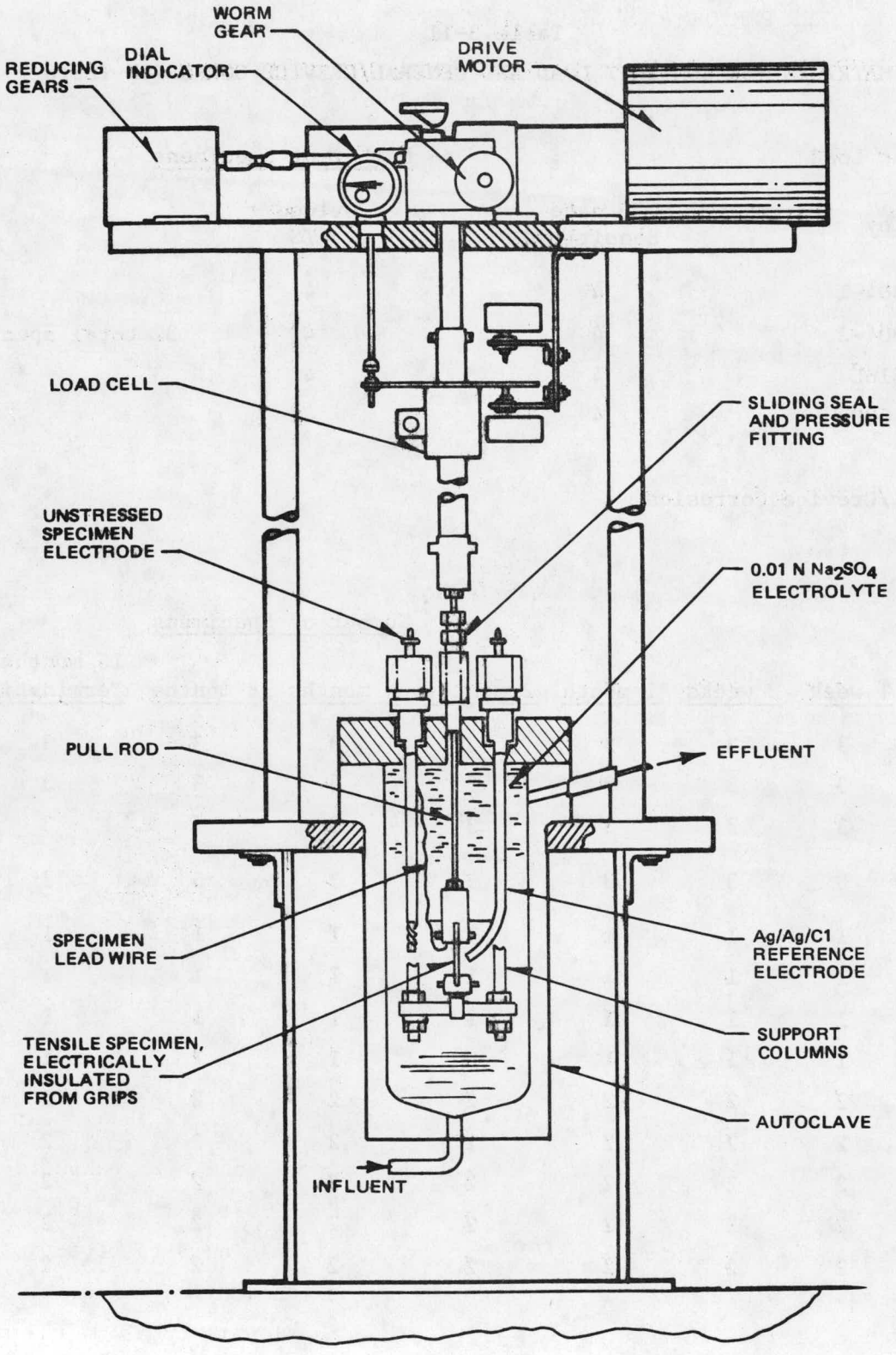

Figure 3-27. Straining Electrode Apparatus

3.6 DEMINERALIZER PERFORMANCE (W. L. Lewis)

Objective. Current BWR practice is to employ hydrogen form (i.e., acid regenerated) cation exchange resin for the bypass clean-up and condensate demeralizers. This practice can be continued when using hydrogen as the AWC additive, but the cation resin will have to be switched to the ammonia form if NH_3 or N_2H_4 is the additive. Use of ammonia-form resins instead of the acid form reduces the demineralizer efficiency for ionic impurity removal. The impact of this reduced efficiency and any other accompanying performance change on both normal operational and shutdown clean-up capability must be evaluated.

3.6.1 Hydrogen Additive

If hydrogen additive is used to suppress oxygen formation, the condensate will contain no new ionic species, and the currently used [H^+ - OH^-] cycle demineralizers will continue to be used. No change in performance would be expected.

3.6.2 Ammonia-Dosed Condensate Treatment

The treatment of high pH, ammonia-dosed condensate in conventional deep-bed mixed-resin demineralizers presents several problems and/or options during operation. The first is the mode of operation of the demineralizer beds: whether to operate in the conventional [H^+ - OH^-] demineralizer mode with a neutral effluent, or to operate in the [NH_4^+ - OH^-] mode with an alkaline or high-pH, NH_4^+-rich effluent. In a conventional [H^+ - OH^-] mixed-ion exchange resin bed, the NH_4^+ ion (from an aqueous solution of ammonia) in the condensate is removed by the cation resin and exchanged from the H^+ ion. Undesirable anions, (Cl^-, $SO_4^=$, etc.) are removed by the anion resins by exchange for the OH^- ion. The effluent from the beds is then pH neutral, and upon exhaustion (partial or total) of the resins (determined by conductivity break) the beds are regenerated in the conventional manner using sulfuric acid to regenerate the cation resins and sodium hydroxide to regenerate the anion resins, following separation of the two resin types. The second option is to allow the cation resins to be operated in the NH_4^+ form until undesirable cations appear in the effluent and then regenerate the resins. There are two distinct methods for

saturating the cation exchange sites with NH_4^+: on-line ammoniation, or separate saturation by treatment of the sulfuric-acid regenerated resins with ammonia hydroxide in the cation regeneration tank. On-line ammoniation merely involved exposing the regenerated cation H^+ resins to the ammoniated stream and allowing the NH_4^+ ions to replace the H^+ ions. As undesirable cations are introduced into the demeralizer bed, these cations replace the NH_4^+ ions at the exchange sites, liberating NH_4^+ into the effluent stream. As NH_4OH is the desired constituent in the feedwater stream, the liberation of NH_4^+ appears to be highly desirable.

The following items are of consideration in determining in which mode $[H^+ - OH^-]$ or $[NH_4^+ - OH^-]$ the condensate demineralizers should be operated.

1. If the $H^+ - OH^-$ mode, required rate of regeneration.

2. If the $NH_4^+ - OH^-$ mode, efficiency of cation removal.

3. Effect of cation slough.

As calculated in Appendix B, if the beds are run on the $[H^+ - OH^-]$ cycle with 18.7 ppm NH_3 in the condensate stream, the hydrogen ion exchange capacity is exhausted at the rate of 153 ft^3 of cation resin per hour. As the demineralizer beds at Dresden contain only 120 ft^3 of cation resin, even if the beds were run to complete theoretical exhaustion it would require turning the beds over (regenerating) every 45 minutes. This is an impossible regeneration frequency to meet which only leaves operation on the $\left[NH_4^+ - OH^-\right]$ cycle as reasonable. (Some fossil-fueled plants and PWR's operate on the $\left[H^+ - OH^-\right]$ cycle with ammonia addition, but the NH_3 levels in these plants are normally below 1 ppm NH_3, not the 18.7 ppm level required in this situation.)

Operation on the $\left[NH_4^+ - OH^-\right]$ cycle presents several problems as to the effects of sodium leakage. From the order of selectivity of several various cations, Reference Dow General Properties Chart for Dowex Ion Exchange Resins, the monovalent series is Ag > Cs > Rb > K > NH_4 > Na > H, and the divalent series

Ba > Sr > Ca > Cu > Mg > Be. This order indicates that although calcium, magnesium, and potassium may be removed from the condensate stream, releasing NH_4^+ ion, difficulties may be experienced in removal of the sodium ion.

The effect of the sodium which passes into the reactor is of some concern as, depending upon the condition of the anion exchange resins, it may appear in the form of NaOH, $NaHCO_3$, or Na_2CO_3.* If the sodium appears as NaOH, with the very real possibility of concentrating in the reactor, the preliminary AWC study may have traded the stress-corrosion cracking problem for one of caustic attack. In addition, there is some evidence of increased turbine deposits operating on the $\left[NH_4^+ - OH^-\right]$ cycle. According to Dr. Carl Cain's comments,** in six units operating in the $\left[NH_4^+ - OH^-\right]$ cycle, both powdered and deep bed resins showed turbine deposits; whereas one unit operating on the $\left[H^+ - OH^-\right]$ cycle showed none.

3.6.3 Hydrazine Addition

Operation of the ion exchangers on a hydrazine additive flow sheet will present the same problems as discussed for the ammonia additive. Hydrazine with its very short half-life and decomposition to ammonia results in condensate compositions essentially identical to those encountered during the use of ammonia.

3.7 TASK B-6. RADWASTE SYSTEM IMPACT (J. M. Jackson, T. Yuoh)

Objective. Predict the liquid and solid radwaste loads (amount and composition) accompanying the potential changes in water chemistry. Evaluate the effect of these loads on equipment capacity, construction materials, processing sequence, etc. Determine the cost of the resulting, modified radwaste system.

The task has just started. There are no results as yet.

---

*Reference comments by I.B. Dick to L.F. Wirth's "Condensate Polishing by Use of Ion Exchange," presented at Liberty Bell Corrosion Course, September 17, 1975, Philadelphia, Pennsylvania.

**Reference Dr. Carl Cain's comments to I.M. Abrams' article, "New Requirements for Ion Exchange in Condensate Polishing," Proceedings of Am. Water Conference, 1976.

3.8 TASK B-7. INJECTION AND CONTROL EQUIPMENT SELECTION (G. VonNieda, J. Holloway)

Objective. Identify the proper system locations for injecting each of the potential additives and the appropriate equipment for this purpose. Similarly, select the position for obtaining a representative sample of the additive concentration and the correct instrumentation for the measurement.

3.8.1 Alternatives

The flow sheets which were reviewed are the mass balance flow paths prepared by H. C. Pellow,[17] are given in the first quarterly report of this Alternate Water Chemistry Program.[28] The flow sheets were prepared for current BWR chemistry (no additive, neutral pH), hydrogen additions, ammonia additions, and hydrazine additions. Hydrogen, ammonia, or hydrazine and combinations of two or all of these additives are being evaluated as potential BWR AWC's. Although the required additive amounts and expected additive concentrations in the system may change with refined calculations, these flow sheets provide adequate information to choose the optimum locations for additive injections during operation.

To select the locations in the BWR plant as optimum injection points for each of the additives, lists of parameters affected by the injection location and of potential injection locations were prepared by evaluation of the impact of the additive on the plant chemistry control at each of these locations.

The items considered in selecting the optimum additive injection points for alternate BWR water chemistries were:

a. Equipment required for additive addition - low pressure versus high pressure addition/cost.

b. Effect of location on additive concentration control philosophy.

c. Will isolation of plant component during operation result in loss of additive control?

d. Effect of additive on condensate demineralizer performance.

e. Effect of additive on pump operation.

f. Effect of additive on corrosion or corrosion protection of feedwater train.

g. Will injection location provide for oxygen control during shutdown?

The available locations as potential additive injection points are numerous and could be almost any location from the condenser hotwell to the feedwater inlet to the core. In addition, the injection point could be located in the recirculation flow loop or in the clean-up system. Nine locations considered for injection points were:

a. Feedwater system, upstream of condensate pumps.

b. Feedwater system, downstream of condensate pumps and upstream of condensate demineralizers.

c. Feedwater system, downstream of condensate demineralizers and upstream of condensate booster pumps.

d. Feedwater system, downstream of condensate booster pumps and upstream of reactor feed pumps.

e. Feedwater system, final feedwater.

f. Clean-up system, upstream of demineralizer.

g. Clean-up system, downstream of demineralizer.

h. Recirculation flow loop, outlet of reactor vessel.

i. Recirculation flow loop, downstream of clean-up system connection.

3.8.2 Hydrogen Additions

If hydrogen gas is chosen as the AWC additive, the control philosophy most likely would be based on a hydrogen addition rate to the plant as a function of power level rather than feedback from reactor water oxygen or hydrogen analyses. The addition rate could be based on feedwater flow rate and injection of the hydrogen directly into the feedwater system would be a logical choice. Use of the clean-up for injection of hydrogen (or any AWC additive) during normal operation is not attractive since this system can be isolated during operation and would result in loss of control of additive concentration and oxygen levels in the reactor water. Addition of hydrogen to the feedwater system upstream of the condensate pumps also should be eliminated since the system pressure is insufficient to cause the hydrogen to go into solution and may cause damage to the condensate pumps. Of the remaining possible locations in the feedwater system or the recirculation loop, all of these locations would be satisfactory for additive injection locations. The preferred location is the feedwater system upstream of the reactor feedwater pumps because of the lower system pressure at these locations. Of the several locations in the feedwater train upstream of the reactor feedwater pumps, the optimum locations has yet to be selected, based on temperature, pressure, hydrogen solubility and dissolution kinetics at each point. As observed during hydrogen addition tests at the Humboldt Bay Reactor Plant in 1968, dissolution kinetics are less favorable than might be expected. The design of the hydrogen addition equipment will be given special emphasis to ensure that added hydrogen is totally dissolved.

3.8.3 Ammonia Additions

If ammonia is chosen as the AWC additive, the control philosophy probably will be based on results of reactor coolant conductivity measurements. The addition rate would respond to a feedback signal from the conductivity analysis. This type of control is similar to the control of ammonia chemistry at Gentilly.

For the choice of additive injection location in the plant with ammonia as the additive, two concerns in addition to these concerns evaluated for hydrogen addition must be considered. These concerns are the effect of ammonia on feedwater system corrosion and on condensate demineralizer performance and reactor water clean-up demineralizer performance. The ammonia addition will increase the pH of the water to which it is added. The resulting basic water chemistry environment will be beneficial in minimizing the general corrosion of carbon steel materials in the feedwater system. In order to provide corrosion protection in the feedwater train, it is expected that the pH should be maintained above about 9.5 which corresponds to a minimum ammonia concentration of about 1.5 ppm.

Based on the mass balance flow sheet developed by Pellow,[28] with sufficient ammonia addition to limit the reactor water oxygen concentration to 10 ppb, a feedwater ammonia concentration of about 10 ppm is expected. This concentration corresponds to a feedwater pH of ∿10.2. If the cation resin used in the condensate demineralizer is hydrogen-form resin, then the ammonia will be removed from the feedwater resulting in neutral water chemistry. At an ammonia concentration of 19 ppm, the capacity of the hydrogen-form cation resin in five beds would be rapidly depleted unless the resin is operated beyond the ammonia breakpoint. It appears highly likely that an ammonia-form resin will be required in the condensate demineralizers with ammonia chemistry control unless the carried-over ammonia is stripped from the steam and returned to the feedwater downstream of the condensate demineralizers. If the ammonia concentrations in the steam were low enough to permit use of hydrogen-form resins, which will remove the ammonia producing neutral water, then ammonia additions downstream of the demineralizers would be required to yield the corrosion protection for the carbon steel materials of the feedwater system.

If the cation resin used in the condensate demineralizers is ammonia-form resin, then the ammonia carried over with the steam will not be removed significantly from the feedwater and the basic pH conditions will be maintained in the feedwater independent of the ammonia injection location in the plant. However, the optimum location again would be immediately downstream of the condensate

demineralizers due to the lower system pressure. Also, the injection of ammonia upstream of the condensate demineralizers which use ammonia-form cation resin may result in ammonia concentrations high enough to cause washoff of corrosion product ions or sodium ions from the demineralizer. The testing of demineralizer performance, which is part of the AWC program (Task B-5 of Reference 1), will provide information concerning the suitability of ammonia-form resin for condensate treatment and the magnitude of the potential problem of washoff of impurity ions with ammonia additions.

Just as in the case for hydrogen additions, locations of an additive injection point for ammonia in the reactor water clean-up system would be a poor choice since isolation of the clean-up system would result in loss of reactor water oxygen control. The removal of ammonia by hydrogen-form cation resin in the reactor water clean-up system probably also will require ammonia-form cation resin for this system. Selection of any location downstream of the feedwater pumps for the ammonia injection would require most expensive equipment due to higher system pressures.

3.8.4 Hydrazine Additions

If hydrazine is chosen as the water chemistry additive, its optimum addition location would be in the final feedwater piping just upstream of the core. This choice is necessary to minimize exposure of the carbon steel feedwater piping to hydrazine and to minimize thermal decomposition before the hydrazine can react with reactor water oxygen. Choice of an additive injection point in the reactor water clean-up system for normal operation is eliminated again since the clean-up system can be isolated during operation. Injection into one of the recirculation loops was eliminated by the additional thermal decomposition of hydrazine which would occur.

3.8.5 Shutdown Control

If the AWC demonstration includes oxygen control during shutdown, layup, and start-up conditions, then either chemical injection capability for the reactor

water system or some form of deaeration system would be required. In Reference 29, a deaeration system which normally would limit the reactor vessel, reactor recirculation system, reactor water clean-up system, and the shutdown cooling portion of the residual heat removal (RHR) system to 300 ppb oxygen concentration has been described. This system primarily depends on vacuum deaeration of the condensate storage tank and use of this deaerated water for supply water to the reactor.

If reactor water system oxygen control by chemical addition (such as hydrazine) is to be considered, the same addition point as proposed for power operation will be satisfactory since it is included in a flow stream resulting from reactor water clean-up system operation. Alternate injection locations for hydrazine addition during shutdown are the control rod drive (CRD) water flow stream or RHR water flow stream. If oxygen control during shutdown by chemical additions is to be considered, further detailed review of system parameters during the shutdown conditions is required to establish optimum injection locations.

3.9 TASK B-8. OPERATIONAL CONSIDERATIONS - SAFETY/TOXICITY HAZARDS (R. Stevens)

Objective. Consider the effect of each of the AWC additive approaches on normal plant operation, e.g., additional manpower requirements, subcontracted service work, special safety or toxicity precautions, employee acceptance, etc. Enter these factors into the selection criteria. There has been no significant progress on this task.

3.10 TASK B-9. ADDITIVE CONSUMPTION AND SOURCE - (D. P. Siegwarth, M. Siegler)

Objective. Predict the consumption of each AWC additive as a function of required coolant concentration and the consequent increase in plant operating cost from using each of the chemicals.

3.10.1 Hydrogen Storage Requirements

Hydrogen storage facilities would be required, if hydrogen addition is chosen as the method to reduce the reactor water oxygen concentration. Discussions of the storage methods with commercial gas vendors have resulted in the recommendation of liquid hydrogen storage facilities. Estimated installation costs of liquid storage facilities with an expected 15-year life are about $80,000 for the storage vessel, and $25,000 for regulating equipment and installation. The cost of liquid hydrogen would be approximately $0.80 per 100 standard cubic feet. Hydrogen costs based on the usage rates in Figures 3-28 and 3-29 are given in Table 3-12. These costs could be substantially reduced if a portion of all of the hydrogen in the condenser offgas were to be recycled.

Table 3-12

HYDROGEN COSTS FOR NO RECYCLE

Reactor Water O_2 Conc. (ppb)	Hydrogen Required (scfm)	Hydrogen Costs ($/day)
10	61.9	713
50	32.3	372

3.10.2 Hydrogen Recycle

Potential recycle methods are shown in Figure 3-30. The SJAE effluent is not suitable for direct recycle because of the high steam and oxygen content. If the conditioning system separated the noncondensible gases from the steam and recombined the oxygen with hydrogen, the gas at Point A would be suitable for recycle. The recombination method of removing the oxygen requires that low air in-leakage rates (<20 scfm) be maintained. If the air in-leakage is not controlled, most of the hydrogen in the offgas will be oxidized in the recombiner by the oxygen from air in-leakage.

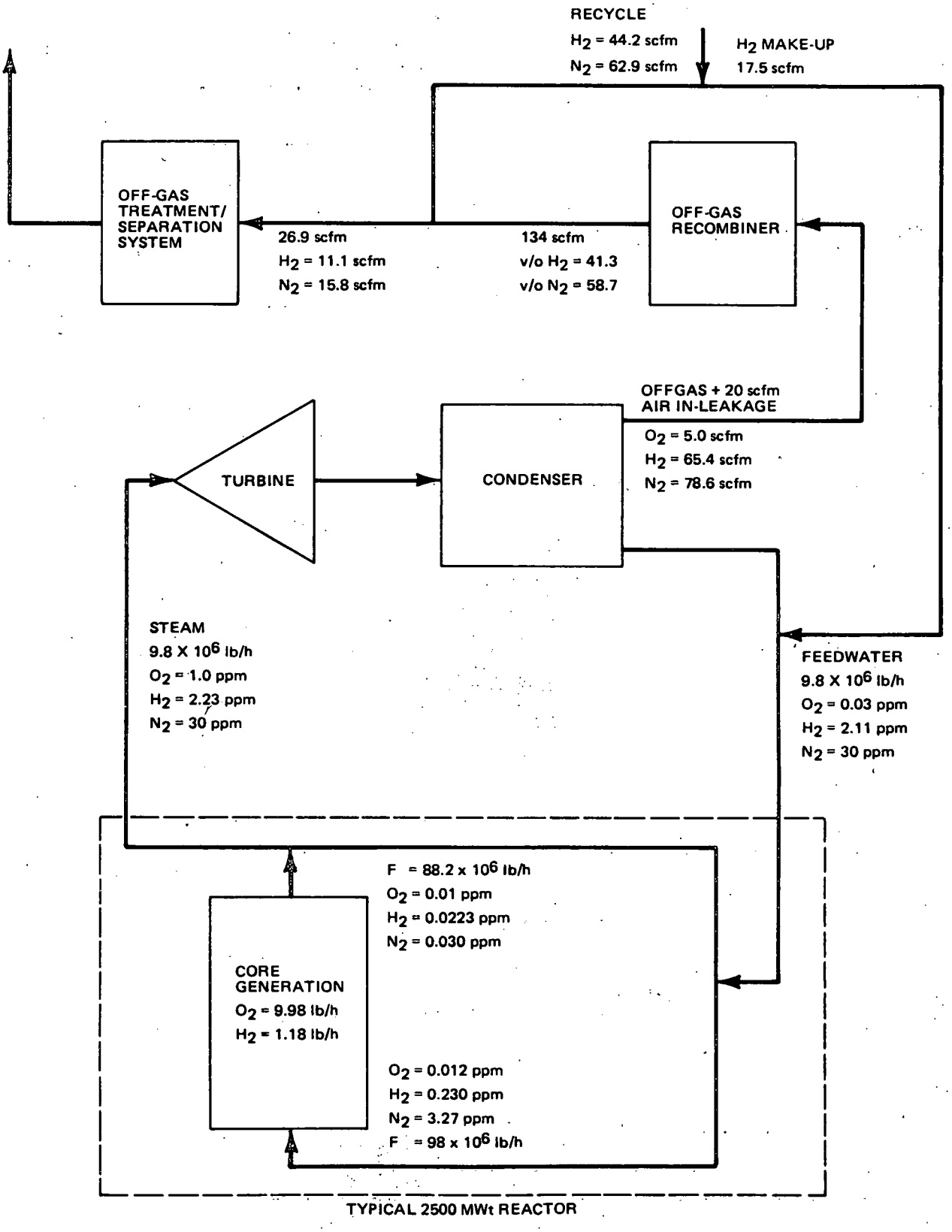

Figure 3-28. Hydrogen Recycle for the Case of 10 ppb Oxygen in the Reactor Water

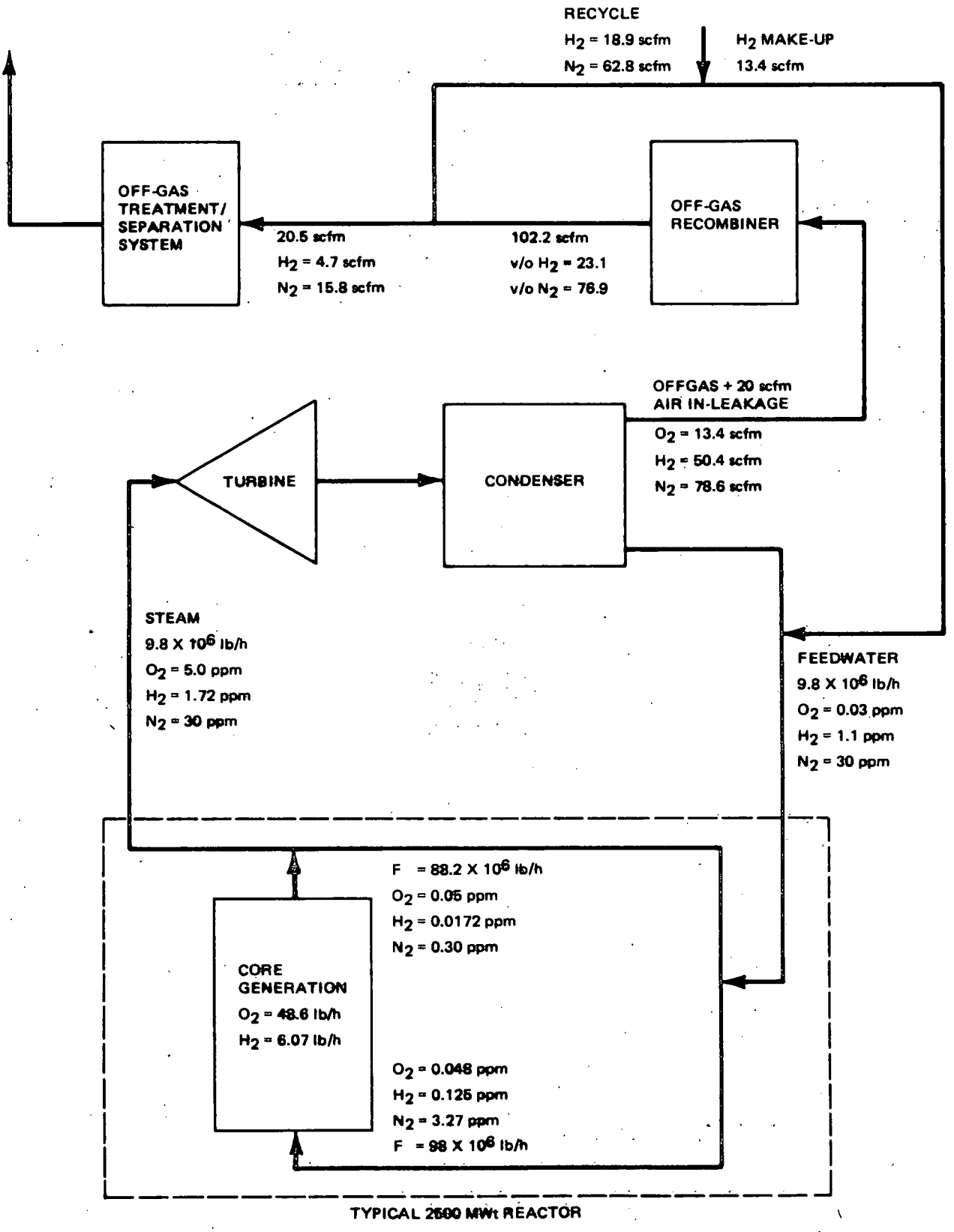

Figure 3-29. Hydrogen Recycle for the Case of 50 ppb Oxygen in the Reactor Water

3.10.2.1 Hydrogen Separation

The separation of hydrogen from the off-gas stream and recycle of the pure hydrogen from Point B would not be as sensitive to the air in-leakage rate. In addition to condensing the steam, conditioning of the non-condensible gases (i.e., drying, etc.) might be required upstream of the hydrogen separation system. Potential hydrogen separation methods are:

1. Swing-cycle adsorption beds;

2. Use of a hydrogen sponge alloy to separate the hydrogen as a hydride and regeneration of the hydride;

3. Thin porous membranes which selectively separate hydrogen; and

4. Hot porous metals which selectively separate hydrogen.

Literature has been collected on some of these methods, but the detailed evaluation of their relative potentials has not been completed.

3.10.2.2 Recycle Without Purification

Probably the simplest hydrogen recycling scheme is the condensation of the steam and removal of the off-gas oxygen by recombination with hydrogen. This method has an additional advantage in that the necessary conditioning of the recycle and bleed streams can probably be accomplished with the presently installed off-gas treatment system equipment. Therefore, calculations were performed to determine the savings which could be realized for the two hydrogen addition cases shown in Table 3-12. The RECHAR system design basis condenser air in-leakage rate of 20 scfm was assumed for these calculations. The calculations were performed for a typical 2500 MWt BWR (Dresden 2) utilizing the mass balance data shown in Figures 3-3 and 3-4. The results of these calculations are shown in Figures 3-28 and 3-29. As indicated in these figures, nitrogen is recycled to the feedwater with the hydrogen. It was assumed that the amount of nitrogen which could be recycled was limited only by the solubility of nitrogen in the feedwater. The point of minimum solubility in the feedwater

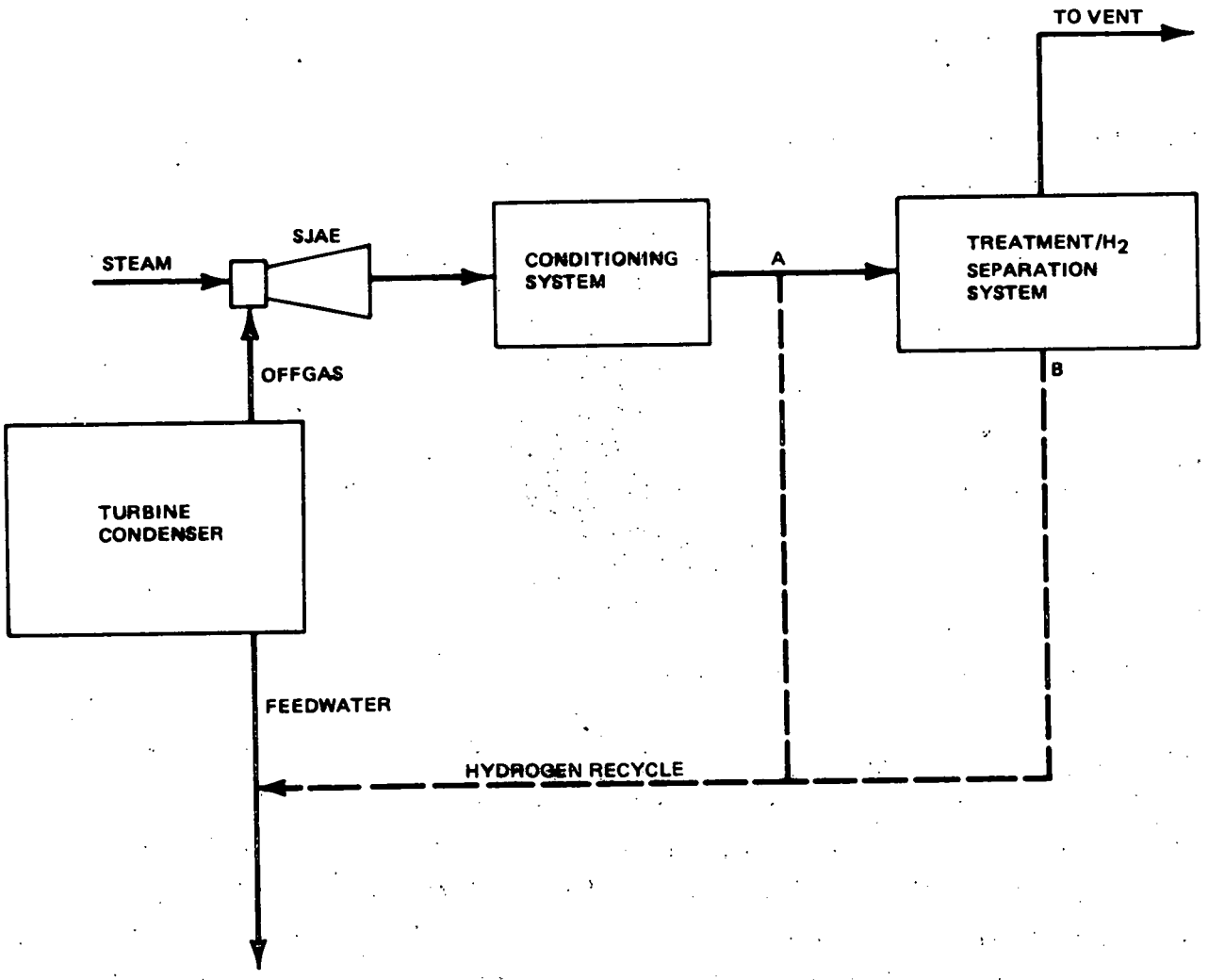

Figure 3-30. Hydrogen Recycle Methods

chain would be at the booster pump suction (approximately 100 psig and 120 to 200°F). The maximum solubility of nitrogen at these conditions is about 37 ppm. Therefore, nitrogen concentration of 30 ppm in the feedwater was assumed for these calculations.

This recycle method reduces the hydrogen make-up requirement from 61.9 scfm to 17.5 scfm and from 32.3 scfm to 13.4 scfm for the cases of 10-ppb and 50-ppb reactor water oxygen concentrations, respectively. The corresponding daily reductions in hydrogen costs would be $511 for the 10-ppb oxygen case and $218 for the 50-ppb oxygen case. However, analysis of additional equipment costs, operating costs and pumping costs are required before it can be determined if this method of recycle would be economical. Also, the effect of the diluent nitrogen on hydrogen dissolution kinetics must be evaluated. One of the major problems with hydrogen addition is finding the mechanism and equipment to assure rapid and complete hydrogen dissolution in the feedwater.

4. REFERENCES

1. J. S. Bromberg and C. E. Kent, *The Boiling Water Reactor Process Environment*, September 1975 (NEDE-12577).

2. C. R. Breden, "Boiling Water Reactor Technology Status of the Art Report. Volume II, Water Chemistry and Corrosion", February 1963 (ANL-6562).

3. R. G. Sowden, "Radiolytic Problems in Water Reactors", *J. Nuc. Mater.*, *8*, No. 1, p. 81, (1963).

4. F. J. Brutschy, "Water Decomposition Studies in the VBWR," Unpublished Internal Memorandum (March 3, 1958).

5. L. Hammar, et al., "Water Chemistry Research at the Halden Boiling Heavy Water Reactor (HBWR)," HPR 55 (June 1967).

6. *Experience from the Experimental Operation of the HBWR on Its Second Fuel Change*, October 1964 (HPR 45).

7. *The EBWR Experimental Boiling Water Reactor*, US Atomic Energy Commission Nuclear Technology Series, prepared by Argonne National Laboratory, May 1957 (ANL 5607).

8. A. W. Kramer, "Boiling Water Reactors," Addison - Wesley Publishing Co., Inc., Reading, Mass. (1958).

9. "Directory of Nuclear Reactors, Vol. III, Research, Test and Experimental Reactors (Supplement to Vol. II)," International Atomic Energy Agency (1960).

10. G. E. Jenks, *Effects of Reactor Operation on HFIR Coolant*, October 1965 (ORNL-3848).

11. J. E. LeSurf and G. M. Allison, "Ammonia Suppresses Oxygen Production in Boiling Water Reactors," *Nucl. Technol.*, *29*, p. 160 (May 1976).

12. L. Hammar, R. Rose, and G. M. Allison, "Water Chemistry Research at the Halden Boiling Water Reactor," Third International Conference on the Peaceful Uses of Atomic Energy, Geneva, 8/31/64 to 9/9/64.

13. Unpublished Internal Communication, D. L. Kavanagh to D. P. Siegwarth (4/11/78).

14. H. S. McLain, "Treatment of the HRT Steam System Water," CF-56-11-132, Oak Ridge National Labs (1956).

15. H. E. Zittel, Nuclear Safety Program Annual Progress Report for Period Ending December 31, 1968, Section 4.3 - Radiation, Thermal, and Chemical Stability of Spray Solutions, June 1969 (ORNL-4374).

16. S. V. Narasimhan, K. S. Krishna Rao and K. S. Vendateswarly, "Water Chemistry Studies VIII - Deoxygenation of Reactor Coolant Water - A Status Report," BHABHA Atomic Research Centre, Bombay, India (1972).

17. H. C. Pellow, "An Investigation of Alternate Water Chemistries for the GE BWR," GE Internal Report (February 1978).

18. H. R. Helmholz, "Specifications for Nitrogen Activity Test Program," December 5, 1977 (Draft)

19. G. F. Palino, "Test Procedures for Nitrogen Activity Measurements at Dresden 2," January 3, 1977, TP-268-0306, Rev. A.

20. a. ATR-268-GFP-0227780001; February 27, 1978
    b. ATR-268-GFP-032178-0002; March 21, 1978

21. H. R. Helmholz, "Installation of Eberline Area Monitors at Dresden-3," March 23, 1978, TP-268-0306, Rev. A.

22. G. F. Palino, *Radioisotope Activities on BWR Primary System Piping, Part 1: Calibration*, May 1977 (NEDC-12646-1).

23. C. K. Neulander, Personal Communication, August 1974.

24. M. Povich, "Effect of Deaeration on Stress-Corrosion of Stainless Steels by CERT," MOR-77-054.

25. M. Povich, "Effect of Shot-Peening on Stress-Corrosion of A508 Low Alloy Steel as Determined by CERT in Air Saturated Water," MOR-76-152.

26. E. L. White, W. E. Berry, and W. K. Boyd, "The Influence of Combined Environmental Effect on Stress-Corrosion of Welded Stainless Steel Piping," EPRI agreement RP311-3 3rd Quarterly Report, 1977.

27. W. L. Clarke, R. L. Cowan, and W. L. Walker, *Comparative Methods for Measuring Degree of Sensitization in Stainless Steel*, May 1977 (NEDO-12669).

28. E. L. Burley, *Alternate Water Chemistry Program Quarterly Report 1*, August 1978 (NEDO-23856).

29. R. M. Fairfield, BWR Services Information Letter No. 136 "BWR Oxygen Control," October 31, 1977.

APPENDIX A

CALCULATIONAL DETAILS AND COMPUTER PROGRAMS FOR HYDROGEN, AMMONIA, AND HYDRAZINE

A general schematic and the definition of the flow and concentration terms for hydrogen, ammonia and hydrazine flow sheets are shown in Figure A-1. For each additive, the concentration terms necessary to describe that additive were used. The flow rates common to the three flow sheets (based on the Dresden 2 Plant) were:

$$F_1 = 9.77 \times 10^6 \text{ lb/h}$$

$$F_2 = 88.23 \times 10^6 \text{ lb/h}$$

$$F_3 = 9.77 \times 10^6 \text{ lb/h}$$

$$F_4 = 98 \times 10^6 \text{ lb/h}$$

A.1. HYDROGEN ADDITION

The data for hydrogen addition tests at five test reactors (ALPR, BORAX III, BORAX IV, EBWR, and HBWR) were reported as steam oxygen concentration (X_{O_2}) as a function of feedwater hydrogen concentration (Z_{H_2}). Based on these data, the core inlet hydrogen concentrations required to maintain 10 and 50 ppb oxygen in the core exit water were calculated for each test reactor. The pertinent data used for the calculations are summarized in Table A-1.

The core-exit-water and the core-inlet-water oxygen concentrations were determined by the following mass balances.

$$Y_{O_2} = X_{O_2}/h_{O_2}$$

$$U_{O_2} = (F_2\, Y_{O_2} + F_3\, Z_{O_2})/F_4$$

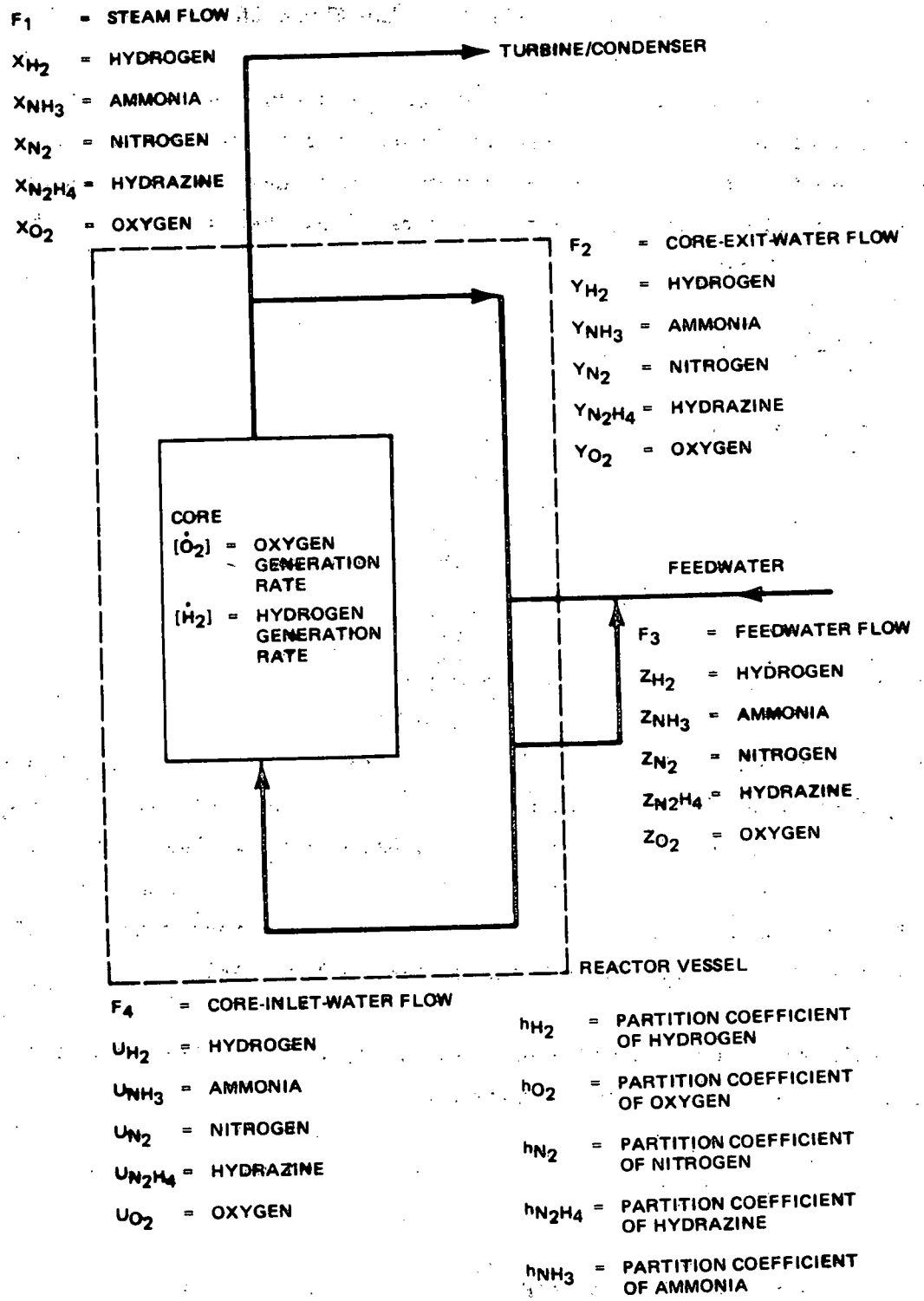

Figure A-1. General Flow Sheet Schematic

Table A-1

PARAMETERS FOR TEST REACTOR CALCULATIONS

Reactor	Flow Rates (lb/h)				Partition Coefficient*		Concentrations (lb/lb)					
							10 ppb O_2 in Core Exit Water			50 ppb O_2 in Core Exit Water		
	F_1	F_2	F_3	F_4	O_2	H_2	X_{O_2}	Z_{O_2}	Z_{H_2}	X_{O_2}	Z_{O_3}	Z_{H_2}
EBWR	6.0×10^{4}	3.8×10^{6}	6.0×10^{4}	3.86×10^{6}	100	100	1.0×10^{-6}	0	3.13×10^{-6}	5.0×10^{-6}	0	2.236×10^{-6}
BORAX III	3.0×10^{4}	2.465×10^{6}	3.0×10^{4}	2.51×10^{6}	100	100	1.0×10^{-6}	0	13.6×10^{-6}	5.0×10^{-6}	0	6.95×10^{-6}
ALPR	9020	1.164×10^{6}	9020	1.173×10^{6}	100	100	1.0×10^{-6}	0	3.1×10^{-6}	5.0×10^{-6}	0	2.007×10^{-6}
BORAX IV	7.5×10^{4}	3.925×10^{6}	7.5×10^{4}	4.0×10^{6}	100	100	1.0×10^{-6}	0	11.16×10^{-6}	5.0×10^{-6}	0	6.25×10^{-6}
HALDEN	9.4772×10^{4}	1.617×10^{6}	9.4772×10^{4}	1.792×10^{6}	100	100	1.0×10^{-6}	0	1.52×10^{-6}	5.0×10^{-6}	0	0.447×10^{-6}

*Based on Experimental Data for the BWR

The oxygen generation rate in the core is

$$[\dot{O}_2] = F_1 X_{O_2} \times F_2 Y_{O_2} - F_4 U_{O_2}$$

The relation between the mass of oxygen and hydrogen generated is

$$[\dot{H}_2] = [\dot{O}_2]/8.0$$

The core-exit and core-inlet-water hydrogen concentrations were determined by an iterative method with the following equations.

$$Y_{H_2} = (F_4 U_{H_2} + [\dot{H}_2])/(F_1 hH_2 + F_2)$$

$$X_{H_2} = hH_2 Y_{H_2}$$

$$U_{H_2} = (F_3 Z_{H_2} + F_2 Y_{H_2})/F_4$$

The first approximation for the iterative method was

$$U_{H_2} = F_3 Z_{H_2}/F_4$$

The computer program used for the above calculation is listed on Table A-2. The calculated results are shown on Figure 3-2 in subsection 3.12 of the main report.

Using Figure 3-2 the core inlet hydrogen concentrations required to maintain 10 ppb and 50 ppb oxygen in the core exit water of a BWR (Dresden 2) were determined to be 230 and 125 ppb, respectively. The concentrations of the oxygen and hydrogen for the different streams were calculated using these core inlet concentrations and the mass balances previously presented. The computer program for calculating the hydrogen addition requirements is listed in Table A-3.

Table A-2

COMPUTER PROGRAM
TEST REACTOR HYDROGEN CALCULATIONS

```
80C     HYDROGEN FLOWSHEET CALCULATIONS-REACTOR DATA
90C            REV 0        3/12/78      T. L. WONG
100 PRINT:"READ:F1,F2,F3,F4"
110 READ:F1,F2,F3,F4
120 PRINT:"READ:H02,HH2"
130 READ:H02,HH2
140 PRINT:"READ:X02,Z02,ZH2"
145 READ:X02,Z02,ZH2
150 Y02=X02/H02
160 U02=(F2*Y02+F3*Z02)/F4
170 GEN02=F1*X02+F2*Y02-F4*U02
180 GENH2=GEN02/8.0
190 UH2=F3*ZH2/F4
200 100 CONTINUE
210 YH2=(F4*UH2+GENH2)/(F1*HH2+F2)
220 XH2=HH2*YH2
230 X=UH2
240 UH2=(F3*ZH2+F2*YH2)/F4
250 TEST=ABS((UH2-X)/UH2)
260 IF(TEST-0.001)200,200,100
270 200 PRINT:"HYDROGEN CONC:XH2,YH2,ZH2,UH2"
280 PRINT:XH2,YH2,ZH2,UH2
290 PRINT:"OXYGEN CONC:X02,Y02,Z02,U02"
300 PRINT:X02,Y02,Z02,U02
310 STOP
320 END
```

Table A-3

COMPUTER PROGRAM
HYDROGEN ADDITION CALCULATIONS

```
10C    PROGRAM BWRH2
100    F1=9.77E06
110    F2=88.23E06
120    F3=9.77E06
130    F4=98.0E06
140    H02=100.
150    HH2=100.
160    X02=1.E-06
170    Z02=30.E-09
180    Y02=X02/H02
190    UH2=110.E-09
200 100 CONTINUE
210    U02=(F2*Y02+F3*Z02)/F4
220    REN02=F1*X02+F2*Y02-F4*U02
230    RENH2=REN02/8.0
240    YH2=(F4*UH2+RENH2)/(F1*HH2+F2)
250    XH2=HH2*YH2
260    HADD=F4*UH2-F2*YH2
265    ZH2=HADD/F3
270    PRINT:"FLOWRATES: F1,F2,F3,F4"
280    PRINT: F1,F2,F3,F4
290    PRINT:"DISTRIBUTION FACTORS:02,H2"
300    PRINT: H02,HH2
310    PRINT:"REGENERATION : (02),(H2) (LB/HR)"
320    PRINT: REN02,RENH2
330    PRINT:"OXYGEN CONC: X02,Y02,Z02,U02"
340    PRINT:X02,Y02,Z02,U02
350    PRINT:"HYDROGEN CONC: XH2,YH2,ZH2,UH2"
360    PRINT: XH2,YH2,ZH2,UH2
380    PRINT 10,HADD
390 10 FORMAT(/,1X,"HYDROGEN ADDITION =",F6.2," (LB/HR)",///)
400 STOP
410 END
```

A.2. AMMONIA ADDITION

The ammonia addition requirement was determined by using the decomposition rate expression discussed in subsection 3.1.3. The calculation was made to determine the ammonia addition required to maintain 10 ppm ammonia in the core-exit water. The parameters used in the calculation are listed in Table A-4 as part of the ammonia addition computer program.

The core-inlet and core-exit-water hydrogen and ammonia concentrations and the ammonia decomposition rate were determined by an iterative method. The core-inlet ammonia and hydrogen concentrations are given by:

$$U_{NH_3} = (F_3 Z_{NH_3} = F_2 Y_{NH_3})/F_4$$

$$U_{H_2} = (F_3 Z_{H_2} + F_2 Y_{H_2})/F_4$$

The decomposition rate is

$$D = K \text{ (Power) } (U_{NH_3})/[(454) (11.2) (U_{H_2})]$$

and the feedwater ammonia and core-exit hydrogen concentrations are:

$$Z_{NH_3} = (D + F_1 X_{NH_3})/F_3$$

$$X_{H_2} = (D\ 6.0/34.0) + F_4 U_{H_2})/(F_1 + F_2/h_{H_2})$$

$$Y_{H_2} = X_{H_2}/h_{H_2}$$

The iterative method was started by assuming initial values for Z_{NH_3} and Y_{H_2}.

Table A-4

COMPUTER PROGRAM AND PARAMETERS
AMMONIA CALCULATIONS

```
10C     PROGRAM AMMONIA,4/4/78,R J STEVENS
20      POWER=2527.
40      N=0
50      F3=9.765E06
60      F4=98.E06
70      F1=9.765E06
80      F2=88.235E06
90      HH2=100.
100     ZNH3=24.E-06
110     UNH3=0.
120     XNH3=0.
130     YNH3=10.E-06
140     HN3=3.77
150     ZH2=3.0E-9
160     UH2=100.E-09
170     YH2=100.E-09
180     PRINT:" DO YOU WANT TO MODIFY FLOWS 1=YES,0=NO"
190     READ: Z
200     IF(Z.NE.1.0) GO TO 50
210     PRINT:" ENTER F1,F2,F3,F4"
220     READ: F1,F2,F3,F4
230 50  PRINT:" DO YOU WANT TO MODIFY AMMONIA CONCENTRATIONS 1=YES"
240     READ:Z
250     IF(Z.NE.1.0) GO TO 60
260     PRINT:" ENTER XNH3,YNH3,ZNH3,UNH3"
270     READ:XNH3,YNH3,ZNH3,UNH3
280 60  PRINT:" DO YOU WANT TO MODIFY HYDROGEN CONCENTRATIONS 1=YES"
290     READ:Z
300     IF(Z.NE.1.0) GO TO 70
310     PRINT: " ENTER YH2,ZH2,UH2"
320     READ:YH2,ZH2,UH2
330 70  PRINT:" DO YOU WANT TO MODIFY HH2 & HN3 1=YES"
340     READ:Z
350     IF(Z.NE.1.0) GO TO 80
360     PRINT:" ENTER HH2, HN3 "
370     READ:HH2,HN3
380 80  D=0.0
390 100 CONTINUE
```

Table A-4 (Continued)

COMPUTER PROGRAM AND PARAMETERS
AMMONIA CALCULATIONS

```
400    N=N+1
410    UNH3=(F3*ZNH3+F2*YNH3)/F4
420    UH2=(F3*ZH2+F2*YH2)/F4
430    X=ZNH3
440    D=8.2*POWER*UNH3/(454.0*11.2*UH2)
450    XNH3=HN3*YNH3
460    ZNH3=(D+F1*XNH3)/F3
470    XH2=((D*6.0/34.0)+F4*UH2)/(F1+(F2/HH2))
480    YH2=XH2/HH2
490    TEST=ABS((X-ZNH3)/ZNH3)
500    IF(TEST-0.001) 4,4,100
510 4 PRINT 5,N
520   5 FORMAT(1H,I5)
530    PRINT 10,ZNH3,UNH3,XNH3,YNH3
531 10 FORMAT(//,1X,"AMMONIA CONCENTRATIONS:",/,2X,"FEEDWATER =",
532&E10.3,/,2X,"CORE =      ",E10.3,/,2X,"STEAM FLOW=",E10.3,/,2X,
533&"RETURN     =",E10.3)
540    PRINT 20,ZH2,UH2,XH2,YH2
541 20 FORMAT(//,1X,"HYDROGEN CONCENTRATIONS:",/,2X,
542&"FEEDWATER =",E10.3,/,2X,"CORE       =",E10.3,/,2X,
543&"STEAMFLOW =",E10.3,/,2X,"RETURN     =",E10.3,//)
560    PRINT:" THE AMOUNT OF NH3 DECOMPOSED IS (LB/HR):"
570    PRINT 30,D
571 30 FORMAT(1H,E10.3)
580    N=0
590 110 CONTINUE
600 STOP
610 END
```

A.3. HYDRAZINE ADDITION

The computer program and input values for the hydrazine addition calculations are listed in Table A-5. The program calculates the hydrazine requirement in two steps. The first step consists of calculating the hydrazine decomposed by radiolytic and thermal decomposition. This step was accomplished by numerically integrating the following equation:

$$(C_{N_2H_4})_n - (C_{N_2H_4})_{n+1} = (A_1 B_1 C_{N_2H_4}^m + kB_2 C_{N_2H_4}) \Delta\ell$$

After the hydrazine decomposition had been determined for a given initial hydrazine concentration, the decomposition products (NH_3, N_2 and H_2) provided the basis for the ammonia decomposition portion of the program which is also shown in Table A-5.

Two hydrazine-addition cases were calculated. In the first case, the quantity of hydrazine required to maintain 1 to 10 ppb in the core exit water was determined. In this calculation, the decomposition of ammonia was not considered. The parameter, DAM, (Line 540 in Table A-5) was set equal to zero.

In the second case, the decomposition of ammonia was considered. The quantity of hydrazine required in the feedwater to obtain 10 ppm ammonia in the core-exit water was determined. As shown in Table A-5, the ammonia decomposition rate (DAM in Line 540) is the same equation as previously given in the discussion of ammonia addition.

Table A-5

COMPUTER PROGRAM
HYDRAZINE CALCULATION

```
60C     HYDRAZINE FLOWSHEET CALCULATIONS
70C       4/11/78 REV 0      T. L. WONG
80 N=0
90 M=0
100 XMW=100.
110 DELT=20.
112 TOTAM=0.0
114 TOTH2=0.0
116 TOTN2=0.0
120 XN=50000.0
130 A=26.3
135 F=9.77
140 B=0.22
150 C0=100
155 C1=C0
160 XK=0.26
170 A2=XMW/XN
180 A3=DELT/XN
185 PRINT:"    RADIOL          THERMAL          C0          C1"
190 200 CONTINUE
195 IF(C0.LT.0.0)GO TO 100
200 DUM1=A*(C0)**XK*A2/F
205 TOTAM=TOTAM+DUM1*F*17.0/32.0
207 TOTH2=TOTH2+DUM1*F/32.0
209 TOTN2=TOTN2+DUM1*F*14.0/32.0
210 DUM2=B*C0*A3
211 TOTAM=TOTAM+DUM2*F*4.0*17.0/(3.0*32.0)
213 TOTN2=TOTN2+DUM2*F*28.0/(3.0*32.0)
240 C1=C0-DUM1-DUM2
250 IF(M-1000)300,300,400
260 400 PRINT:DUM1,DUM2,C0,C1
263 M=0
265 300 IF(N.EQ.49999)GO TO 100
270 N=N+1
280 M=M+1
290 C0=C1
300 GO TO 200
310 100 PRINT:DUM1,DUM2,C0,C1
311 PRINT:N
312 PRINT:"TOTAL GENERATION: NITROGEN,HYDROGEN,AMMONIA"
313 ZN2=TOTN2*1.0E-06/F
314 ZAM=TOTAM*1.0E-06/F
315 ZH2=TOTH2*1.0E-06/F
317 IF(C1)710,710,720
318 710 XN2H4=0.0
319 GO TO 730
320 720 XN2H4=C1*1.0E-06
321 730 YN2H4=XN2H4/5.0
325 ZN2H4=C1*1.0E-06
327 POWER=2527.0
```

Table A-5 (Continued)

COMPUTER PROGRAM
HYDRAZINE CALCULATION

```
328 PRINT:TOTN2,TOTH2,TOTAM
330 F1=9.77E06
340 F2=88.23E06
350 F3=9.77E06
360 F4=98.0E06
370 HH2=100.0
380 UAM=0.0
390 XAM=0.0
400 YAM=0.0
410 HAM=3.77
420 UH2=0.0
430 YH2=0.0
440 XH2=0.0
450 HN2=100.0
460 UN2=0.0
470 YN2=0.0
480 XN2=0.0
490 600 CONTINUE
500 UAM=(F2*YAM+F3*ZAM)/F4
510 UH2=(F2*YH2+F3*ZH2)/F4
520 UN2=(F2*YN2+F3*ZN2)/F4
530 X1=YAM
532 X2=YN2
534 X3=YH2
540 DAM=8.2*POWER*UAM/(454.0*11.2*UH2)
550 DH2=DAM*3.0/17.0
560 DN2=DAM*14.0/17.0
570 YAM=(F4*UAM-DAM)/(F1*HAM+F2)
580 XAM=HAM*YAM
590 YH2=(F4*UH2+DH2)/(F1*HH2+F2)
600 XH2=HH2*YH2
610 YN2=(F4*UN2+DN2)/(F1*HN2+F2)
620 XN2=HN2*YN2
630 TEST1=ABS((X1-YAM)/YAM)
640 TEST2=ABS((X2-YN2)/YN2)
650 TEST3=ABS((X3-YH2)/YH2)
660 IF(TEST1-0.001)610,610,600
670 610 IF(TEST2-0.001)620,620,600
680 620 IF(TEST3-0.001)630,630,600
685 630 CONTINUE
690 PRINT:"HYDRAZINE CONC:ZN2H4,XN2H4,YN2H4"
700 PRINT:ZN2H4,XN2H4,YN2H4
710 PRINT:"AMMONIA CONC:ZAM,UAM,XAM,YAM"
720 PRINT:ZAM,UAM,XAM,YAM
730 PRINT:"HYDROGEN CONC:ZH2,UH2,XH2,YH2"
740 PRINT:ZH2,UH2,XH2,YH2
750 PRINT:"NITROGEN CONC:ZN2,UN2,XN2,YN2"
760 PRINT:ZN2,UN2,XN2,YN2
770 STOP
780 END
```

APPENDIX B

PERFORMANCE OF BWR CONDENSATE AND RWCU SYSTEMS (DEEP-BED AND FILTER DEMINERALIZERS)

To find: Length of runs in deep-bed condensate systems

Basis: 1 hour of operation

The amount of NH_3 in the hotwell = 183 lb/h (from 18.7 ppm carryover x 9.765×10^6 lb steam/h).* Then the lb equivalent of NH_3 in

$$\text{condensate} = \frac{183 \text{ lb/h}}{17.03 \text{ lb/eq}} = 10.72 \text{ lb equiv/h}$$

The following, excerpted from technical data manuals, is typical for cation resins (strong). Capacity, based upon use of 8 lb of 66°-Baume H_2SO_4 regenerant/ft^3 of cation resin is:

	AMBERLITE				DOWEX				
	200	122	120	252	HCRS	HCRW	HGR	HGRW	MSC-
Exhaustant	NaCl	NaCl	NaCl	NaCl	NaCl				
Level (as $CaCO_3$)	200	500	500	500					
Corrected Capacity kgr/ft^3 as $CaCO_3$	19.7	23	23	21	24	24	19	19	17.5
Corrected Capacity lb equiv/ft^3	0.056	0.066	0.066	0.060	0.068	0.068	0.054	0.054	0.050

For resin of the highest capacity (0.068), in 1 hour

$$\frac{10.72 \text{ lb equiv/h}}{0.068 \text{ lb equiv/ft}}$$

or 153 ft^3 cation resin will reach the ammonia break.

Then if operation proceeds beyond the ammonia break, we would expect (from info by Rohm and Hass) that resin would have the same exchange capacity as

*E. L. Burley, "Alternate Water Chemistry Quarterly Report 1," August 1978 (NEDO-23856).

H^+ form resins if run to same point of sodium leakage. However, Dow points out (TD 634.92 & 634.93) that the cation resins (either NH_4^+ and H^+ form) are affected by the pH. That is, the exchange capacity at pH = 7 is greater than at pH = 9. For example, Dow's highest capacity resin (Dowex HGR-W) shows a capacity of only 3.21 kgr/ft^3 for 5% sodium leakage with a 413-ppb sodium input in the presence of ammonia at a pH of 9.3 to 9.5, not 10.2 as obtained by Pellow. (L. F. Wirth* notes that the degree of regeneration required, to effect low sodium and chloride leakage at a pH of 9.6, is over 99% for cation resin and 96% for the anion resin.) Dow also mentions (TD 634.92 & 634.93) in passing that the anion resin is adversely affected and the silica removal effectiveness drops off rapidly when operating at high pH levels. This may require changing the in-place demineralizers to a 1:1 or even a 2:3 cation: anion (volume) resin ratio.

*L. F. Wirth, "Condensate Polishing by Use of Ion Exchange," Presented at Liberty Bell Corrosion Course, September 14, 1975, Philadelphia, Pennsylvania.

DISTRIBUTION

Name	M/C
L. D. Anstine	V04
R. G. Bock	110
E. L. Burley (25)	585
R. N. Carter	H02
J. D. Clark	772
R. L. Cowan	407
W. R. DeHollander	110
C. F. Falk	165
P. Ford	SCH
B. M. Gordon	138
G. M. Gordon	138
R. Hanneman	SCH
H. R. Helmholz	V04
M. Indig	V17
J. Isaacson	154
J. M. Jackson	195
C. E. Kent	772
R. J. Law	V15
J. C. Lemaire	138
M. F. Lyons	110
L. E. Nesbitt	761
G. F. Palino	V04
H. H. Paustian	151
H. Pellow	110
W. Pitt	195
R. A. Proebstle	146
R. R. Roof	870
C. P. Ruiz	V04
M. Siegler	585
J. M. Skarpelos	110
L. L. Sundberg	585
J. S. Wiley	110
C. D. Wilkinson	164

DISTRIBUTION

Name	M/C
T. L. Wong	585
J. C. Blomgren (10)	
Commonwealth Research Corp.	
1319 S. First Ave.	
Maywood, IL 60153	
NEBG Library (5)	328
VNC Library (1)	V01